# DIPLOMARBEIT

# Palynological Investigation on Plio-Pleistocene Sediments of the Lukundol Formation, Kathmandu Basin, Nepal

Angestrebter akademischer Grad
**Magistra der Naturwissenschaften (Mag.rer.nat.)**


| | |
|---|---|
| Verfasser: | Andrea Kern |
| Matrikelnummer: | 0301595 |
| Studienrichtung: | Paläobiologie (A 443) |
| Betreuer: | Ao. Prof. Dr. Reinhard Zetter |


Wien, am 27. Januar 2009

# Content

Abstract

The Himalaya is an area, which underwent significant change influencing the whole world since the Eocene. The raising of this unique in its size mountain massive change not only for the local environment, but further did cause a different world climate due to the raising of the Asian Monsoon climate. Therefore local data is needed to get a better understanding of the raise and its influence.
Especially palynologists have tried to reconstruct ancient vegetation, but limited their work mostly to the light microscope only.

For this investigation, sediment of the Lukundol Formation from the Kathmandu Basin is analyzed by the light microscope and the scanning electron microscope to get a more detailed impression. 78 taxa were processed, containing 25 spores from ferns and mosses, 7 different gymnosperms, 45 angiosperms and 1 freshwater cyst.
It is shown, that some taxa, which are often missing in a normal record, are part of this assemblage and can be easily recognized due the use of the SEM. Further, many different species within one genus occurs, which look alike in the light microscope (e.g. Composites, Euphorbiaceae). Especially when it comes down to common taxa of the Kathmandu Valley, such as *Quercus* or *Pinus*, the identification down to the species level narrows down the paleoenvironment.

## Zusammenfassung

Das Gebiet des Himalayas durchlief seit dem Eozän eine entscheidende Veränderung und beeinflusste die ganze Welt. Die Hebung dieses großen und einzigartigen Gebirgsmassivs veränderte nicht nur die vorherrschenden lokalen Bedingungen, sondern verursachte weiter eine Änderung des Weltklimas durch die Entstehung des asiatischen Monsunklimas. Deshalb sind Daten aus diesem Gebiet notwendig, um deren Entstehung und den Einfluss besser zu verstehen.
Besonders Palynologen versuchten die vergangene Vegetation zu rekonstruieren, beschränkten ihre Arbeit aber meist nur auf das Lichtmikroskop.

Für diese Untersuchung wurden Proben aus der Lukundol Formation des Kathmandu Beckens analysiert, jedoch sowohl im Lichtmikroskop als auch mit dem

Rasterelektronenmikroskop, um einen detaillierteren Eindruck zu bekommen. 78 Taxa wurden bearbeitet, wobei es sich um 25 Sporen von Farnen und Moosen handelte, 7 verschiedene Gymnospermen, 45 Angiospermen und eine Süßwasser-Zyste.
Es wird ersichtlich, dass einige Taxa, welche häufig in der Vergesellschaftung fehlen, hier auftreten und durch den Einsatz des Rasterelektronenmikroskops leicht identifiziert werden können. Weiter, wurden Arten einer Gattung dokumentiert, die sich im Lichtmikroskop so stark ähneln, dass sie nicht unterschieden werden können (z.B. Composites, Euphorbiaceae). Besonders wichtig ist die Identifikation auf Artniveau bei den weit verbreiteten Arten des Kathmandu Beckens, wie *Quercus* oder *Pinus*, da diese bei der Interpretation des Paläoumwelt von entscheidender Bedeutung sind.

# Introduction

Nepal, as we know it today, is mainly characterized by the high mountains of the Himalaya.
These are the result of the collision between the Indian continent with the Eurasian plate in the Paleogene (60-55 Ma), when the raising of the mountains set in.
The northward drift of India began in the Mesozoic, caused the closure of the remaining Tethys ocean in the Cretaceous/Paleogene and the rise of the Himalaya during the Neogene. The Tethys was replaced by a terrestrial environment, which did not only change the local situation, but influenced the global climate by emergence of the Asian Monsoon Climate.

By now, this orogeny is not fully understood. Scientists have multiple theories about the evaluation rate as well as about how in detail these huge mountains arose. This aberrancy is often caused by the different source of data they used, such as fossil floras or studies of the sediment.
Recent studies suggest that the southern Tibet may have reached its present evaluation by 15 Ma (Spicer et al., 2003.).
For sure is, that towards the end of the Cenozoic, the mountains reached a high enough elevation to alter wind circulation pattern and to create the current monsoon pattern (West, 1996).

Important information about the rising of the Himalaya was received from the Ocean drilling of deep sea sediments of the Arabian Sea. These supported the theory, that the Himalayan and Tibetan plateau reached an altitude high enough to lead to the Indian summer monsoon about 10 Ma. At about 8 Ma, this system got more intense (e.g. Kroon et al., 1991; Prell and Kutzbach, 1992; Rea, 1992).
This data get support from the Ocean Drilling in the Bengal Deep Sea Fan. Furthermore they indicate acceleration in the uplift of the Higher Himalaya between 11 and 10 Ma and after 9 Ma (Amano and Taira, 1992; France-Lanord and Derry, 1994; Derry and France-Lanord, 1996).

It is well documented, that at about 8 Ma ago, the environment of the Punjab of India and the Potwar Plateau of Pakistan were becoming drier. This is linked with the important event of the dramatic expansion of $C_4$ grasses, which happened between 8 and 6 Ma. The typically monsoon weather with dry winters and a high summer precipitation is more

suitable for $C_4$ plants than for $C_3$. (Cole and Monger, 1994; Cerling et al., 1997) The $C_4$ cycle is more energy-consuming, but has a more effective utilization of the $CO_2$. Therefore these grasses need less water, thus they are better adapted to a dry climate.
This is reflected in the nature of the grasses, understood from their pollen, as well as the rapid evolution of xeric rodents and the general reduction in the abundance of irregular occurring aquatic fish, turtles, crocodiles and snakes (Siwalik fauna).

First studies in the Himalaya were all based on India, while Nepal was left aside till the second part of the 20th century in the case of geology and paleontology. Then scientist finally tried to describe the major geology and the tectonics in this area, which are yet still not fully understood.
It was obvious, that some parts of Nepal are more suitable for doing paleontology, such as the Siwaliks, which can be easily correlated with localities in India. But also of great interest was put into the Kathmandu Basin, an intramontaine basin in the middle of the Lesser Himalaya between the Mahabharat Mountains in the south and the Shivapuri Mountains in the north.

Hagen (1968, 1986) mentioned that the elevation of Mahabharat range at the south of the Kathmandu Valley is very important for the regional meteorology and climate in the Himalaya. It is well known, that basin fill sediments preserve a very good record for paleoclimatic investigations due of their normally high sedimentation rate.

With more than 600 m thick sedimentation overlying the basal conglomerate and its position at the at the south of the slopes of the Greater Himalaya, the Kathmandu Valley is very suitable for paleoclimatic investigation, because the area is directly influenced by the monsoon climate.

Next to trying to interpret the climate in this area, the idea of the connection between the Himalaya orogeny and a change in the global climate, today known as the Late Cenozoic Cooling, was already published in the year 1899 b T.C. Chamberlin, who wrote about the effect of chemical weathering in connection with the atmospheric $CO_2$ concentration. In the 80ies, this concept was taken to modern science by studying the role of tectonic movement in controlling the world climate.
The basic idea is that an increase of chemical weathering causes a drawdown of atmospheric greenhouse gas carbon dioxide, leading to a decrease in temperature. Fact is that the Cenozoic temperature is more or less well documented by isotopes of organisms in the deep ocean sediments. The ratio of $^{18}O/^{16}O$ gives information about the ice sheet volume (ice contains a higher amount of the lighter $^{16}O$, which leads to more $^{18}O$ in the

ocean water) and the ocean temperature. Oxygen isotopes from the past 55 Ma show a long-time increase with several fluctuations, especially in the Oligocene, when the Antarctic ice shield grew intensively, and in the middle Miocene and Late Pliocene. Raymo and Ruddiman (1992) proposed that the uplift of the Tibetian plateau is the main driving force behind the Cenozoic climate change. Mountain elevation occurred more often in the Miocene, including the Alps, East Africa and parts of the Cordillera of North and South America (Ruddiman et al., 1989), but their location and size cannot be compared with the one of the Himalaya.
The direct connection between the atmospheric temperature and the $CO_2$ concentration was analyzed in detail in the 140 000-year Vostock ice core record for the last glacial – interglacial cycle, but also during the whole Phanerozoic. For the long-time carbon cycle, the balance between the chemical weathering, which reduces the $CO_2$ concentration in the atmosphere and the volcanic input from the Earth's interior as well as $CO_2$ from sea floor spreading, is of great importance.

Further information about the climate can be received by working on the fossils of this area. Especially palynological investigations are very suitable for these climate studies, because easily many samples can be studied showing changes over the time span.

But for this investigation, the main focus lay on further taxononomical analyses. Until now, not many scientists have studied their Nepalese pollen samples with the light microscope and the scanning electron microscope, which is necessary to get more detailed information, and therefore for a better interpretation. Exceptions are Paudayal (2002 and 2004), who specialized on comparing recent material with samples from the Pleistocene of the Kathmandu Basin, and Nakagawa et al. (1996), who did interesting research in the common taxa *Quercus* and *Pinus*. These groups are highly abundant in this area, covering a wide range of altitude, but especially *Quercus* cannot be distinguished with the light microscope only.
Another aim was to compare the assemblage of this sample with previous work from Yoshida and Igarashi (1894), Fujii and Sakai (2002) and Goddu (2004) as well as with the pollen grains found by Paudayal (2004).
All present taxa should in the end be analyzed in relation to paleoclimate, paloecology and paleovegetation as well as possible.

# Geology of Nepal

The mountains of Nepal are part of the Himalaya, which orogenesis started back in 60-55 Ma, shortly after the collusion between the Indian continent and the Asian landmass (Bossart and Ottinger, 1989).The uplift is well documented from the late Eocene on, especially also by the sediments in the Himalayan foreland and the Bengal and Indus fan systems (Cochran, 1990; Bookfield, 1993; Burback et al., 1993; France-Lenord et al., 1933). The northward drift of India still continues, thus the mountains are still raising and changing.
This active zones result into several thrusts and folds.
Scientists have published different classification of the geology of Nepal.
Upreti (1999) distinguished five major tectonic zones of Nepal, changing for approximately from south to north, as described following.

## Major Tectonic Zones of Nepal

The Terai Zones represents the southernmost tectonic division of Nepal. It is part of the Indo-Gangetic Plain ranging from the Indian Shield in the south to Main Frontal Thrust (MFT) in the north.
It represents alluvial deposits from Pleistocene to recent with an average thickness of 1500 m, which lie on the Churia Group (Middle Miocene to Pliocene).
The sediment, which is exposed in outcrops along the southern front of Churia Range, is mostly comprised of boulders and gravel, but also of finer sediments (clay and silt) which can be found farther in the south.
This zone already shows significant sighs of the development of thrusts, especially in the northern part, consequential, in the future an elevation will happen here as well.

The Churia Zone, equivalent to Siwalik and also often named the Sub-Himalaya, forms a big foreland basin consisting of Neogene to Quaternary fluvial sediments extending from the east the west. These are the southernmost hills of Nepal.
This group lies between two big thrusts, the Main Boundary Thrust in the north and the Main Frontal Thrust in the south. Due to the folding of the mountains of the Lesser Himalaya, a lot of Churia sediments are today covered by this zone.
It is equivalent to the three folded Siwalik zone in the Potwar region of Pakistan and the western Indian Himalaya. But unlike these sediments, the Nepalese are rare on vertebrate

fossils (Siwalik fauna), therefore the correlation is difficult. Still, as in Pakistan, the formation can also be divided into a lower, middle and upper part based on lithology.
The sediment is normally comprised of sandstones, sandstones with feldspars and quartz, mudstone or clay, in which often plant fossils can be found and locally freshwater mollusks occur. The vertebrate assemblage includes pisces, reptilia and mammalia (comparable to the typical Siwalik fauna of India and Pakistan).
The whole sequence represents a coarsening-upwards, which reflect the rising of the Himalayan mountains (Gansser, 1964).

The Lesser Himalaya Zone, also named Lower Himalaya or the Midlands, is located between the Main Boundary Thrust (MBT) in the south and the Main Central Thrust (MCT) in the north. This group takes up a large part of Nepal, but is clearer exposed in western Nepal. It consists of non-metamorphosed to low-grade metamorphic rocks, but it is normally unfossilerous.
Two groups are separated by an unconformity, the Great Lesser Himalayan Unconformity. The older part ranges from Paleoproterozoic to Precambrian age (approximately 1800-2000 Ma up to 570 Ma), the younger are marine Gondwana sediments from Perm/Carboniferous to Eocene age. In the south, the Precambrian rocks thrust the Churai Group along the MBT. Additionally several crystalline nappes can be distinguished in this zone.
Because of the lack of fossils and the complicated structure of the whole zone, stratigraphy and correlation is rather difficult; therefore no equivalent is defined somewhere else in the Himalaya.
From the east to the west the tectonics of the Lesser Himalaya are very diverse. In the east, a big thrust sheet covers nearly the whole area, similar to the center part, where the Kathmandu nappe occupies to a great extant. The western part is mostly limited due to the cover of the Higher Himalaya sediments.

The Higher Himalayan Zone was first described as the Central Crystalline zone of the Kumaon Himalaya (Heim and Gansser, 1939), which lies above and at the north of the MCT and below the fossiliferous Tibetan-Tethys Zone.
Also this zone extents from the east to the west throughout Nepal.
The sediment forms up to almost 10 km thickness of crystalline rocks, commonly called the Himal Group, comprised of mostly gneiss, schists and migmatites. These define the highest peaks of the Himalayan Mountains, e.g. Everest, Manaslu, Annapurna, Dhaulagiri and Kanjiroba.
There were different opinions about the Kathmandu- Langtang section. Some scientists define the border of the Higher Himalayan Zone at the south of Kathmandu with the MCT reaching very close to the MBT. Newer maps instead locate the MCT at the north of

Kathmandu valley, which makes these rocks a separated tectonic unit.
The north of the zone is marked by the North Himalayan Normal Fault (NHNF), also know as the South Tibetian Detachment System (STDS).

The crystalline part of this zone was mostly studied along the gorges, that were cut deep into by the major rivers, which expose the up to 12 km thick rocks as well as thick section of the overlying Thetyan zone in some parts. Thus the best known areas of the High Himalaya are along the rivers Upper Karnali, Kali Gandaki, Modi, Marshyangdi, Burhi Gandaki and Trisuli.

The Tibetan-Tehtys zone is the most northern tectonic zone of the Himalaya. These rocks are sedimentary rocks known as the Tethyan Sedimentary Series (TSS), but close to the Higher Himalayan zone, metamorphism can occur. Mostly shale, limestone and sandstone can be found.
This zone lies between the South Tibetian Detachment Fault System (STDFS) and the Indus-Tsangpo Suture Zone (ITS) and is known for fossils dated from Cambrian to Late Cretaceous. These rocks show a nearly continuous series from lower Paleozoic up to lower Paleogene with marine sedimentary succession. They are considered to be deposited as a part of the Indian passive continental margin (Liu and Einsele, 1994).
In Nepal this area is only limited to a small area in the west, located around Annapurna-Dhalagiri and the Dolpa regions.

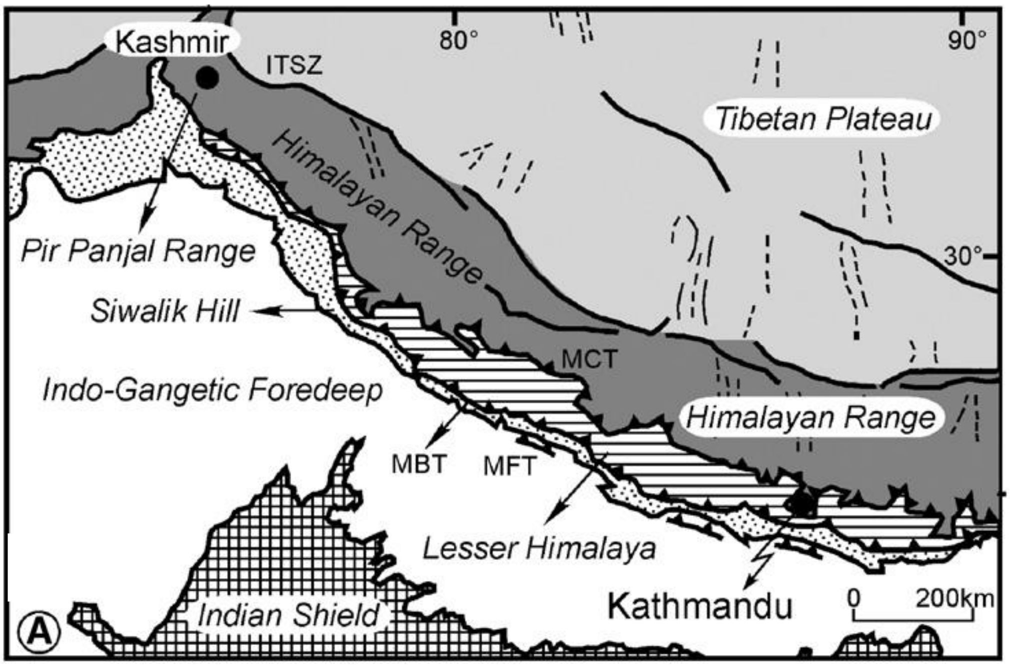


**Fig.1. after Sakai et al., 2006.**
**The main tectonostratigraphic units of the Himalaya.**

## Tectonics

As mentioned before, the Himalaya tectonics are controlled by three major thrusts; the Main Central Thrust (MCT), the Main Boundary Thrust (MBT) and the Main Frontal Thrust (MFT). These thrusts come all together on one surface named the Main Himalayan Thrust (Upreti, 1999).

The MCT is the oldest one and was the first that broke the Indian crust, thus it was first described my Indian scientist. Because the oldest rocks overlying belong to the Dumnri Formation, late Eocene (Sakai et al., 1999), it is thought to be the actual age. Confusing are the metamorphic rocks in this Formation (26 to 17 Ma), which are described as crystalline rocks from the Higher Himalayan Zone.
Hagen (1969) was the first, who worked on the geology of Nepal, but he did not name any thrust similar to the MCT.

But locating the MCT is essential, because it separates the Lesser and the Higher Himalaya, a zone a low metamorphosed zone from one with high grade metamorphism. Years later this was published by some French researchers (Bordet, 1961; Bordet et al., 1972; Le Fort 1975a,b; Pêcher, 1975,1977), who characterized it as a thick ductile shear zone (MCT zone).
But Japanese scientists (Hashimoto et a., 1973) published that the MCT is divided into two parts in Nepal (MCT 1 as the lower MCT and MCT 2, the upper MCT). MCT 1 is known from India, but MCT 2 is the one, the French thought to be the Nepalese MCT.
In western Nepal, this two-parted MCT thrust can be recognized as well, published by Frank and Fuchs (1970).
The MCT is of great importance because it is defined as the base of the Tibetan Slab, which is a distinctive tectonic unit of the Higher Himalaya.

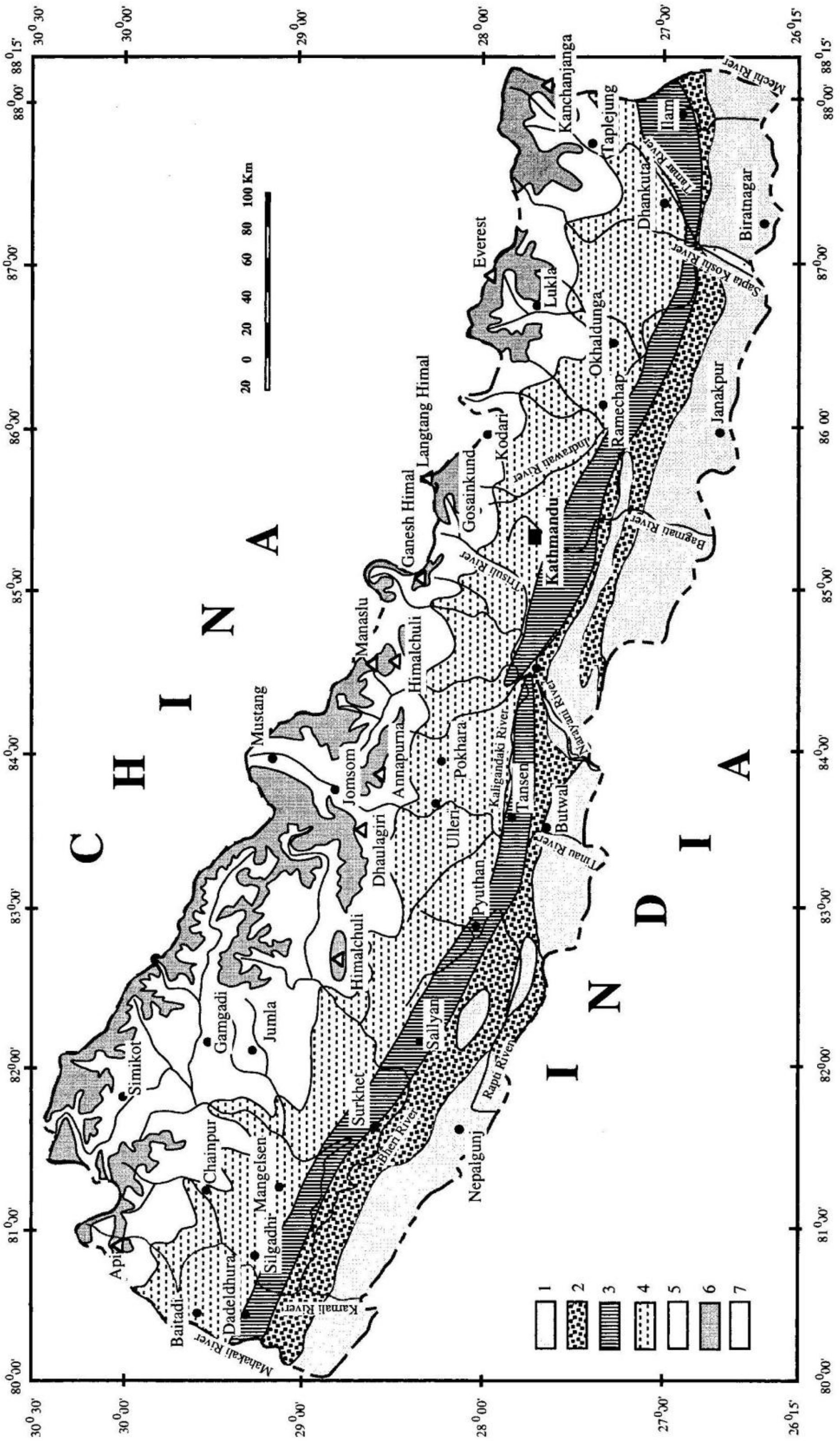


**Fig.2. after Upreti, 1999.**

**Physiographic subdivisions of Nepal. 1: Terai (Northern Gangetic Plain) and Dune Valleys (100-200 m) 2: Churia Range (Siwalik equivalent) (200-700m) 3: Mahabharat Range (1000-2500 m) 4: Lesser Himalaya (Midlands) (300-2000 m) 5: Fore Himalaya (200-4500 m) 6: Higher Himalaya (>4000 m) 7: Inner Valleys (2500-4000 m).**

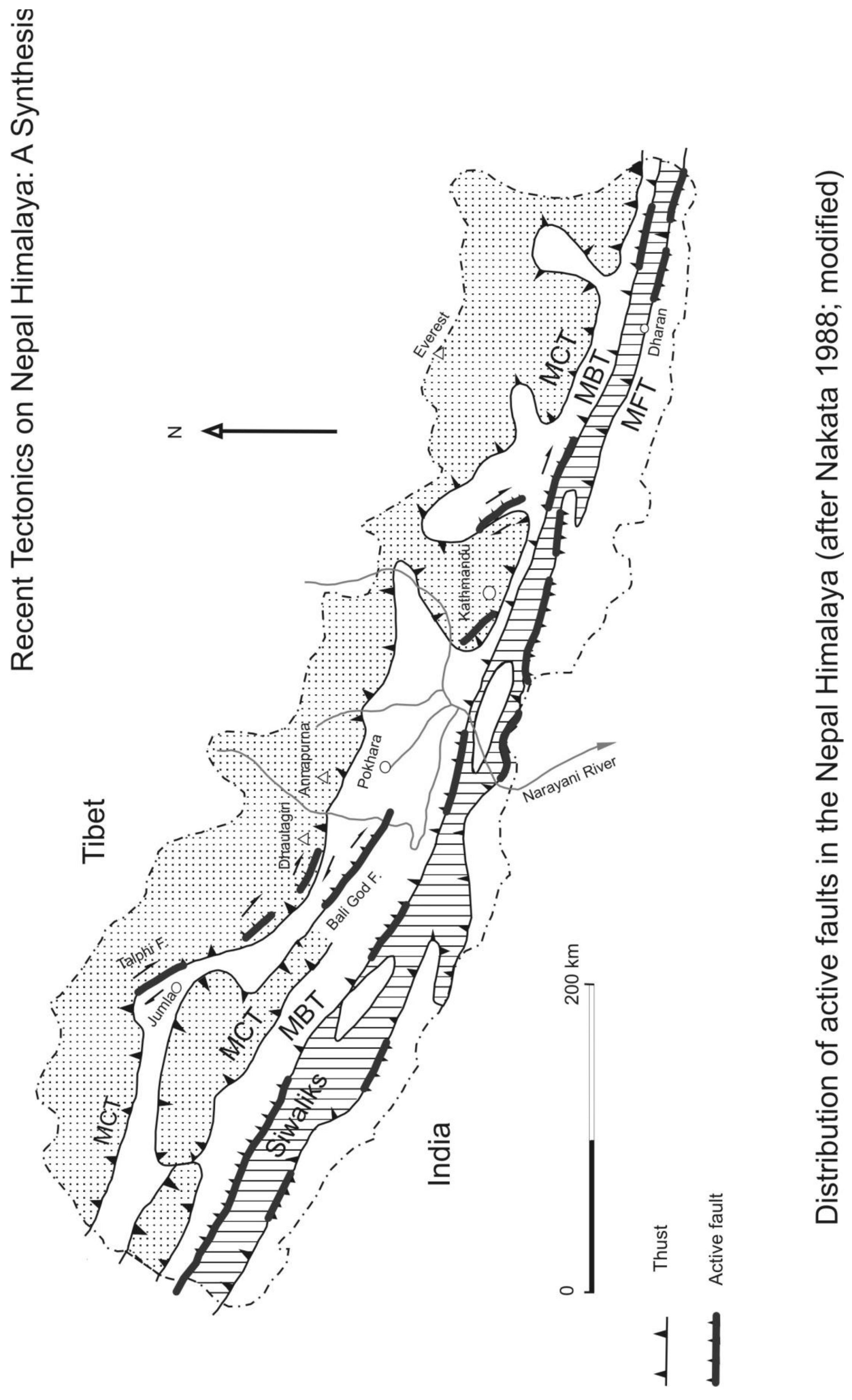


**Fig.3. after Nakata, 1988; modified.**

# The Kathmandu Basin and the Paleo-Lake Kathmandu

The Kathmandu Basin is an intramontaine basin located within the Lesser Himalaya. After the Kashmir Valley in India, it is the second biggest basin system in the whole Himalayan Mountains and the biggest n Nepal. With a diameter of 30 km in the east-west and of 25 km north-south direction it has a more or less circular outline covering an area of about 650 $km^2$. The average elevation today is around 1340 m.

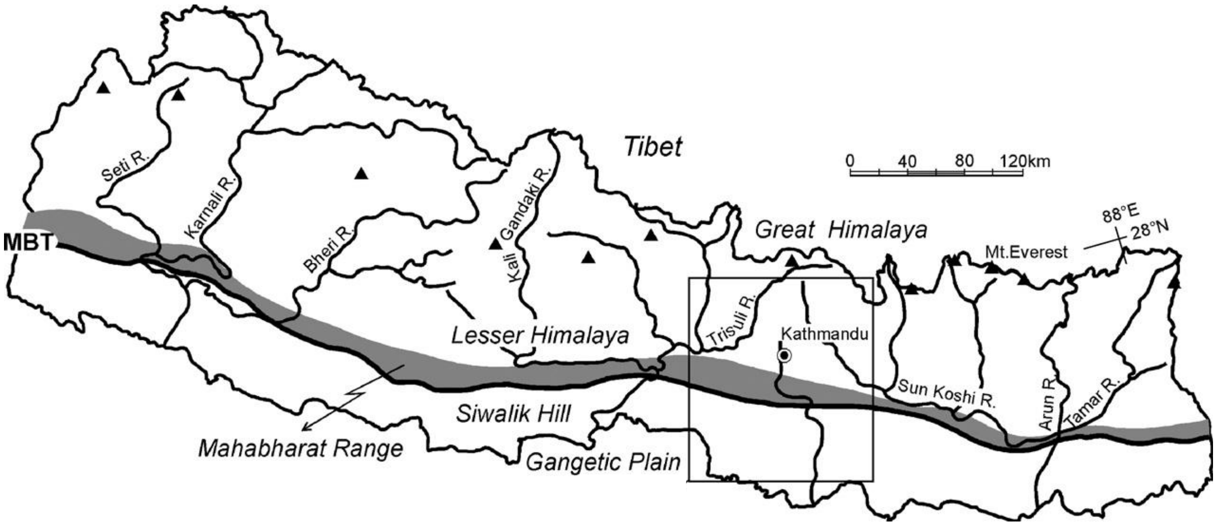


**Fig.4. after Sakai et al., 2006.**
**Drainage pattern of the Himalayan rivers and distribution of the frontal range of the Himalaya, called Mahabharat Range in Nepal (shaded). The rivers flowing along the transverse valley from the north to the south change their direction to eastwards or westwards along the longitudinal valley, because of the recent uplift of the Mahabharat Range.**

With its location on the southern slopes of the Himalaya, the alley is surrounded by the Mahabharat Mountains (2000 to 2800 m above sea level) in the south and the Shivapuri Mountains in the north.
The Shivapuri slope in the north is mostly comprised of gneiss and granite, unlike the northwestern part, where Paleozoic Tethyan rocks of the Phulchauki Group are outcropping, which nearly surround the rest of the basin.

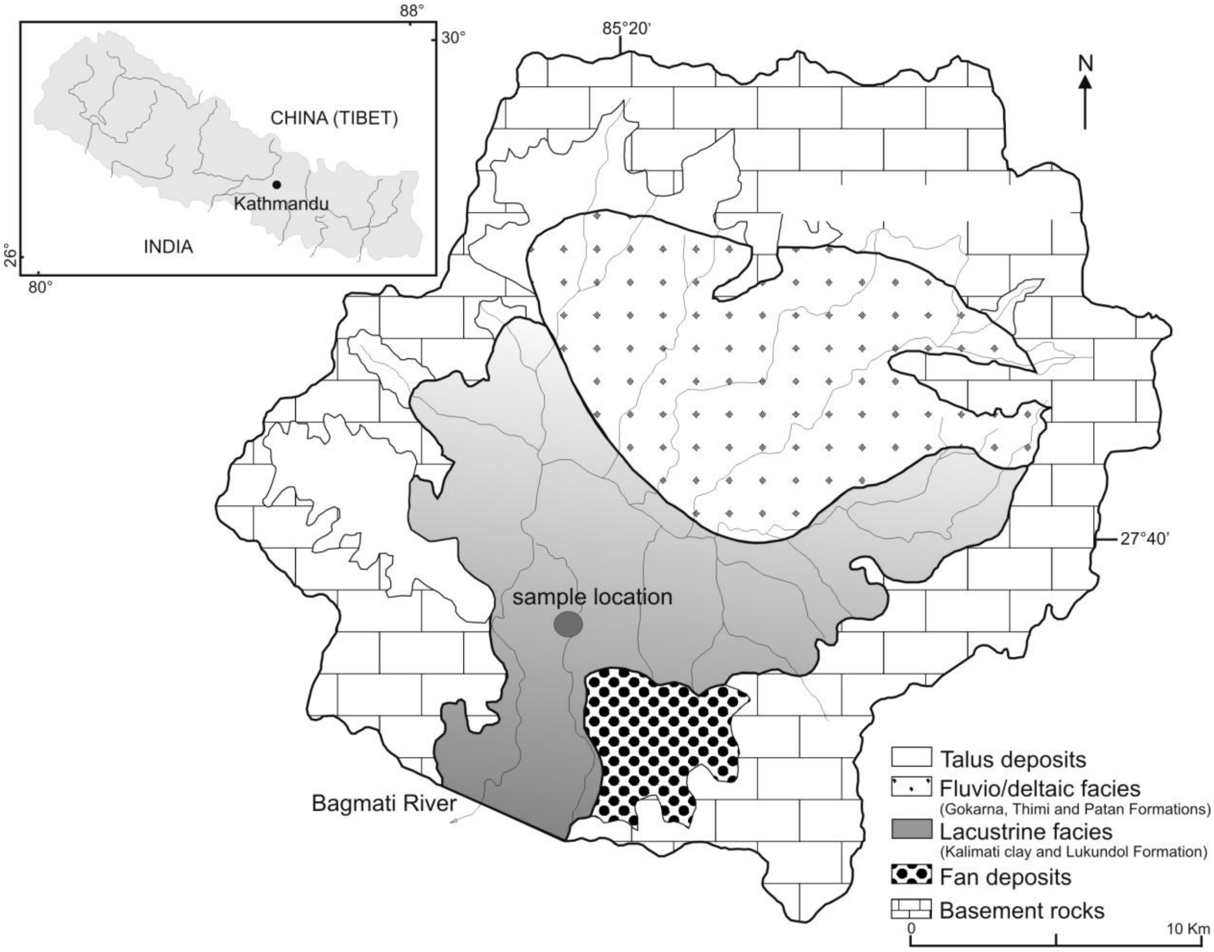


**Fig.5. after Paudayal (personal communication).**
**The sedimentary deposition of the Kathmandu Valley the sample location.**

## Paleo-Lake Kathmandu

The Kathmandu Valley is filled with unconsolidated clay, silt, sand and gravels from Upper Pliocene to Quaternary age (Yoshida and Gautam, 1988; Fort and Gupta, 1981), which overly consistent the Precambrian Bhimphedi group and the early Paleozoic Phulchoki Group (Stöcklin and Bhattarai, 1981).
The sediment can be divided into three facies types, an open-lacustrine facies in the central part of the basin, mainly marginal fluvio-deltaic facies in the north and an alluvial fan facies in the southern part. All these originate from a lake, which once filled the basin, therefore it is called the Paleo-Lake Kathmandu.
Gravity measurements showed a maximum thickness of about 650 m in the basin (Moribayashi and Maruo, 1980).

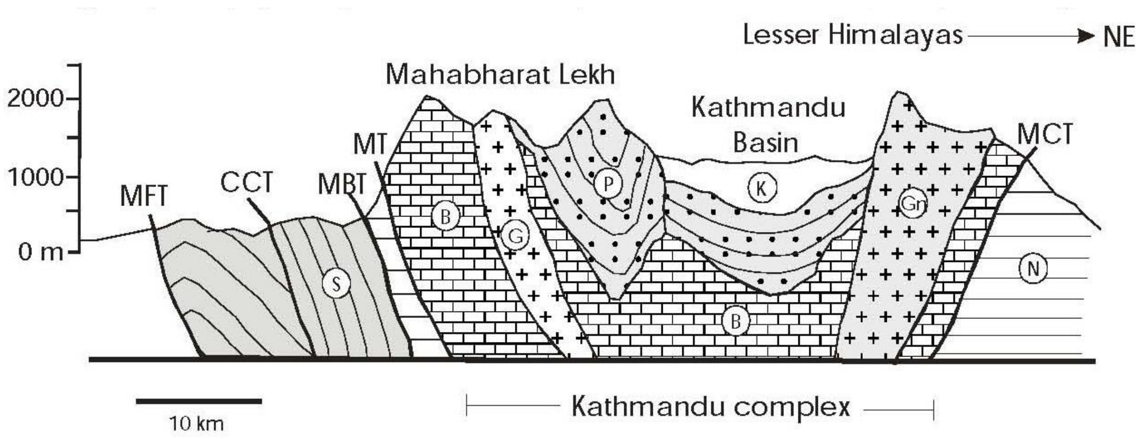


**Fig.6. after Upreti, 1999.**
**A schematic geological cross section in the Central Nepal Himalayas (modified after Stöcklin and Bhattarai, 1981).**
**S: Shivalik group, B: Bhimphedi group, P: Phulcauki group, N: Nawakot complexes, G: Granite, Gn: Gneiss complex, K: Kathmandu complex, MFT: Main Frontal Thrust, CCT: Central Churia Thrust, MBT: Main Boundary Thrust, MT: Mahabharat Thrust (Main Central Thrust: MCT).**

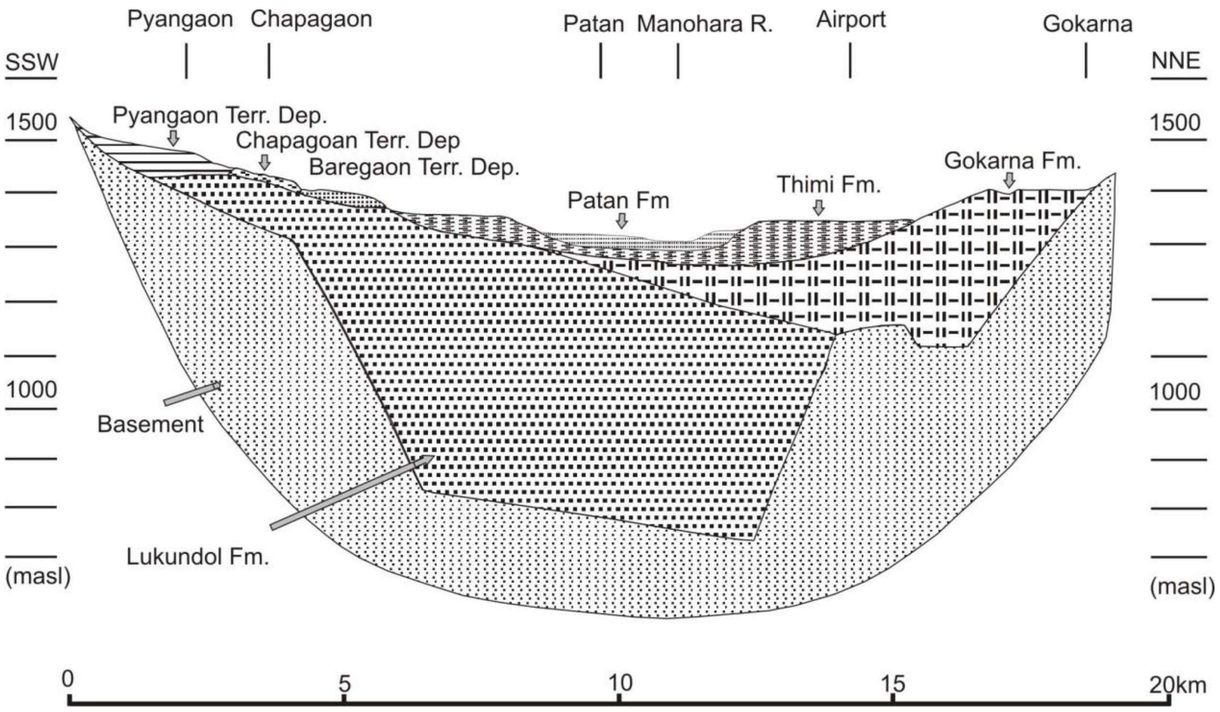


**Fig.7. after Yoshida and Igarashi, 1984; modified.**
**Schematic geological section of the Kathmandu Valley. The topography of the basement is after Moribayashi and Maruo (1980).**

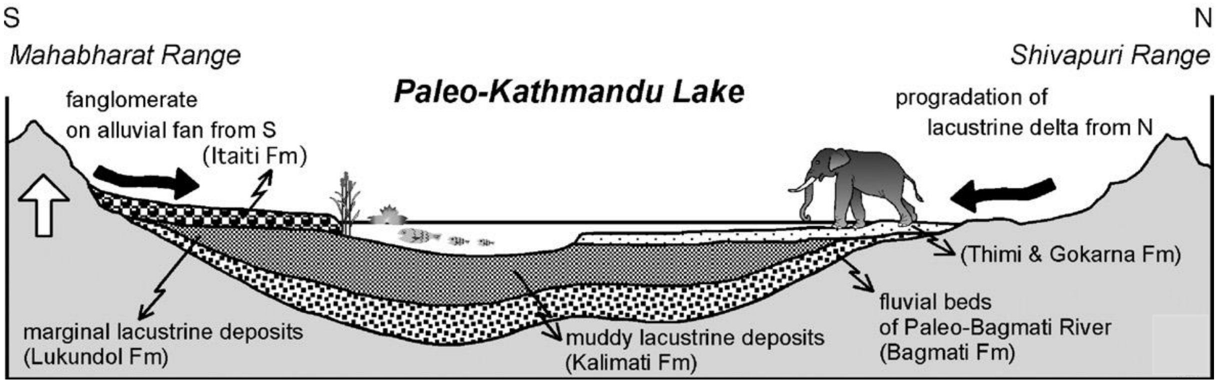


**Fig.8. after Sakai et al., 2006.**
**A schematic cross section showing the stratigraphic framework and depositional environments of the basin fill sediments in the Kathmandu Valley (modified from Sakai et al, 2002).**

Also the drainage system in the valley is of great importance, because the river drainage pattern and therefore the sedimentation has been disturbed by the uplift of the Mahabharat Range.
The rivers normally flow southwards from the Tibetan Plateau and the Great Himalaya, but due to the Mahabharat Mountains, the flow direction changes to the east or west. After passing these mountains, the rivers alter again to the south and finally drain in the Gangetic Plain. These changes in the basin Group are also an evidence for the uplift (Sakai et al., 2006).
Due to the rise, the mountains dammed the river water in the basin at their northern part, leading to the formation of the Paleo-Lake Kathmandu.
The main drainage system today is the Bagmati River, which leaves to the gangetic delta in the south. One of his main tributaries is the Nakhu Khola, the river that allowed us to collect these samples by exposing surface outcrops of the Lukundol Formation.

The dominating sediments from Paleo-Lake Kathmandu (Fujii and Sakai, 2001) are divided into three different facies, starting with the Kalimati clay as open-lacustrine conditions. Within the clay, also several layers of lignite are interbedded (Natori et al., 1980; Katel et al., 1996).
But at about 1 Ma, the deposition system in the valley chanced, which led to the deposition of a four meter thick fossiliferous sandbed in the otherwise monotonous mud-predominant sequence (Sakai et al., 2002). This change in the environment does not only occur on the margin of the lake, but can also be found almost in the center of the Kathmandu basin.
There fossil shells of bivalves, opercula of gastropods as well as fish teeth are described. The large extent of this sandbed (it covers an area of 320 m$^2$) suggests, that this change

indicates a decrease in the lake level due to a conversion of the paleocurrent from south to north because of the rise of the Mahabharat Mountains.

Above the sand bed, silty mud was deposited representing shallow lacustrine facies. In there the green algae *Pediastrum* has a high abundance, which is a typical sign for shallow water conditions.

However, the junction between this could not be described due to too coarse sampling. Basically, there are two possible explanations for the decrease in the lake level. One is climatic, but pollen spectra do not show a significant shift to a dryer climate. The other one is tectonic, which means, that due to further change in the rise of the Mahabharat Lekh the drainage system conducted more water out of the basin.

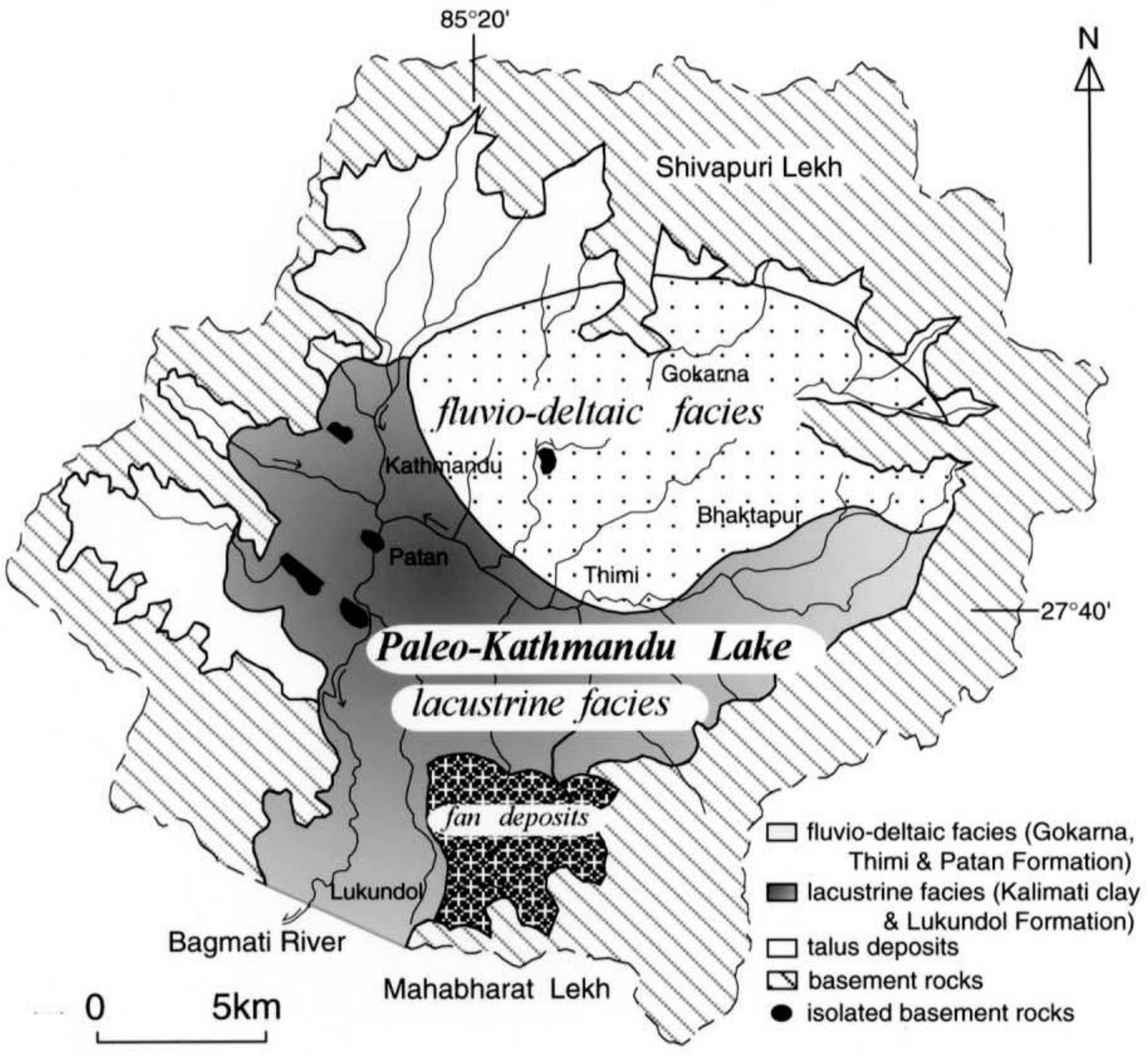


**Fig.9. after Fujii and Sakai, 2002.**
**A sedimentary facies map showing the distribution of interpreted lacustrine and alluvial depositional environments of the Paleo-Lake Kathmandu during the late Pleisocene.**

## The Lukundol Formation

The Lukundol Formation is the oldest part of the basin fills of the Kathmandu Basin, dated due to paleomagnetic studies to a range from Gauss Chron to the early Brunhes Chron (from late Pliocene to early-middle Pleistocene; from 2.9 to 1.5 Ma) (Yoshida and Gautam, 1988; Fort and Gupta, 1981). Hence it is correlated to the Pliocene Karewa Formation in the Kashmir Basin and Siwalik Group (Gupta, 1975; Fort Gupta, 1981; West and Munthe, 1981; Tuladhar, 1982). Newer investigations by Goddu (2004) with magnetic susceptibility along with amino-acid dating suggest an age between ~0.75 – 1.1/1.8 Ma.
This formation is exposed in the south of the Kathmandu Basin, mostly along the Bagmati River, where also the type locality along the river Khahare Khola, can be found.
The main occurring sediments are consolidated clay, silt and sand beds with lignite layers. The clay and silt beds are sometime carbonaceous; therefore they often bear plant fossils.

At the bottom of the formation the sedimentary facies is a marginal lacustrine, rich in coarse gravel and sand deposited by a braided river of the Paleo-Bagmati River containing boulder and muddy swamp elements (Sakai et al., 2002). These are meta-sediments coming from the Kathmandu complex or the Shivapuri Lekh.
The situation changes to lake margin sediments (fluvio-deltaic and back swamp environment) as the Mahabharat Lekh rose. Based on the shift of the sedimentation area, there occurred also a transfer in the paleocurrent (northeast and the northwest to the southwest and southeast). This change appeared at about 1 Ma at the base of the member V, correlated with the Jaramillo Event at 0.99 Ma (Yoshida and Gautam, 1988), hence the Mahabharat Lekh stated its rapid uplift at that time. Goddu dates this event to 0.9 Ma., where he describes also an iron oxide layer in a silt bed with a thickness of approximately 1 cm. This is linked to dry climate reconstructed by pollen data with high amount of *Artemisa*, Chenopodiaceae and Gramineae. He also investigated the sediment closely following the sand bed deposits, which change quickly back to mud and clay and sequential gravel. An explanation suggests an climatic event or high tectonic stress from the Mahabharat Lekh.

This change in the lake level is additionally documented at another part of the Kathmandu Basin as well (Kartel et al., 1996, Sakai et al., 2002).
The uppermost deposits are gravel and sand dominated originated from braided river and alluvial fans.

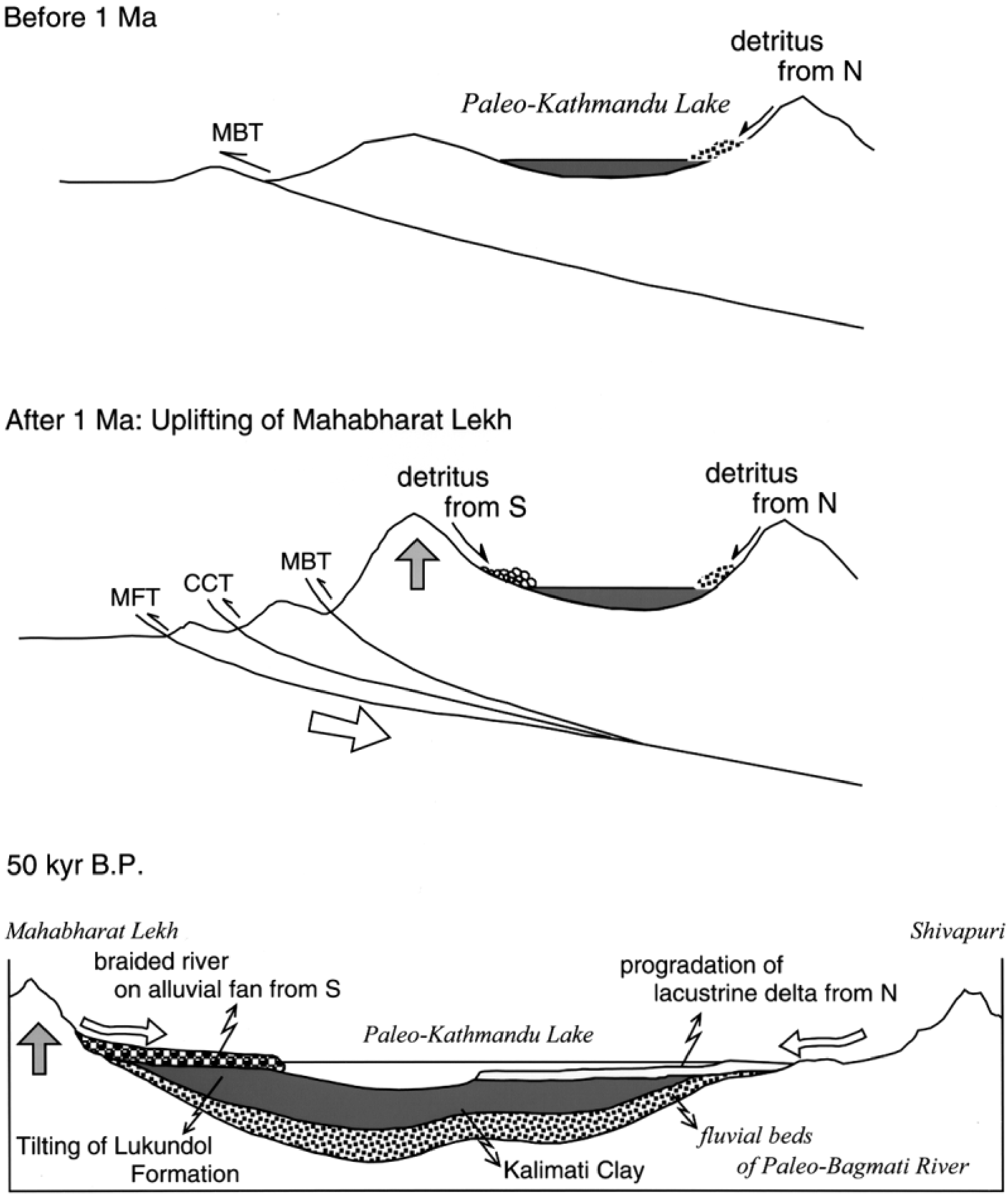


**Fig.10. after Sakai et al., 2002.**
**A schematic model to explain differences of depositional environments of the Paleo-Kathmandu Lake before and after 1 Ma, and their linkage to the uplift of the Mahabharat Lekh by faulting and subsequent intracontinental underthrusting along the Main Boundary Thrust System. Depositional environments of sedimentary bodies in the Kathmandu Basin at around 50 000 years BP is shown in the figure at the bottom.**

Due to the still ongoing uplift of the mountains sediments quickly filled the ancient lake, but also caused migration of the Lukundol sediments further north.

The Lukundol Formation is unconformably overlaid by the Pleistocene formations by the Gokarna Formation (younger lacustrine sediments), the Thimi Formation and finally the Patan Formation (fluvio-deltaic sediments). These deposits well document the ice ages by the changing of coarse and fine sediments.
The lake decreased during this time, forming terrace landforms at the shorelines, where these formations are well exposed in the north of the basin.
The Paleo-Lake Kathmandu had its maximum extension at about 30 000 years BP, when it covered nearly the whole basin, therefore the level reached a depth between 1400 and 1440 m (Fujii and Sakai, 2001; Sakai, Fujii and Kuwahara, 2001, Saijo and Kimura, 2007).

The Lukundol Formation is also known for vertebrate fossils, also known as the Lukundol fauna. A similar fauna was found in Pinjor and Tatrot Formations of the Siwalik Group (Gupta, 1975; West and Munthe, 1981).


**Fig.11. after Goddu, 2004.**
**Fossil leaves from the Lukundol Formation.**

In the Lukundol Formation also macrofossils of plants are known. But until now no publication with detailed information could be found.

| Yoshida and Igarashi (1984) Yoshida and Gautam (1988) | Dongol (1985, 1987) | Shrestha et al (1998) | Sakai (2001) | Sakai (2001) Southern parts | Sakai (2001) Central parts |
|---|---|---|---|---|---|
| Patan Fm | Kalimati clays | Gokarna Fm Takha Fm Kalimati Fm and Chapagaon Fm | | Itaiti Fm | |
| Thimi Fm | | | | | |
| Gokarna Fm | | | | | |
| Borrogaon Terrence deposits | Champi Ithari Gravel | | Lukundol Formation: Upper member | | |
| Chapagaon Terrence deposits | | | | | |
| Pyangaon Terrence deposits | | | | | |
| Lukundol Fm, Members: V | | | | | |
| IV | | | | | |
| III | Nakhu Khola Mudstone and Kaseri-Nayankhandi Lignite | Lukundol Fm and Kobgaon Fm | Middle member | Lukundol Fm | Basal Lignite member |
| II | | | | | |
| I | Tarebhir Basal Gravel | Basal Boulder bed | Lower member | Trebhir Fm | Bagmati Fm |
| | | | | | |

**Fig.12. after Goddu, 2004; modified.**
**Correlation of the Lukundol Formation with the newly proposed stratigraphy (Sakai, 2001) and other workers.**

# Previous work on Pollen of the Kathmandu Basin

## Palynological investigations

Franz and Kral (1975) and Kral and Havinga (1979) were the first, who did palynological investigations on pollen originated from the Kathmandu Valley. But they focused on several samples of the younger sediments of the Paleo-Lake Kathmandu of the Late Glacial Period. Because their assemblage contained temperate trees and herbaceous elements, they interpreted the climate to be more continental than at present. Recognizing the potential of these sediments, further investigations were performed (Kral and Havinga, 1979), which allowed insights into the vegetational succession during the Pleistocene and additionally the first radiocarbon dates.

Scientists from Japan tried to reconstruct paleoclimate of the Kathmandu Valley based on pollen assemblages. At first, discontinuous surface outcrops were investigated (Yoshida and Igarashi, 1984; Igarashi et al., 1988; Nakagawa et al.; 1996).
Yoshida and Igarashi (1984) divided the Lukundol Formation into 5 pollen zones:

| | |
|---|---|
| Luk-1 | Dominance of arboreal trees (*Pinus, Quercus, Castanopsis, Ulmus, Zelkova*<br>Low percentages of *Alnus, Betula, Acer, Carpinus, Juglans, Fraxinus* and *Podocarpus*<br>Little amount of *Picea, Abies and Tsuga*<br>High abundance: herbs, Graminiae, *Artemisia, Trapa.* |
| Luk-2 | Dominance of conifers (*Picea* and *Abies*)<br>Decrease of *Quercus, Castanopsis, Ulmus, Zelkova*<br>Appearance of Graminiae, *Trapa, Sparganium*, Apiaceae, Nymphoides, *Persicaria, Alnus, Tsuga* and *Betula.* |
| Luk-3 | Dominance of *Quercus, Castanopsis, Alnus, Betula*<br>Appearance of *Myrica, Acer, Carpinus, Ulmus, Zelkova, Sapium, Juglans, Ilex*<br>*Pinus* is dominant, but other conifers are not frequently found. |
| Luk-4 | *Pinus* occurs in high percentages<br>Dominance of *Tsuga, Picea, Abies, Podocarpus*, Cupressacae, *Quercus*<br>Less amount of Ericaceae, *Ulmus, Zelkova, Clerodendrum, Alnus, Betula,* |

| | |
|---|---|
| | *Weigela, Ilex*<br>*Pediastrum* can be found. |
| Luk-5 | *Pinus* decreases – *Tsuga* and *Alnus* increase instead<br>High abundance of *Quercus*<br>Appearance of *Juglans, Carya, Corylus, Acer, Murus, Styrax, Lonicera,* Araliaceae, *Eleagnus*. |

Compared to the recent flora (Schweinfurth, 1957), Yoshida and Igarashi, described the Luk-1 and Luk-3 as a "tropical evergreen lower montane forest" and Luk-4 and 5 as a "tropical evergreen upper montane forest".
Luk-2 is situated in between, characterized by an assemblage named as "tropical evergreen upper montane forest, lower belt".
They relate this to the climatic situation, which may have been relatively mild and/or warmer and moister than present, containing also a distinctive cold spell.
But in the upper deposits, the climate changed to one comparable to recent, but becoming drier at the top of the formation.

Fujii and Sakai (2002) instead laid their focus on the interpretation of the Himalayan uplift as well as the reconstruction of the rising of the monsoon. Therefore they needed a continuous sequence, which can be most likely found in clay ("Kalimati" clay = black clay), thus they worked on a 284 m-long-drilled-core beneath Kathmandu city.
They reported a dominance of *Quercus*, which can appear with more than 50% of the whole aboreal pollen sum. Also high abundant are *Pinus* and *Alnus* (5-20%), followed by *Castanopsis* (5-10%). The most common herbs are Graminiae with a frequency of 5 to 20%. The whole assemblage was divided into three zones:

| | |
|---|---|
| Zone I<br>(older than 2.58 Ma) | Common occurrence of *Tsuga*; high frequency of *Pinus* and *Betula* (compared to zone II). |
| Zone II<br>(warmer period, about 2.1 to 1.1 Ma) | High abundance of spores and *Castanopsis*. Coniferous pollen (*Pinus, Abies, Tsuga*) are extremely rare. In some samples *Cyclobalanopsis* appears with 40-50%. |
| Zone III | Antiparallel cyclic change in the appearance of *Pinus* and *Quercus* and |

| | |
|---|---|
| (between 0.8 and 1 Ma) | *Cyclobalanopis* – while one is dominant, the other is very rare.<br>low frequency of *Picea, Abies* and *Tsuga.*<br>Dominant peaks of *Betula* and Graminae in some samples. *Artemisa* and Chenopodiaceae increase in the upper part.<br>*Pediastrum* occurs in this zone and gets more important though the whole sequence. |

Zone I is the only one, that could contain samples from the Lukundol Formation. This suggestion is based on a correlation of the paleoclimatic data and the cores lithology. This period is characterized by a dominance of cold climate taxa and shows only little fluctuations in the pollen frequencies.

Goddu (2004), with the help of Igarashi, also did some work on sediments from the Lukundol Formation. The main aim was dating and furthermore to reconstruct the paleoclimate by the palynological assemblage.
Samples were taken from the whole Lukundol section (143, but only 77 contained pollen), and the results were grouped into 14 pollen zones:

| Zone | Pollen assemblage | Reconstructed climate and vegetation |
|---|---|---|
| Zone 14 | High percentage of *Pinus*, *Trapa* and ferns. | Pine forest around open water under moist climate. |
| Zone 13 | Dominance of *Quercus, Pinus* and *Alnus*; high percentage of algae and *Typha*. | Open forest vegetation; open water under moist/cool climate. |
| Zone 12 | Low percentage of arboreal pollen and dominance of ferns. | Expansion of bog under moist climate. |

| | | |
|---|---|---|
| Zone 11 | Dominant *Tsuga, Abies* and *Quercus* together with *Alnus, Juglans* and *Ulmus*. *Trapa* occurs. | Hemlock-fir-oak forest of cool temperate to subalpine under cold/moist climate. |
| Zone 10 | *Quercus, Tsuga, Ilex, Alnus, Juglans* and *Ulmus* have a high abundance, but also ferns. | Oak-hemlock forest under cool/moist climate. |
| Zone 9 | Low occurrence of arboreal pollen except *Pinus, Typha* and ferns are dominant. | Expansion of the bog under moist climate. |
| Zone 8 | *Quercus* and *Pinus* are dominant, but also *Castanopsis*. *Trapa, Botrycoccus* and *Typha* appear. | Oak-pine forest under temperate/moist climate. |
| Zone 7 | Low percentage of arboreal pollen, but high occurrence of ferns and *Persicaria*. | Bog development under moist climate. |
| Zone 6 | High abundance of *Castanopsis, Pinus* and ferns. | Chinquapin forest under warm/moist climate. |
| Zone 5 | *Pinus, Quercus* and *Tsuga* are dominant, herbs and ferns are rare. | Closed pine-oak-hemlock forest under cool/moist climate. |
| Zone 4 | Dominant of non arboreal pollen e.g. *Artemisia*, Gramineae, Chenopodiaceae. | Dry climate. |
| Zone 3 | Dominant of *Quercus, Alnus* and *Pinus* together with *Betula, Picea* and ferns. | Oak-alder-pine forest under cool/moist climate. |

| | | |
|---|---|---|
| Zone 2 | *Pinus* is dominant with *Querus, Tsuga*. Graminiae, *Persicaria* and ferns are predomninant. | Pine forest under cool/moist climate. |
| Zone 1 | *Quercus, Pinus*, Graminea are dominant next to a high percentage of *Castanopsis*. | Oak-pine forest under warm/moist climate. |

Next to pollen they analyzed magnetic susceptibility to support dating. Higher magnetic concentration can be found in colder climate times, but is also a signal for a dryer situation. Except for the periods in zone 6 and 1, the climate is cooler and moister than in the Kathmandu Basin today. This could be due to the influence of the Indian monsoon or tectonics, second seem to be more likely. Their theory says that coarser material from the surrounding mountains was transported into the basin, which destroyed the lake or bog vegetation, which led to the dry steppe-like pollen record in zone 4. Equally this dry period was also recognized by Igarashi et al (1988) and Igarashi (1984).
Their newer magnetostratigraphic investigations dated the Lukundol Formation between ~0.75 to 1.1/1.8 Ma (Goddu, 2004).

Detailed work on the Kathmandu lake sediments was done by Khum N. Paudayal under the support of David K. Ferguson, who collected my samples as well. Paudayal specialized his dissertation at the University Vienna on the pollen from the Pleistocene (Gokarna, Thimi and Patan Formation) comparing the fossil pollen with recent material.
He showed all the occurring pollen and spores with a light microscope picture as well as with a scanning electron microscope picture (Paudayal and Ferguson, 2004), which allowed identification even at the species level.

Another publication, that allows an identification down to species level is by Nakagawa et al. (1996), who compared fossil pollen grains from *Quercus* and *Pinus* from Kathmandu Valley sediments (Gorkarna area) with recent ones of the basis of the scanning electron microscope. These two genera are very important in that area, because they can form large forests. Though the genera are widespread over different altitude, on species level, zoning can be distinguished due to climate (Stainton, 1972, Tabata et al., 1988).
*Pinus roxburghii* is common in warm areas, where *P. wallichiana* lives in a colder

environment. Therefore their abundance can be used as a climatic indicator.
Today, these species do not usually share the same habitat, *P. wallichiana* lives above 2000 m up to 3500 m. Because *P. wallichiana* is dominant in their fossil samples, they estimated a temperature 4 to 13 °C below the recent in the Kathmandu Valley.
Even more information can be concluded from the different species of *Quercus*. *Q. semecarpifolia* is a typical element in cold areas, but for wet and dry conditions. In today's Himalaya the trees are distributed from 2500 to the tree line at 3600 m. Contrasting is *Q. incana*, which is restricted to warmer zones; it does not occur in wet areas, but is not only common in dryer parts as well. The most precise information results from *Q. glauca*, which is limited to warm and wet areas.
Therefore *Q. semecarpifolia* and *Q.incana* are used for temperature reconstruction and *Q. glauca* as an indicator for wet conditions.
In the Gorkarna sediments, *Q. semicarpifolia* has a high abundance, therefore is the second taxa, that points to a colder climate in the Pleistocene.

## Vertebrate fossils from the Lukundol Formation

The first fossils ever described from the Lukundol area were vertebrates; in particular they discovered a mandibel of an elephant *Stegodon ganesa* (Sharma, 1973).
After this West and Munthe (1981) worked on vertebrate assemblages of this formation in the Nakkhu Khola area, which allowed the correlation with the Karewa Formation of the Kashmir and the Pinjor Formation of the Siwaliks (India).
The latest most important Lukundol fauna was collected my Dongol (1985) along the lower reaches along the Bagmati River.
Among these fossils were many proboscideans, e.g. *Hexaprodon sivalensis, Elephas planifrons*, *Elephas* cf. *hysudricus*, but also *Crocodylus* sp., suids (*Potamochoerus palaeindicus, Potamochoerus cf. ehobaldo*), stegodontidae (*Stegodon insignis*), Trionychidae (*Lissmys* sp.) and several bovids and cervids (West et al, 1988; Corvinus, 1988, Sah, 1992).

Also an occurrence of pharyngeal teeth of the cypriniformid fish *Tor* and a jaw and scales of another teleost fish is described (West et al, 1988).

# Recent vegetation of Nepal

Nepal is located at the southern slopes of the Himalaya Mountain Range. It covers an area of 147 181 $km^2$, but its expansion from east to west is much greater than from the north to the south.
83 percent of the country is occupied by high mountains; the rest of 17 percent is the Terai land.

There are many factors that determine vegetation in Nepal.
One of the major aspects is the rainfall, which originates from the summer monsoon.

This forms at the Bay of Bengal and the Arabian Sea and reaches Nepal at June to September. Winter rainfall is only common in the western part. The eastern part is earlier hit by heavy rainfall, so during the whole year, a higher precipitation can be found here. On the other hand, more snowfall is common in the western part, which leads to a lower snow line in the west compared to the east.

Due to the great difference in altitude and climate of whole Nepal, there appears a diverse separation in vegetation zones.

During the last 50 years scientists tried to characterise the vegetation of Nepal while using different methods. Schweinfurth (1957) was one of the first, who described the recent vegetation types of the entire Himalaya, where he divided the Nepalese flora into three distinct zones due to the main drainage system.
Stearn (1960) was convinced, that a better subdivision is made into Western Himalayan flora and Eastern Himalayan flora, with a mix of these two occurring in Central Nepal, without paying any attention to the altitude.

While others published different regions based on the river systems (Banerji, 1963).

Two important publications appeared in the year 1972, where they combined climatic and phytogeographic regions. These are still used today; the one was created by Stainton, the other by Dobremez.

Stainton (1972) divided the vegetation of Nepal into seven climatic and phytogeographic regions:

- Terai and Bharbar
- Foothills
- Mahaharat Range
- Midlands
- Himalaya
- Inner Himalaya
- Arid zone

Within these zones, he further classified 35 forest types, which can be grouped into 10 mayor zones.

The Terai is part of the Gangetic delta, where the land is mostly flat. Therefore it is intensively used for agriculture. But originally a lowland evergreen forest grew in this area. The Bharbar is the belt in the north of Terai, also known as the Siwalik or in Nepalese Chuiya. Water only reaches this area as streams from higher mountains after the monsoon. Further north, the Siwalik or Churiya hills can be found, where are characterised by high cultivation today, that includes the removal of the forest. As consequence a lot of soil erosion problems appeared.
In the Marabharat Range rivers are dominant, e.g. Bagmati, Babai or Rapti, which are flowing from the north to the south. They also form a natural barrier to the midlands and the foothills.
The average altitude of the midlands is about 2000 m. They include high valleys such as the Kathmandu Valley, Pokhara, Trishuli and Banepa.
In the north of the midlands the Himalaya follows, which continuously ranges from the east to the west of Nepal. It is characterized by alpine to subalpine ecological zones. Even the high located parts still plants live till approximately 6000 m, where the nival zones begins.
The Inner Himalaya zone is found in valleys above 3600 m, which are very dry. Therefore high altitude desert flora is present including *Juniperus indica*, *Sophora moorcroftiana* and *Caragana brevispina*.
The arid zone is found in the northern part of the Dhaulagiri and Annapurna Himal, but too high for forest vegetation. The location allows plants similar to Tibet, such as *Lonicera spinosa*, *Hippophae tibetana* and *Cragana geradica*.

In the Kathmandu Valley today two of these can be found, which is the subtropical broad-leaved evergreen forest and the subtropical pine forest. For these taxa such as *Alnus* *nepalensis*, *Castanopsis indica*, *Schima wallichii* and *Pinus roxburghii* can be commonly found.

Dobremez (1972) worked out a more detailed classification. He structured the vegetation into four vegetation belts, western, north-western, central and eastern, but further he published 11 bioclimatic zones, 35 forest types, 75 vegetation types and 118 ecosystems.

The Land Resource Mapping Project (LRMP) finally divided Nepal into five zones correlating approximately with the altitude (HMHN, 1986).

| Region | Altituide | Percents of Nepal |
|---|---|---|
| Terai | Below 500 m | 10.46 |
| Siwaliks | 500-1000 m | 25.78 |
| Midhills | 1000-3000 m | 31.95 |
| High mountains | 3000-5000 m | 29.05 |
| High Himalaya | Above 5000 m | 2.75 |

Within these zones, several types of forest vegetation are recorded:

- Lowland evergreen forest
- Warm temperate evergreen forest
- Cool temperate forest
- Deciduous forest
- Coniferous forest
- Tree line – Rhododendron shrub
- High alpine meadow

Next to the big vegetational zones, the river valleys create their own microclimates, which lead to big changes in the vegetation on a very limited area.

The most common taxa in the Himalaya are oaks (*Quercus*), which are mainly evergreen. There are 35 species, being spread from an evaluation between 800 m and 3800 m. Today, eight of these can be found in Nepal (*Q. floribunda, Q. glauca, Q. lamellose, Q. lanata, Q. leuchotrichophora, Q. mespilifolioides, Q. oxodon, Q. semecarpifolia*).

## Vegetation of the Kathmandu Valley

In the Kathmandu Valley today two types of forests are common.
One can be found at the valley floor, which is today highly reduced by the humans. Only some limited areas are protected, such as Pashupati forest, Gokarna forest, Swayambhu forest and Hattiban forest, where a typical subtropical vegetation can be found. *Quercus glaucana*, *Castanopsis tribuloides*, *Schiima wallichii*, *Acer ablongum*, *Osmanthus fragrans* or *Engelhardia spicata* are elements with a high abundance (Paudayal, 2002)

The other forest type is surrounding the mountains, but is also influenced by the humans. This can be divided into four major parts, which all consist of subtropical temperate vegetation. Only different elements appear in the different directions due to the change of ecological situation.
The first are Schima-Castanopsis forests, that grow together with *Pinus roxburghii* and *Quercus glauca*. Higher above them the vegetations shifts to an oak-laurel forest, where also *Rhododendron arboretum*, *Lyonia ovalifolia, Quercus glauca, Quercus lanada* are common. More important are *Lithocarpus spicata*, *Litsea lancifolia*, Linderanacusua, frequently found together with *Carpinus viinea*, *Symplocos spp.*, *Acer oblongum*, *Querus lamelllosa*.
Only in wetter parts, *Alnus nepalenis* appears.
*Quercus semecarpifolia* grows in the highest parts of this forest, along with *Rhododenron arboretum* or *Lyonia sp*.

## Material and methods

The material for this investigation was collected by Dr. David K. Ferguson and Dr. Khum N. Paudayal during their field trip in the year 1998. The locality is known from leaf fossils near the place called Bungmati (27°37'53.62''N and 85°18'28.29''E, altitude 1336 m amsl) at the left and right bank of Nakkhu Khola, where the Lukundol Formation is exposed approximately 11 m.

The first preparation was done on the sample LL1/LL7. After the sediment was crushed into small pieces and squelched in a mortar, some drops of HCl conc. were added to check, if the sample contains calcareous matter. Because no reaction was visible, directly the second step of the preparation was started to remove the silica with HF. The sediment was put into a copper pan above a Bunsen burner, but before adding the HF we moistened the sample to avoid a heavy reaction. The material had to be boiled between 10 and 15 minutes before it was put into a 4 to 5 liter HF-resistant vessel with water to neutralize the acid.
After waiting about one hour for the sediment to settle down, the liquid was decanted and the sample was put into a glass vessel (600 ml). HCl conc. had to be added before it was again put above the Bunsen burner to boil the sample for another 10 to 15 minutes to avoid fluorspar/fluorite.
Then another hour later the next decantation had to be done before the sample was filled into centrifuge tubes. To neutralize the acid water was added and the tube was turned in the centrifuge (Heraeus Instruments Laforfuge 400) up to 3000 revolutions per minute. This step was repeated approximately 3 times.

Now to follow is acetolysis, which starts with chlorination. In the centrifuge tube, glacial acetic acid is the be added, before the same amount of saturated sodium chlorate was added till the tube is filled three-quarters before you add 4 to 5 drops of concentrated hydrochloric acid. During the whole procedure a glass stab should be in the centrifuge tube.
Each tube shall now be held in boiling water for approximately 5 minutes and sometimes stirred. There the oxidation happens, which can be often recognized in a chance of the color.
Afterwards the centrifuge has to be used another three times washing the sample with water before the water is replaced by glacial acetic acid.
This had to be done because in the next working step, no water particles are allowed to remain in the sample while adding the acetolysis liquid (Erdtman, 1954), which contains

$H_2SO_4$ conc.
The liquid contains nine parts of acetic anhydride and one part $H_2SO_4$ conc. which should be mixed in this order. Acetolyis is performed to color the organic matter (sporopollenin part of all palynomorphs).
After adding the acetolysis liquid, the sample has to be put into boiling water, where it should remain for about 5 to 10 minutes. Often the reaction is visible due to the lightening of the sample in the dark liquid. The samples is then centrifuged and decanted. Afterwards the sediment needs again to be centrifuged with glacial acidic acid, before you have to repeat the same steps of spinning and decanting again with water for approximately 3 times till the shacked sample with water does not show any more bubbles (then the sample is surrounded by water only).

Decanting the last time has to be done very carefully because as much water as possible has to be removed, because the sample is then kept in glycerin.

For the second preparation (sample LL22) I followed the same steps excluding the HF part. Instead of heating the sample with HF up, I put the sample simply into a HF-resistant plastic vessel (1 liter) and waited for 3 days, stirring it every couple of hours (Faegri and Iversen, 1989). The reaction is the same, but without the heat it is much slower.

For the microscope the material in glycerin was put on a slide, but not covered with a cover glass. For light microscopy photography the pollen got transferred to a second slide, using a human short hair clued on a dissecting needle.
All the work on the microscope had been done on a Nikon Eclipse 80i microscope (magnifications 10x, 20x, 40x, 60x).

The most interesting pollen and spore were moved outside the glycerin, where it sticks on the hair. As soon as the pollen touches a small drop of glycerin on a second slide, it departs the hair. This way pictures can be taken without any organic material covering parts of the pollen. A Samsung Digimax V70 digital camera was used to take the light microscopic pictures.
For the SEM the pollen grains were first collected also with the hair on the needle outside the glycerin, before they were put on the stub in a drop of ethanol absolute, which removes the glycerin even from the pollen surface. No special fixing was done (Zetter, 1989 and Zetter and Ferguson, 2002). All work was performed with a Joel JSM 6400 Scanning Microscope owned by the University of Vienna.

For identification the pollen several books were used (Pollen Analysis by Moore, Webb, Collision, 1995; Leitfaden der Pollenbestimmung by Beug, 2004; The Pollen Flora of Yunnan, China by Fujiki, Zhou and Yasuda, 2005; Pollen Flora of NW Himalaya by Gupta,

Sharma and Sahn, 1986), as well as some internet data bases like the palynological database from University Vienna (www.paldat.org) or the palynological homepage of the University of Arizona (http://www.geo.arizona.edu/palynology).
But the biggest support for identifying was Dr. Khum Paudayal's dissertation "Pleistocene Environment of the Kathmandu Valley, Nepal, Himalaya" (2002) and the knowledge of my supervisor Dr. Zetter.

# Taxonomy

## Spores

*Davallia* sp.
size: medium (40 – 50 µm)
shape: oblate; elliptic in equatorial view; elliptic in polar view
aperture type: monolet
exospore: LM: verrucate like structure elements
SEM: verrucate and additionally irregularly scattered granulae.

Davalliaceae gen. indet.
size: medium(42 – 46 µm)
shape: oblate; elliptic in equatorial view; elliptic in polar view
aperture type: monolet
exospore: LM: verrucate like structure elements
SEM: verrucate; the large verrucae form reticulum-like structure, the rugulae are larger at the distal pole, where around the aperture, they get smaller; the surface of the rugulae shows a mircoverrucate suprasculpture.

*Lepisorus* sp.
size: large (29 – 33 x 50 – 58 µm)

shape: oblate; elliptic in the equatorial view; elliptic in polar view
aperture type: monolet
exospore: LM: verrucate like structure elements
SEM: foveolate to perforate; on the surface, granulae are irregularly distributed.

Polypodiaceae gen. indet.1.
size: medium (42 – 48 µm)
shape: oblate; elliptic in equatorial view; elliptic in polar view
aperture type: monolet
exospore: LM: verrucate like structure elements
SEM: verrucate, additionally fossulate.

Polypodiaceae gen. indet.2.
size: medium to large (34 – 37 x 50 – 56 µm)
shape: oblate; elliptic in equatorial view; elliptic in polar view
aperture type: monolet
exospore: LM: verrucate like structure elements
SEM: verrucate with a fossulate and microverrucate surface
It can be best distinguished from Polypodiaceae gen.indet.1 due to bigger and more asymmetric verrucae.

Polypodiaceae gen. indet.3.
size: medium (24 – 26 µm)
shape: oblate; straight obtuse triangular in polar view
aperture type: trilet
exospore: LM: : scabrate to slightly verrucae
SEM: verrucate in the SEM with irregularly scattered granulae.

Pteridaceae gen. indet.
size: medium (37 – 41 µm)
shape: oblate; straight obtuse triangular in the polar view
aperture type: trilet

exospore: LM: psilate in the central area, a random part of verrucae before a broad psilate cingulum

SEM: psilate in the central area, a random part of verrucae before a broad psilate cingulum.

*Pyrrosia* sp.

size: large (60 – 70 μm)

shape: oblate; elliptic in equatorial view; elliptic in polar view

aperture: monolet

exospore: LM: psilate with irregular distributed microverrucae

SEM: psilate with irregular distributed microverrucae.

*Selaginella* sp.

size: medium (23 – 28 μm)

shape: oblate; spheroidal; circular in polar view

aperture type: trilet

exospore: LM: scabrate and pilate

SEM: granulate and roughly fossulate with pilae (on the top granulate as well)

Pilae occur only on the distal side of the spore where the ornamentation is also less distinctive.

*Woodwardia* sp.

size: medium (25 x 32 – 34 μm)

shape: oblate; elliptic

aperture type: monolet

exospore: LM: psilate

SEM: psilate to fossulate.

Spore gen. indet.1.

size: large (65 – 71 μm)

shape: oblate; elliptic in the equatorial view; elliptic in the polar view

aperture type: monolet

exospore: LM: verrucate with baculae and rare clavae
SEM: mircoverrucate and fossulate with baculae and rare clavae.

Spore gen. indet.2.
size: medium (27 – 33 µm)
shape: oblate to spheroidal circular in the polar view
aperture type: trilet
exospore: LM: reticulate-like to gemmate
SEM: spinae-like forked sculpture elements are arranged to a reticulum like sculpturing pattern.

Spore gen. indet.3.
size: medium (22 – 27 µm)
shape: oblate; obtuse triangular
aperture type: trilet
exospore: LM: verrucate
SEM: SEM perforate around the aperture, but granulate close to the cingulum; few pilae on the distal side of the spore.

Spore gen. indet.4.
size: medium (29 – 35 µm)
shape: oblate; obtuse triangular to circular in polar view
aperture type: trilet
exospore: LM: psilate to scabrate; a curva imperfecta can be seen
SEM: psilate with microrugulae around the aperture.

Spore gen. indet.5.
size: small (20 – 23 µm)
shape: oblate; obtuse triangular to circular
aperture type: trilet
exospore: LM: psilate
SEM: psilate.

Spore gen. indet.6.

size: medium (27 – 29 µm)

shape: oblate; circular to obtuse triangular in polar view

aperture type: trilet

exospore: LM: scabrate to rugulate

SEM: shows a reticulum-like sculpture.

Spore gen. indet.7.

size: large (58 – 63 µm)

shape: oblate; elliptic in the equatorial view; elliptic in the polar view

aperture type: monolet

exospore: LM: scabrate

SEM: rugulate and fossulate.

Spore gen. indet.8.

size: medium (38 – 41 µm)

shape: oblate; elliptic in the polar view

aperture type: monolet

exospore: LM: psilate

SEM: fossulate to microrugulate and perforate.

Spore gen. indet.9.

size: medium (27 – 42 µm)

shape: spheroidal to oblate; circular to obtuse triangular in polar view

aperture type: trilet

exospore: LM: echinate

SEM: the echinae are covered leading to an angular scratched looking surface.

Spore gen. indet.10.

size: medium (24 – 30 µm)

shape: oblate; straight obtuse triangular

aperture type: trilet

exospore: LM: scabrate to verrucate

SEM: granulate to fossulate; psilate on the proximal side; around the trilet mark small verrucae appear; distal echinae-like sculpture elements are common.

Spore gen. indet.11.

size: medium (28 – 30 µm)

shape: oblate; straight obtuse triangular

aperture type: trilet

exospore: LM: verrucate

SEM: verrucate and fossulate.

Spore gen. indet.12.

size: small (19 – 24 µm)

shape: oblate; elliptic in equatorial view

aperture type: monolet

exospore: LM: : psilate with few baculae

SEM: granulate with roughly fossulate with baculae.

Spore gen. indet.13.

size: medium (26 – 29 µm)

shape: oblate; straight obtuse triangular

aperture type: trilet

exospores: verrucate in the LM; additionally the granulate to fossulate surface can be seen in the SEM.

Spore gen. indet.14.

size: medium (17 – 20 x 28 – 32 µm)

shape: oblate; elliptic

aperture type: monolet

exospore: LM: baculate to clavate

SEM: sculpturing is characterized by gemmae or clavae.

## Gymnosperms

### Ephedraceae:

*Ephedra cf. intermedia* Schrenk ex C.A. Meyer.
size: medium (39 - 44 x 14 – 17 µm)
shape: oblate; inaperturate
aperture type: polyplicate
aperture number: 6
ornamentation: LM: psilate
SEM: psilate.

### Pinaceae:

*Abies* sp.
size: very large (110 – 115 µm)
shape: bisaccate
aperture type: leptoma
aperture number: 1
ornamentation: LM: corpus is rugulate to verrucate; around the leptoma the ornamentation becomes coarser; the distinguishing feature to the other pinaceae is the strongly thickened cappa
SEM: corpus is rugulate to verrucate; around the leptoma the ornamentation becomes coarser; sacci are perforate.

*Picea* sp.
size: very large (120 – 130 µm)
shape: bisaccate
aperture type: leptoma

aperture number: 1

ornamentation: LM: scabrate; can easily be recognized among the pinaceae because of the low angel between the corpus and the sacci; the sacci seem often to touch each other around the leptoma

SEM: surface of the corpus is rugulate and perforate; the ornamentation is little more coarse between the corpus and the sacci.

*Pinus roxburghii* Sarg.

size: large ( 50 – 60 µm)

shape: bisaccate

aperture type: leptoma

aperture number: 1

ornamentation: LM: scabrate; the sacci show a more acute angel to the corpus

SEM: verrucate on the corpus showing bigger verrucae around the sacci; the sacci itself are granulate and perforate.

*Pinus wallichia* A.B. Jacks.

size: large (60 – 70 µm)

shape: bisaccate

aperture type: leptoma

aperture number: 1

ornamentation: LM: scabrate; the sacci show blunter angel to the corpus

SEM: verrucate on the corpus; the verrucae are next to the sacci; the sacci itself are granulate and perforate.

*Tsuga cf. dumosa* (D. Don) Eichler

size: large (66 – 68 µm)

shape: monosaccate; circular in the polar view; bowl-shaped in the equatorial view

aperture type: leptoma

aperture number: 1

ornamentation: LM: scabrate and echinate

SEM: verrucate or rugulate with irregularly scattered echinae of different size.

### Podocarpaceae:

*Podocarpus* sp.
size: medium (32 µm)
shape: bisaccate
aperture type: leptoma
aperture number: 1
ornamentation: LM: scabrate
SEM: microechinate; microechinae are densely scattered and very small; there is no difference between the ornamentation of the corpus and the sacci.

## Angiosperms

### Aceraceae:

*Acer* sp.
size: small (19 x 25 µm)
shape: prolate; elliptic in equatorial view
aperture type: colpate
aperture number: 3
ornamentation: LM: scabrate to striate
SEM: striate; striae are less than half a µm wide and are irregularly branched and united.

### Apiaceae:

Apiaceae gen. indet.
size: small to medium (10 – 12 x 24 – 27 µm)

shape: prolate; elliptic in the equatorial view; triangular obtuse convex in the polar view
aperture type: colpate
aperture number: 3
ornamentation: LM: psilate; sexine seems to be thicked, especially around the poles
SEM: striate; at the pole area, the striae show another pattern than in the mesocolpium area.

## Arecaceae:

*Palmae* sp.1.
size: small to medium (15 – 19 x 27 – 28 μm)
shape: oblate; elliptic in polar view
aperture type: sulcate
aperture number: 1
ornamentation: LM: psilate to slightly coarse verrucate
SEM: echinate and slightly foveolate; spines are infrequent and sometimes missing due to preservation, they do not have a regular length or shape.

*Palmae* sp.2.
size: medium (14 – 17 x 36 – 42 μm)
shape: oblate; elliptic in polar view
aperture type: sulcate
aperture number: 1
ornamentation: LM: scabrate
SEM: perforate to foveolate with an irregular pattern.

## Asteraceae:

*Artemisia* sp.
size: small (15 – 20 μm)
shape: subprolate; spheroidal in the equatorial view; triangular in the polar view
aperture type: colporate

aperture number: 3

ornamentation: LM: scabrate; sexine is clearly thickened

SEM: microechinate and perforate; bigger echinae with a broad base are surrounded by numerous smaller ones.

Liguliflorae Compositae gen. indet.

size: medium (38 – 40 µm)

shape: spheroidal

aperture type: colporate

aperture number: 3

ornamentation: LM: lophate- echinate

SEM: echinate and perforate; the echinae cover the lophae, but leave our fenestrae, where the surface is visible; perforations are limited to the base of the echinae.

Tubiflorae Compositae gen. indet.1.

size: medium (31 – 33 µm)

shape: spheroidal to slightly oblate

aperture type: colporate

aperture number: 3

ornamentation: LM: echinate; a thick wall can be seen

SEM: echinate and perforate; the perforation is regularly distributed over the whole surface, but gets wider at the base of the echinae.

Tubiflorae Compositae gen. indet.2.

size: small (15 x 16 – 20 µm)

shape: spheroidal to slightly prolate

aperture type: colporate

aperture number: 3

ornamentation: LM: echinate

SEM: echinate; the origin of the echinae is bound together.

Tubiflorae Compositae gen. indet.3.
size: small (18 – 20 x 20 – 21 µm)
shape: spheroidal to subprolate
aperture type: colporate
aperture number: 3
ornamentation: LM: echinate
SEM: echinate and mircoreticulate.

Tubiflorae Compositae gen. indet.4.
size: small to medium (18 – 23 x 25 – 29 µm)
shape: prolate
aperture type: colporate
aperture number: 3
ornamentation: LM: echinate
SEM: echinate and microreticulate; the echinae have, except at the basis, a closed surface.

**Betulaceae:**

*Alnus* sp.
size: small (13 – 17 µm)
shape: oblate; quinquangular obtuse concave
aperture type: porate
aperture number: 4-6
ornamentation: LM: psilate; easy to recognize because of the thickened exine (arcus), that leads from one pore to the next
SEM: microechinate to slightly microrugulate.

*Betula* sp.
size: medium (29 – 33 µm)
shape: oblate; triangular obtuse convex in polar view; elliptic in equatorial view
aperture type: porate
aperture number: 3
ornamentation: LM: psilate; sexine gets clearly thicker around the porus

SEM: microrugulate with microechinae on the top of the microrugulae.

*Carpinus* sp.
size: medium (26 – 50 μm)
shape: oblate; convex triangular in polar view
aperture type: porate
aperture number: 3
ornamentation: LM: psilate
SEM: microrugulate and microechinate; microechinae are locate on the top of the microrugulae.

**Caryophyllaceae:**

Caryophyllaceae gen. indet.
size: small (9 – 12 μm)
shape: spheroidal
aperture type: porate
aperture number: panto
ornamentation: LM: scabrate; thick sexine is visible
SEM: perforate and microechinate with microechinae; the echinae are acuter around the pores and cover also the pore membrane.

**Chenopodiacae:**

Chenopodiaceae gen. indet.1.
size: small (16 – 20 μm)
shape: spheroidal
aperture type: porate
aperture number: panto
ornamentation: LM: scabrate

SEM: perforate with microechinae; the microechinae are irregularly scatted, but also densely cover the pore membrane.

Chenopodiaceae gen. indet.2.

size: small (21 – 23 μm)

shape: spheroidal

aperture type: porate

aperture number: panto

ornamentation: LM: psilate

SEM: perforate and microechinate; microechinae are densely scattered over the whole surface and the pore membrane.

It can be distinguished from the other Chenopodiaceae due to their bigger echinae, which are more than Chenopodiaceae gen.intdet.1, but less than Chenopodiaceae gen.indet.3.

Chenopodiaceae gen. indet.3.

size: small (17 – 19 μm)

shape: spheroidal

aperture type: porate

aperture number: panto

ornamentation: LM: psilate to scabrate

SEM: perforate with many microechinae.

This species can be easily distinguished from Chenopodiaceae gen.indet.1 because of more echinae, which are regularly arranged, and not as deep pores.

## Eleagnaceae:

*Eleagnus* sp.

size: medium (30 – 33 μm)

shape: oblate; triangular in polar view; obtuse elliptic in equatorial view

aperture type: colporate

aperture number: 3

ornamentation: LM: scabrate

SEM: psilate with irregularly scatted granulae.

## Euphorbiaceae:

*Phyllanthus* sp.1.

size: small (15 – 17 x 20 μm)
shape: prolate; elliptic in equatorial view; almost circular in the polar view
aperture type: syncolpate
aperture number: 3
ornamentation: LM: microreticulate
SEM: microreticulate- heterobrochate; no change in the ornamentation around the colpi.

*Phyllanthus* sp.2.

size: small (12 – 16 x 15 – 19 μm)
shape: prolate; elliptic in equatorial view
aperture type: colpate
aperture number: 3
ornamentation: LM: reticulate; the strongly thickened sexine is visible; also the colpi are clearly thickened.
SEM: reticulate-heterobrochate; the muri have a smooth surface.

*Sapium* sp.

size: small (15 – 17 x 19 – 22 μm)
shape: prolate; elliptic in equatorial view; concave obtuse triangular in polar view
aperture type: colporate
aperture number: 3
ornamentation: LM: psilate
SEM: perforate with a slightly fossulate surface.

**Fagaceae:**

*Quercus* sp.1

size: small ( 17 x 25 µm)

shape: prolate; elliptic in the equatorial view; circular to triangular in the polar view

aperture type: colpus

aperture number: 3

ornamentation: LM: scabrate

SEM: striate; the short striae do not have a reoccurring pattern; they often lie parallel to other and unite at a certain point.

*Quercus* sp.2

size: small (15 – 18 x 19 – 22 µm)

shape: prolate; elliptic in the equatorial view; circular to triangular in the polar view

aperture type: colporate

aperture number: 3

ornamentation: LM: scabrate

SEM: surface is characterized by mircoverrucae, which are often combined of several parts.

*Quercus* sp.3.

size: small (15 – 18 x 18 – 24 µm)

shape: prolate; elliptic to in the equatorial view; circular to triangular in the polar view

aperture type: colpus

aperture number: 3

ornamentation: LM: scabrate

SEM: microverrucate; microverrucae show often a slightly striate suprasculpture.

*Quercus* sp.4.

size: small (15 – 17 x 17 -22 μm)

shape: prolate; elliptic in the equatorial view; circular to triangular in the polar view

aperture type: colpus

aperture number: 3

ornamentation: LM: scabrate

SEM: microverrucate and fossulate; microverrucae show a microechinate suprasculpture.

*Quercus* sp.5.

size: small (12 – 14 x 19 – 22 μm)

shape: prolate; elliptic in the equatorial view; triangular in the polar view

aperture type: colporate

aperture number: 3

ornamentation: LM: psilate to scabrate

SEM: striate and perforate; short striae origin around perforations.

## Juglandaceae:

*Engelhardia* sp.

size: small (20 – 22 μm)

shape: oblate; convex obtuse triangular in polar view

aperture type: porate

aperture number: 3

ornamentation: LM: psilate

SEM: microechinate; microechinae are densely placed over the whole surface.

*Juglans* sp.

size: medium (33 – 39 μm)

shape: oblate

aperture type: porate

aperture number: more than 6; more or less regular arranged over the whole pollen grain ornamentation: LM: psilate

SEM: microechinate; the microechinae tent to get bigger around the porus.

**Mimosaceae:**

<u>Mimosaceae gen. indet.</u>

size: polyade, medium (30 – 35 μm)

shape: elliptic

aperture type: unknown

aperture number: unknown

ornamentation: LM: psilate to scabrate; single grains are not always clearly visible

SEM: microverrucate; perforate and fossulate.

**Oleaceae:**

<u>*Fraxinus* sp.</u>

size: small (14 – 19 x 18 – 25 μm)

shape: prolate; elliptic in equatorial view

aperture type: colporate

aperture number: 3

ornamentation: LM: reticulate

SEM: reticulate-heterobrochate; muri are coarse; in the lumina free standing columellae can be seen.

<u>*Ligustrum* sp.</u>

size: small (18 x 22 μm)

shape: prolate; elliptic in the equatorial view

aperture type: colporate

aperture number: 3

ornamentation: LM: scabrate; nexine and sexine are clearly visible, while the sexine is slightly thicker

SEM: reticulate-heterobrochate; with smooth muri.

## Poaceae:

Poaceae gen. indet.1.
size: medium (37 – 42 μm)
shape: spheroidal
aperture type: ulcerate
aperture number: 1
ornamentation: LM: psilate
SEM: verrucate with a microechinate suprasculpture.

Poaceae gen. indet.2.
size: small (19 – 20 μm)
shape: spheroidal
aperture type: ulcerate
aperture number: 1
ornamentation: LM: psilate
SEM: microechinate and perforate.

Poaceae gen. indet.3.
size: medium (27 – 31 μm)
shape: spheroidal
aperture type: ulcerate
aperture number: 1
ornamentation: LM: psilate
SEM: fossulate and microverrucate with a microechinate suprasculpture.

**Rutaceae:**

*Zanthoxylum* sp.

size: small (18 x 24 µm)

shape: prolate; elliptic in equatorial view; circular to triangular in polar view

aperture type: colporate

aperture number: 3

ornamentation: LM: scabrate to slightly striate

SEM: striato-reticulate; striae form a wide and irregular net over the mesocolpium, but get tighter at the poles and next to the colpi.

**Solancaceae:**

Solanaceae gen. indet.

size: small (15 – 19 µm)

shape: oblate to spheroidal; obtuse triangular in the polar view

aperture type: (brevi-)colporate

aperture number: 3

ornamentation: LM: scabrate

SEM: perforate and microechinate.

**Symplocaceae:**

*Symplocos* sp.1

size: small to medium (23 – 28 µm)

shape: oblate; triangular obtuse concave in polar view

aperture type: colporate

aperture number: 3

ornamentation: LM: scabrate

SEM: microreticulate-heterobrochate; the reticulum has not always closed brochae; the vertexes are higher than the rest of the reticulum; the thickness of the muri is varying; surface shows infrequent granulae.

*Symplocos* sp.2
size: small (23 – 24 μm)
shape: oblate; triangular obtuse convex in the polar view; elliptic in the equatorial view
aperture type: (brevi-)colporate
aperture number: 3
ornamentation: LM: scabrate
SEM: rugulate, perforate and fossulate.

**Typhaceae:**

*Typha* sp.
size: small to medium (22 -26 μm)
shape: spheroidal
aperture type: ulcerate
aperture number: 1
ornamentation: LM: reticulate; a thick nexine and a very thick sexine is visible
SEM: reticulate-heterobrochate with rough muri.

**Ulmaceae:**

*Ulmus* sp.
size: small (21 – 23 μm)
shape: oblate; quinquangular obtuse in polar view; elliptic in equatorial view
aperture type: porate
aperture number: 4 to 6 (5)
ornamentation: LM: rugulate
SEM: rugulate with a granulate surface.

*Zelkova* sp.

size: small (21 – 24 μm)

shape: oblate; quadrangular convex in the polar view

aperture type: porate

aperture number: 4 to 5 (4)

ornamentation: LM: rugulate

SEM: rugulate with microechinate suprasculpture.

Compared to *Ulmus* sp., *Zelkova* sp. has shorter and stronger rugulae, which often unite.

Fam. indet.1.

size: small (13 – 16 x 20 - 23 μm)

shape: prolate; elliptic in the equatorial view; trilobate in the polar view

aperture type: colporate

aperture number: 3

ornamentation: LM: scabrate

SEM: perforate, with irregularly scattered granulae.

Fam. indet.2.

size: medium (20 – 23 x 30 – 34 μm)

shape: elliptic in the equatorial view

aperture type: colporate

aperture number: 3

ornamentation: LM: scabrate

SEM: surface appears fossulate and perforate.

Fam. indet.3.

size: medium (17 – 20 x 24 – 34 μm)

shape: prolate; elliptic in the equatorial view

aperture type: colpate

aperture number: 3

ornamentation: LM: reticulate

SEM: reticulate-heterobrochate with small muri.

Fam. indet.4.
size: medium (24 – 28 µm)
shape: oblate; circular lobate in polar view
aperture type: colpate
aperture number: 6
ornamentation: LM: reticulate
SEM: reticulate-heterobrochate; muri are regularly covered with mircoechinae.

## Cyst

Unknown gen. indet.
size: medium (20 – 24 x 29 – 32 µm)
shape: ovoid
ornamentation (LM and SEM): perforate.

# Results and discussion

The investigated samples from the Lukundol Formation show a rich and diverse assemblage. Altogether 78 different taxa were found, including 25 spores from ferns and mosses, 7 gymnosperms, 45 angiosperms and 1 freshwater cyst. 37 of all these were identified to their genus level, only 4 could be determined to their species level due to comparison to recent taxa (Paudayal, 2002). Except 4 angiosperms and 14 spores, all other could be assigned to a family.
For the spores, Polypodiaceae were highly abundant. Among the pollen, no special taxa appeared with a sticking high number.
No algae, such as *Pediastrum*, was seen, despite it seems to be abundant in some parts of the formation, e.g. Fujii and Sakai (2002) or Yoshida and Igarashi (1984).

The assemblage shows well known elements of this area, *Pinus* sp., *Quercus* sp. or Polypodiaceae, but also some rare elements, exemplary *Zanthoxylum* sp. Compared to Paudayal (2002), who published five different Quercus taxa, this investigation also shows five, but only 2 are identical.

Other pollen grains, such as *Acer* sp., *Ephedra* sp. or *Zanthoxylum* sp., occurred in my samples, are known in today's vegetation of Nepal, but were not mentioned by Paudayal (2002). However supposing frequent element, like *Castanopis* sp. is missing in Lukundol sample. Several other taxa of families were found by Paudayal (2002) in a rich number, such as many species of *Polygonum* or Sapotaceae, where none of them was found here. Additionally, aquatic plants do not appear at all, unlike at Paudayal's work, who identified *Trapa* sp. *Nymphoides* sp. and *Myriophyllum spicatum*. He also dealt with more species of Compositae, Cayophyllacae, Sympocaceae and Apiaceae, which are present in my samples with a lower species number. Also no Ericaceae could be detected by myself.
In contrast, I did investigate 3 different taxa of Poaceae, where Paudayal (2002) only described one, which is identical with one of these samples. Also almost the same types of Chenopodiaceae were imaged.
Farther, many taxa are the same between the Lukundol Formaion I worked on, and the younger Formations (Patan, Gokarna, Thimi) , Paudayal (2002) studied. The gymnosperms are, excluding *Ephedra* sp., the same species. Both assemblages show a high abundance in spores, but twice as much pollen taxa could be found. Among the angiosperms, a long list of equal genera and species is termed from more or less common taxa of this area such as *Alnus* sp., *Betula* sp., *Elaegnus* sp, *Engelhardia* sp., *Fraxinus* sp. and many more. Except

the fact, that some of these were identified by Paudayal (2002) by comparing them with recent herbarium material as species.

Mountain valleys, such as the Kathmandu Valley, are very suitable for interpretation based on palynological samples. Because the valley is surrounded by high mountains, only a little amount of pollen can reach there from the outside except from the high areas of the Greater Himalaya, for example *Cedrus* sp. (Yoshida and Igarashi, 1984).

Already from other authors (Yoshida and Igarashi, 1984; Fujii and Sakai, 2002; Paudayal, 2002; Goddu, 2004) it is known, that the climatic conditions in the valley had changed during the deposition of the Lukundol Formation. Yoshida and Igarashi (1984) mentioned a shift from the "tropical evergreen lower montane forest" to a "tropical evergreen upper montane forst", which they took as a climatic signal for a moister and warmer climate more than one million year ago. Especially the top of the formations is said to be dry.
Also Fujii and Sakai (2002) document in their samples out of a drilled core, that at the top (between 0.8 and 1 Ma) dry climate preferring plants such as *Artemisia* and Chenopodiaceae increase.
Since this is not meant as a quantitative work, a direct linking with one of the other worker's zone is not possible. Additionally, a method for dating is missing.

The samples investigated for this work show a mixed pollen record as well. *Artemisia*, Chenopodiaceae, *Ephedra* and Poacea are present, often suggesting an open environment with low precipitation. But unlike these grasses, the high abundance of ferns, which need a moister habitat, documents the plants living around the Paleo-Lake Kathmandu.
An element from the lake itself is *Typha* sp., which grows at the shore.

The area around the Lake seems to be characterized by shifting forest vegetation due to the difference in elevation. Trees such a *Zelkova* or *Fraxinus* were possibly living around the lake, while *Quercus* and *Pinus*, were more common little farer away and higher up in the hills around. *Picea* sp. and *Abies* sp. are also occurring, giving an example for higher elevation vegetation or a cooler climatic zone. The same interpretation can be made from *Tsuga* sp. or *Ephedra* sp. These were often taken as an indicator for a colder climate in the Kathmandu Basin, than it is today (Goddu, 2004).

Generally speaking, many warm temperate taxa are abundant. Plants such as *Engelhardia* sp., *Sapium* sp., *Symplocos* sp., Asteraceae or Rutaceae, as other scientists (Yoshida and Igarashi, 1984; Fujii and Sakai, 2002; Goddu, 2004) observed before, point to a warmer climate. Others, like *Betula* sp., *Carpinus* sp., *Juglans* sp., *Eleagnus* sp. or Oleaceae, are also representatives of warm climate, but sometimes also live in temperate zones.

A typical temperate element, like *Ulmus* sp., is also found. Cold temperate elements may be part of the assemblage, but further identification on species level is needed to give a more precise picture.

For detailed further work on climate, much more samples out of a section are needed. Only then it would be useful to count the samples and compare them with each other.

Many samples do not exclude the use to the scanning electron microscope. From a whole section, it is necessary to investigate only several samples in detail to get a good impression of the whole assemblage. Once, taxa are approved or further defined with the scanning electron microscope, they are easier recognized in the light microscope as well. Working procedure as described above gives a more reliable information for reconstructing paleoclimate and paleoenvironment than work done only on the light microscope.

## Acknowlegdements

At this place I first want to thank my supervisor Dr. Reinhard Zetter for giving me the material and helping me with all my questions.
Further many thanks to Dr. David K. Ferguson and Dr. Khum N. Paudayal for colleting my samples during their field work in Nepal and additionally Dr. Paudayal for sending me interesting papers and maps from the Kathmandu Basin. For further literature about Nepal I have to thank Dr. Ferguson as well as Dr. Christa-Charlotte Hofmann for giving me books as a help for identifying pollen and spores.
For all the technical support on the computer I onwards have to thank Nadja Kavcik.
In the end, I also thank all my fellow students for discussion, helping me and spending my breaks.

# **Plates**

**Plate 1:**

Fig.1: ***Davallia* sp.** LM; equatorial view

Fig.2: ***Davallia* sp.** SEM; equatorial view

Fig.3: ***Davallia* sp.** SEM; detail picture of the surface

Fig.4: **Davalliaceae gen. indet.** LM; equatorial view

Fig.5: **Davalliaceae gen. indet.** SEM; equatorial view

Fig.6: **Davalliaceae gen. indet.** SEM; detail picture of the surface

Fig.7: ***Lepisorus* sp.** LM; equatorial view

Fig.8: ***Lepisorus* sp.** SEM; equatorial view

Fig.9: ***Lepisorus* sp.** SEM; detail picture of the surface

Fig.10: **Polypodiaceae gen. indet.1.** LM; equatorial view

Fig.11: **Polypodiaceae gen. indet.1.** SEM; equatorial view

Fig.12: **Polypodiaceae gen. indet.1.** SEM; detail picture of the surface

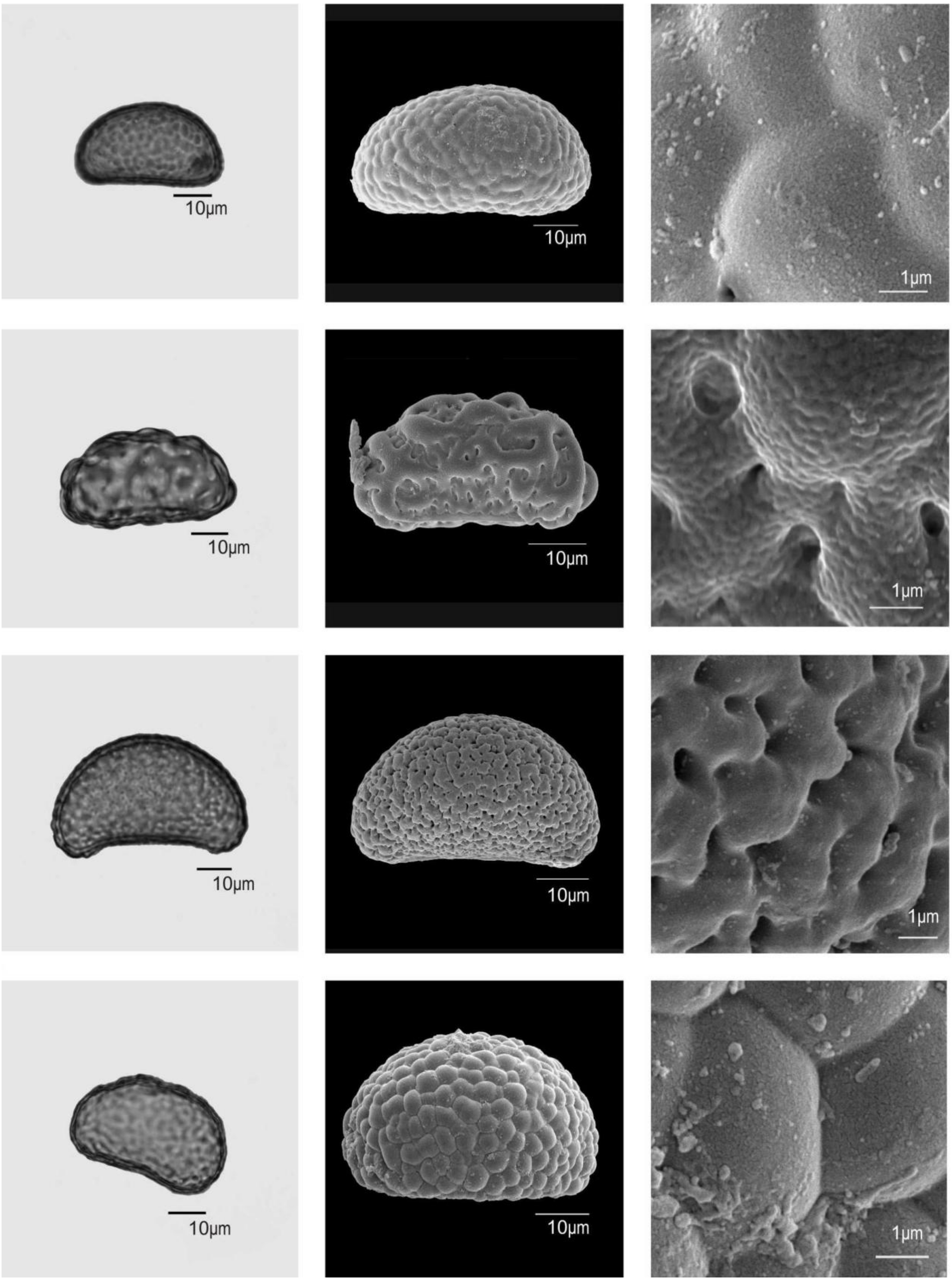
10µm
10µm
1µm
10µm
10µm
1µm
10µm
10µm
1µm
10µm
10µm
1µm

**Plate 2:**

Fig.1: **Polypodiaceae gen. indet.2.** LM; equatorial view

Fig.2: **Polypodiaceae gen. indet.2.** SEM; equatorial view

Fig.3: **Polypodiaceae gen. indet.2.** SEM; detail picture of the surface

Fig.4: **Polypodiaceae gen. indet.3.** LM; polar view

Fig.5: **Polypodiaceae gen. indet.3.** SEM; polar view

Fig.6: **Polypodiaceae gen. indet.3.** SEM; detail picture of the surface

Fig.7: **Pteridaceae gen. indet.** LM; polar view

Fig.8: **Pteridaceae gen. indet.** SEM; polar view

Fig.9: **Pteridaceae gen. indet.** SEM; detail picture of the surface

Fig.10: ***Pyrrosia* sp.** LM; equatorial view

Fig.11: ***Pyrrosia* sp.** SEM; equatorial view

Fig.12: ***Pyrrosia* sp.** SEM; detail picture of the surface

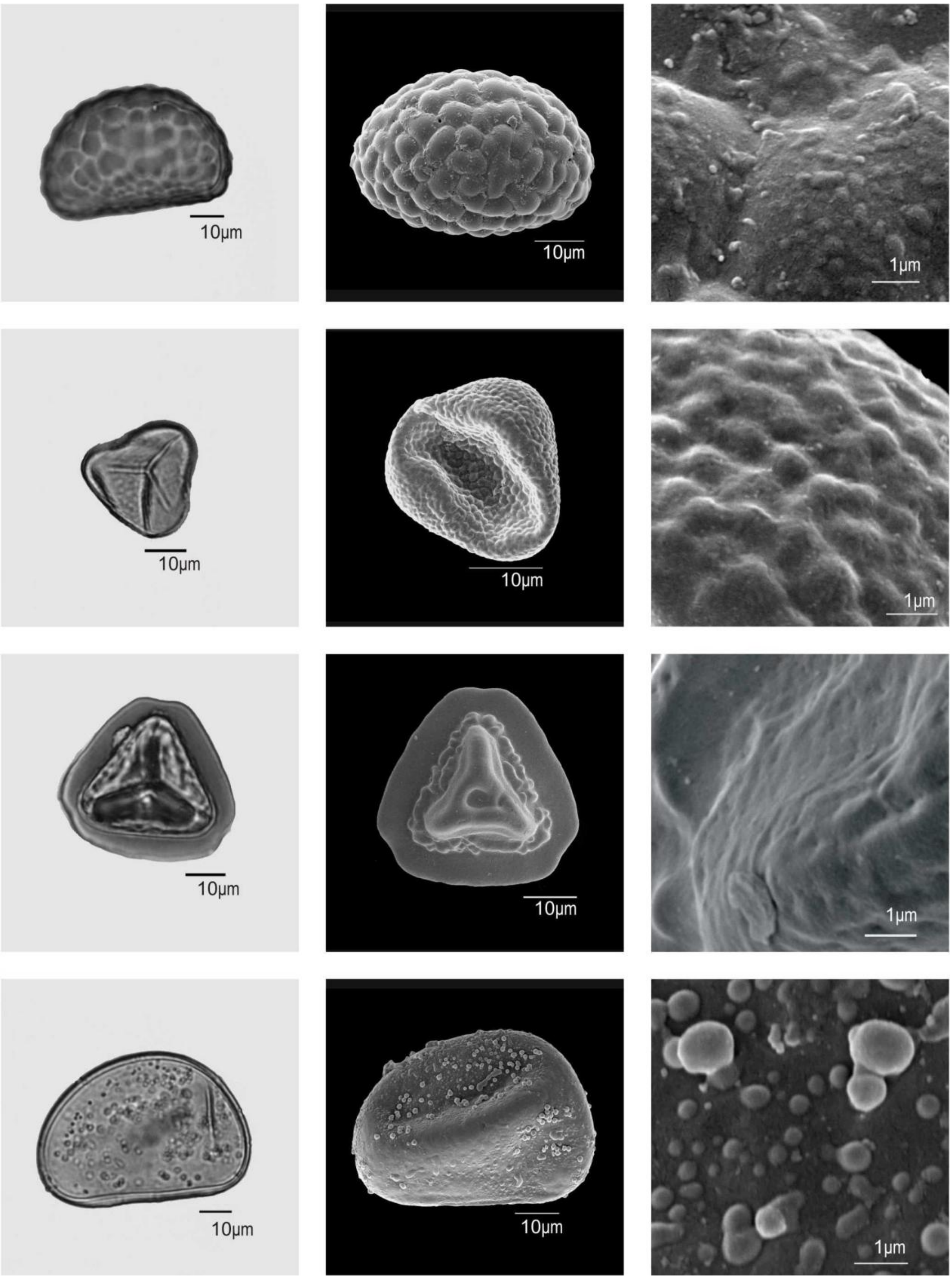
10μm
10μm
1μm
10μm
10μm
1μm
10μm
10μm
1μm
10μm
10μm
1μm

**Plate 3:**

Fig.1: ***Selaginella* sp.** LM; polar view

Fig.2: ***Selaginella* sp.** SEM; polar view

Fig.3: ***Selaginella* sp.** SEM; detail picture of the surface

Fig.4: ***Woodwardia* sp.** LM; equatorial view

Fig.5: ***Woodwardia* sp.** SEM; equatorial view

Fig.6: ***Woodwardia* sp.** SEM; detail picture of the surface

Fig.7: **Spore gen. indet.1.** LM; equatorial view

Fig.8: **Spore gen. indet.1.** SEM; equatorial view

Fig.9: **Spore gen. indet.1.** SEM; detail picture of the surface

Fig.10: **Spore gen. indet.2.** LM; polar view

Fig.11: **Spore gen. indet.2.** SEM; polar view

Fig.12: **Spore gen. indet.2.** SEM; detail picture of the surface

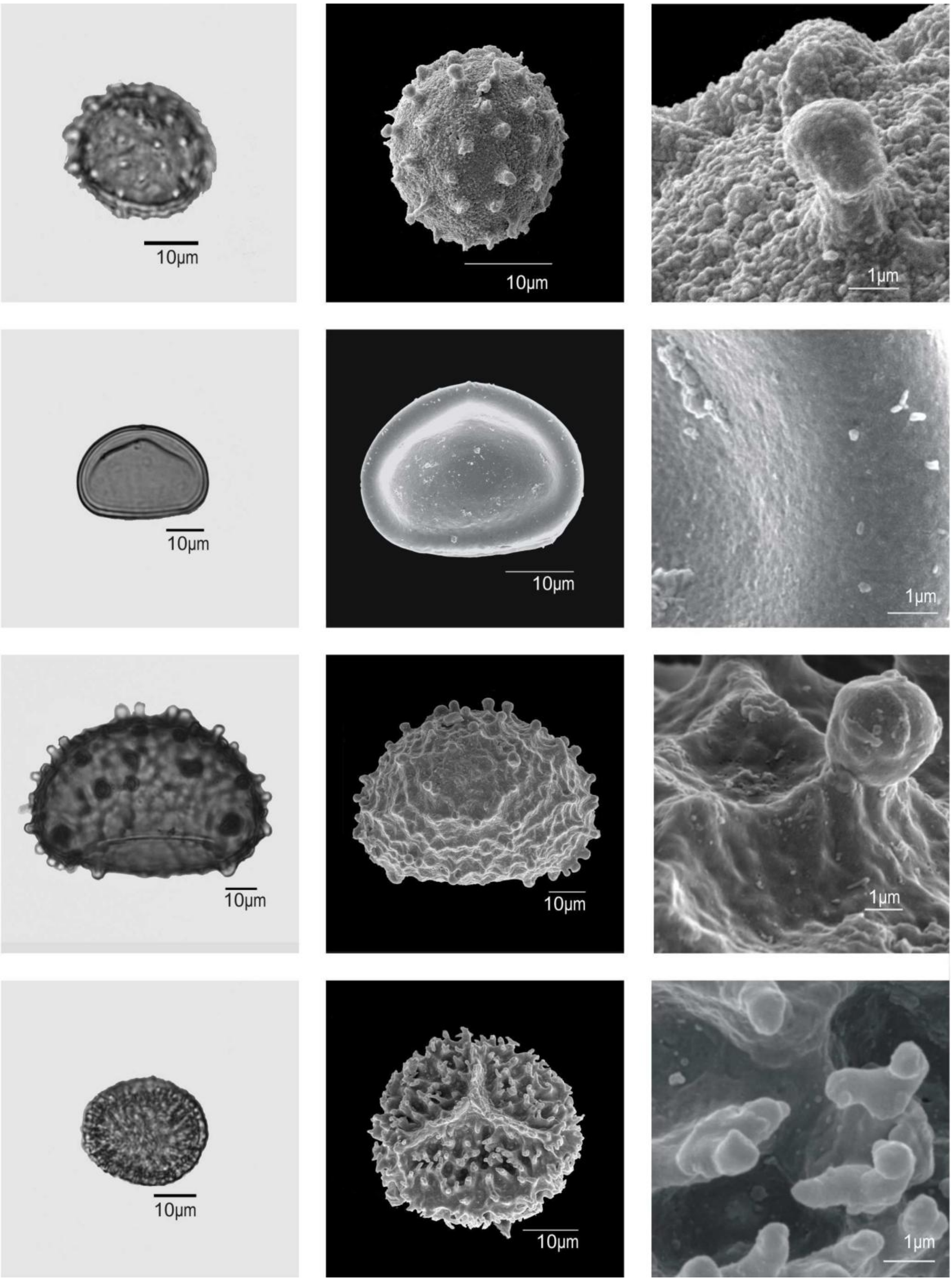
10µm
10µm
1µm
10µm
10µm
1µm
10µm
10µm
1µm
10µm
10µm
1µm

**Plate 4:**

Fig.1: **Spore gen. indet.3.** LM; polar view

Fig.2: **Spore gen. indet.3.** SEM; polar view

Fig.3: **Spore gen. indet.3.** SEM; detail picture of the surface

Fig.4: **Spore gen. indet.4.** LM; polar view

Fig.5: **Spore gen. indet.4.** SEM; polar view

Fig.6: **Spore gen. indet.4.** SEM; detail picture of the surface

Fig.7: **Spore gen. indet.5.** LM; polar view

Fig.8: **Spore gen. indet.5.** SEM; polar view

Fig.9: **Spore gen. indet.5.** SEM; detail picture of the surface

Fig.10: **Spore gen. indet.6.** LM; polar view

Fig.11: **Spore gen. indet.6.** SEM; polar view

Fig.12: **Spore gen. indet.6.** SEM; detail picture of the surface

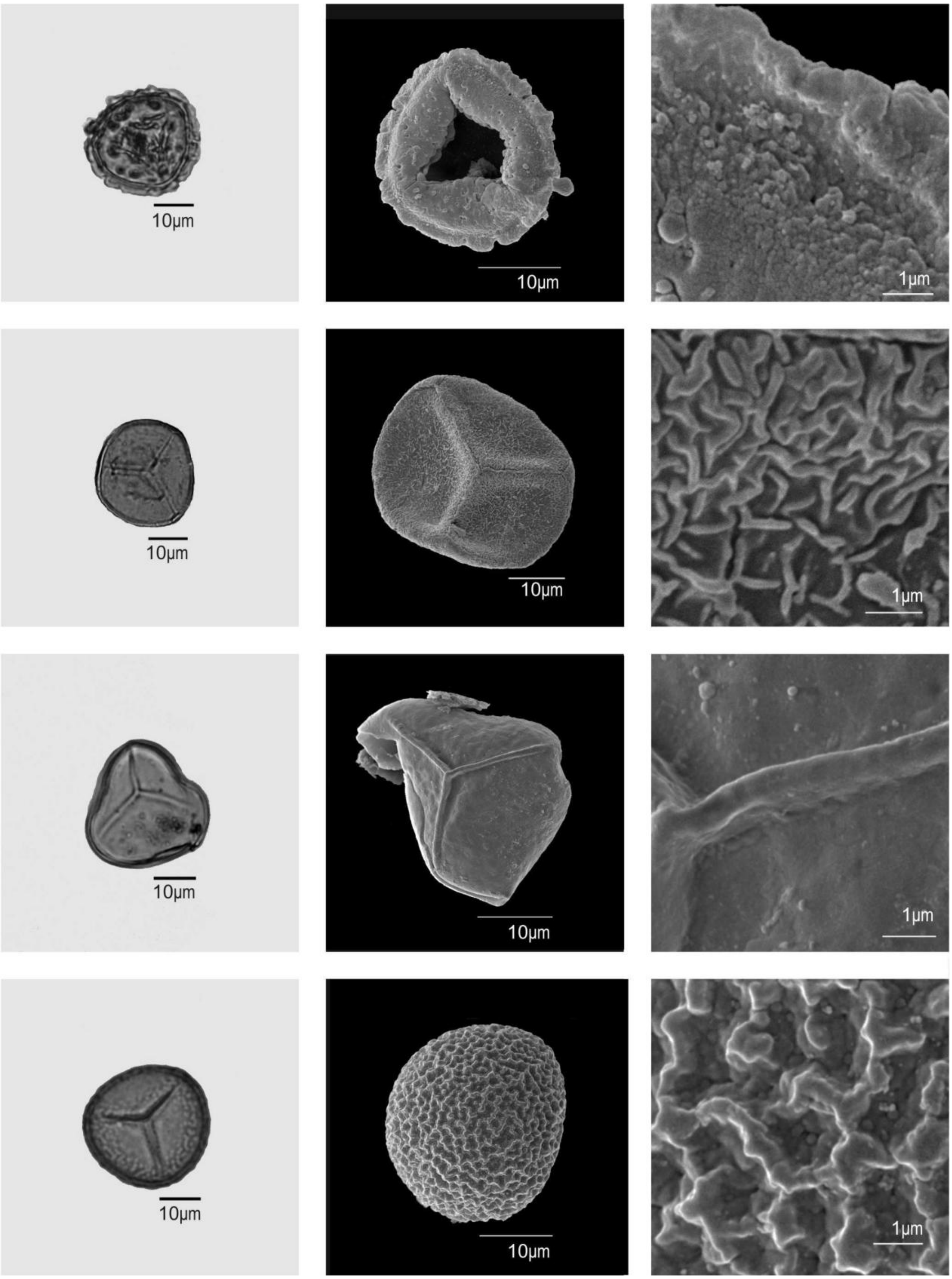
10µm
10µm
1µm
10µm
10µm
1µm
10µm
10µm
1µm
10µm
10µm
1µm

**Plate 5:**

Fig.1: **Spore gen. indet.7.** LM; equatorial view

Fig.2: **Spore gen. indet.7.** SEM; equatorial view

Fig.3: **Spore gen. indet.7.** SEM; detail picture of the surface

Fig.4: **Spore gen. indet.8.** LM; polar view

Fig.5: **Spore gen. indet.8.** SEM; equatorial view

Fig.6: **Spore gen. indet.8.** SEM; detail picture of the surface

Fig.7: **Spore gen. indet.9.** LM; polar view

Fig.8: **Spore gen. indet.9.** SEM; polar view

Fig.9: **Spore gen. indet.9.** SEM; detail picture of the surface

Fig.10: **Spore gen. indet.10.** LM; polar view

Fig.11: **Spore gen. indet.10.** SEM; polar view

Fig.12: **Spore gen. indet.10.** SEM; detail picture of the surface

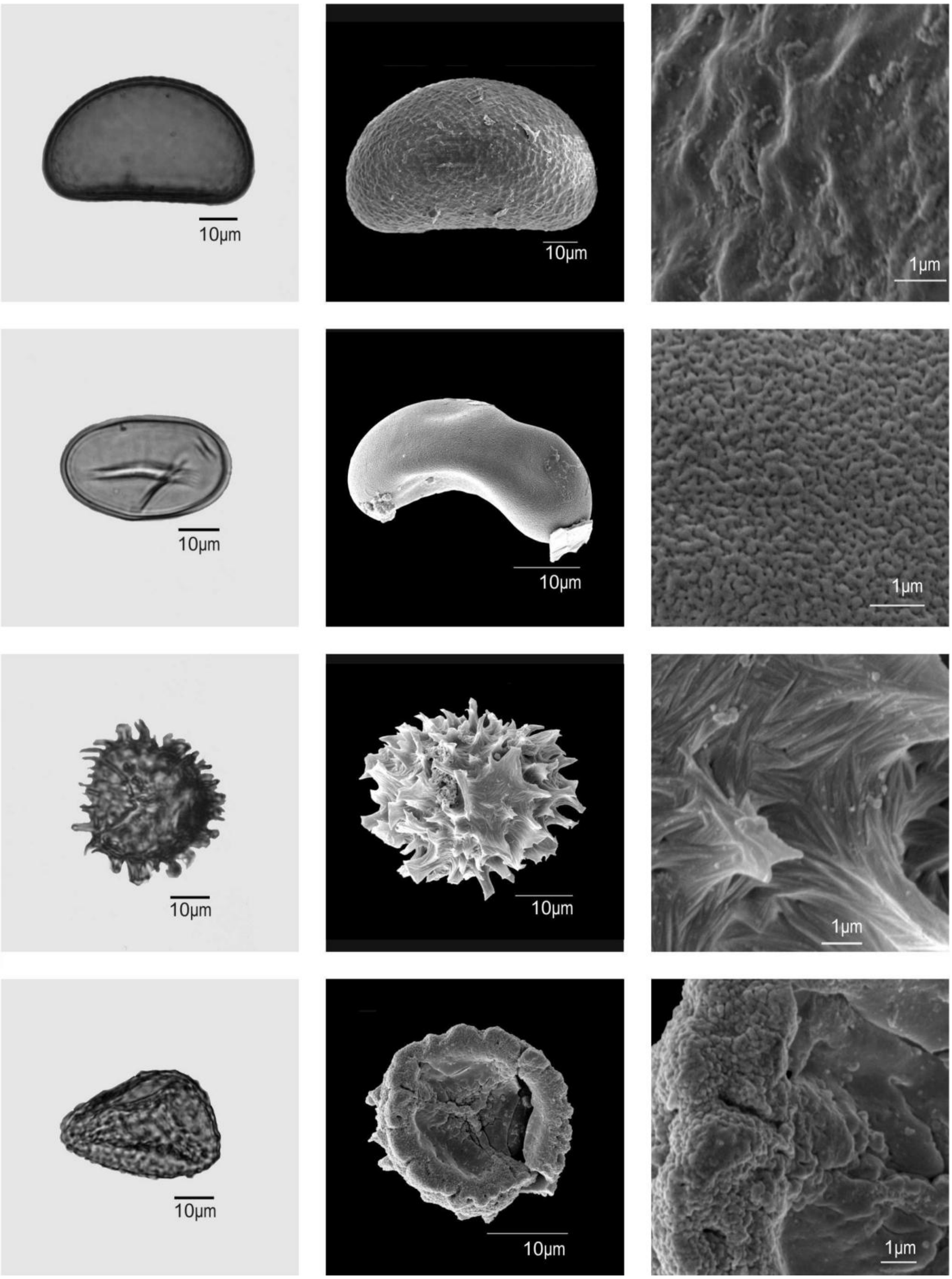
10μm
10μm
1μm
10μm
10μm
1μm
10μm
10μm
1μm
10μm
10μm
1μm

**Plate 6:**

Fig.1: **Spore gen. indet.11.** LM; polar view

Fig.2: **Spore gen. indet.11.** SEM; polar view

Fig.3: **Spore gen. indet.11.** SEM; detail picture of the surface

Fig.4: **Spore gen. indet.12.** LM; equatorial view

Fig.5: **Spore gen. indet.12.** SEM; equatorial view

Fig.6: **Spore gen. indet.12.** SEM; detail picture of the surface

Fig.7: **Spore gen. indet.13.** LM; polar view

Fig.8: **Spore gen. indet.13.** SEM; polar view

Fig.9: **Spore gen. indet.13.** SEM; detail picture of the surface

Fig.10: **Spore gen. indet.14.** LM; polar view

Fig.11: **Spore gen. indet.14**. SEM;

Fig.12: **Spore gen. indet.14.** SEM; detail picture of the surface

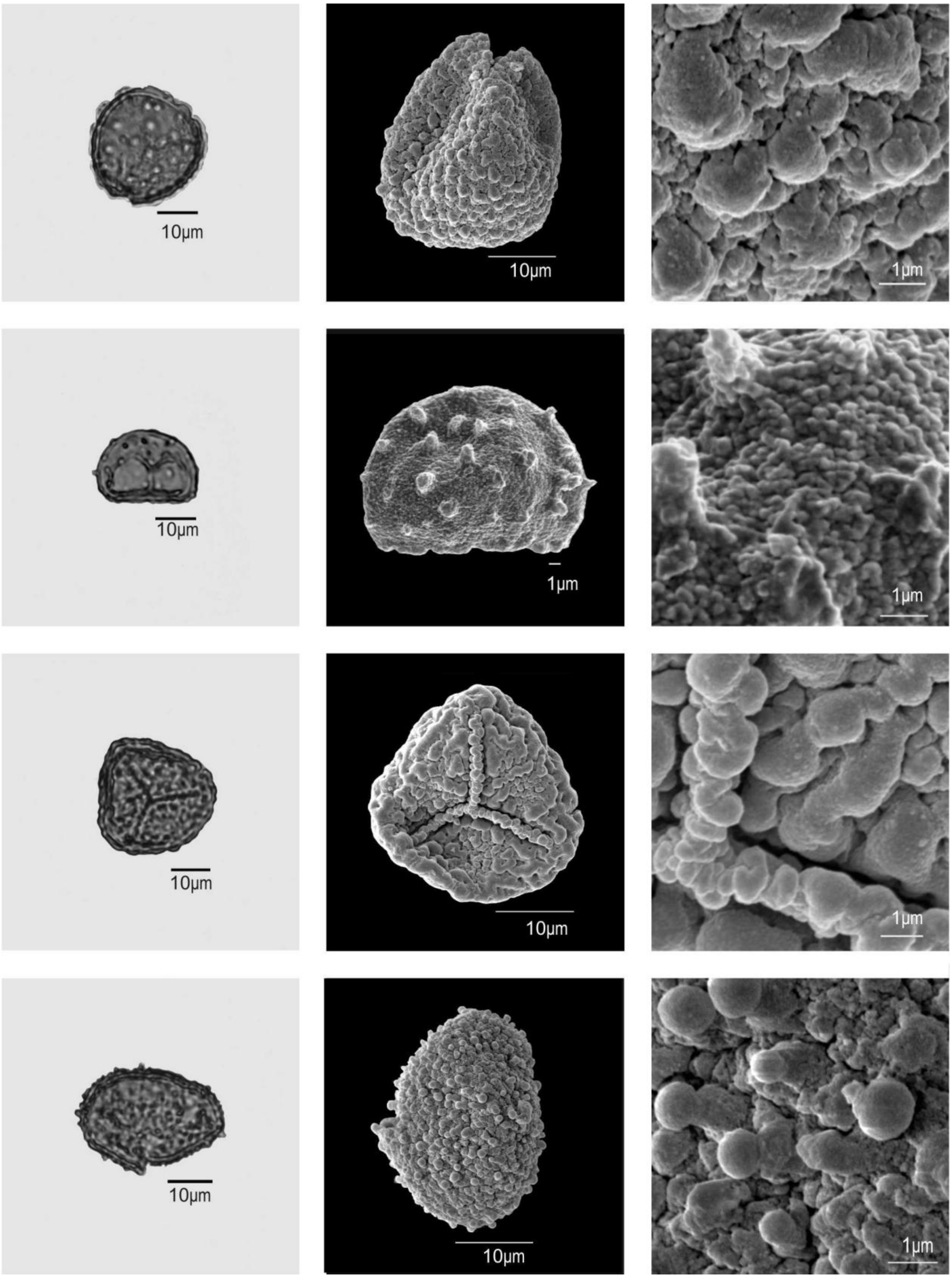
10µm
10µm
1µm
10µm
1µm
1µm
10µm
10µm
1µm
10µm
10µm
1µm

**Plate 7:**

Fig.1: ***Ephedra cf. intermedia***. LM;

Fig.2: ***Ephedra cf. intermedia***. SEM;

Fig.3: ***Ephedra cf. intermedia***. SEM; detail picture of one plica

Fig.4: ***Abies* sp.** LM; equatorial view

Fig.5: ***Abies* sp.** SEM; equatorial view

Fig.6: ***Abies* sp.** SEM; detail picture of the surface

Fig.7: ***Picea* sp.** LM; equatorial view

Fig.8: ***Picea* sp.** SEM; equatorial view

Fig.9: ***Picea* sp.** SEM; detail picture of the surface

Fig.10: ***Pinus roxburghii***. LM; equatorial view

Fig.11: ***Pinus roxburghii***. SEM;

Fig.12: ***Pinus roxburghii***. SEM; detail picture of the surface

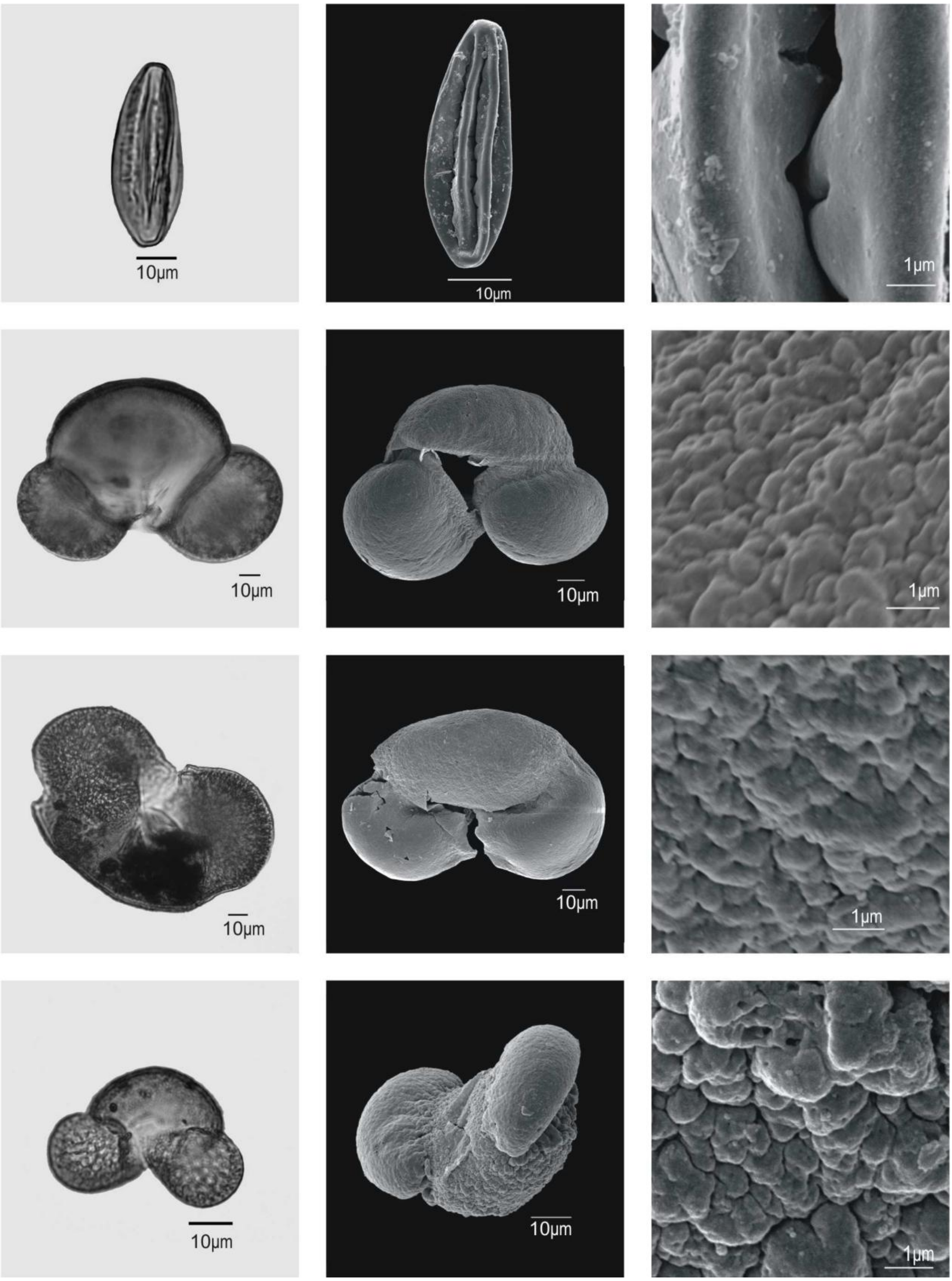
10µm
10µm
1µm
10µm
10µm
1µm
10µm
10µm
1µm
10µm
10µm
1µm

**Plate 8:**

Fig.1: ***Pinus wallichia***. LM; equatorial view

Fig.2: ***Pinus wallichia***. SEM; equatorial view

Fig.3: ***Pinus wallichia***. SEM; detail picture of the surface

Fig.4: ***Tsuga cf. dumosa***. LM; polar view

Fig.5: ***Tsuga cf. dumosa***. SEM; polar view

Fig.6: ***Tsuga cf. dumosa***. SEM; detail picture of the surface

Fig.7: ***Podocarpus* sp.** LM; polar view

Fig.8: ***Podocarpus* sp.** SEM; polar view

Fig.9: ***Podocarpus* sp.** SEM; detail picture of the surface

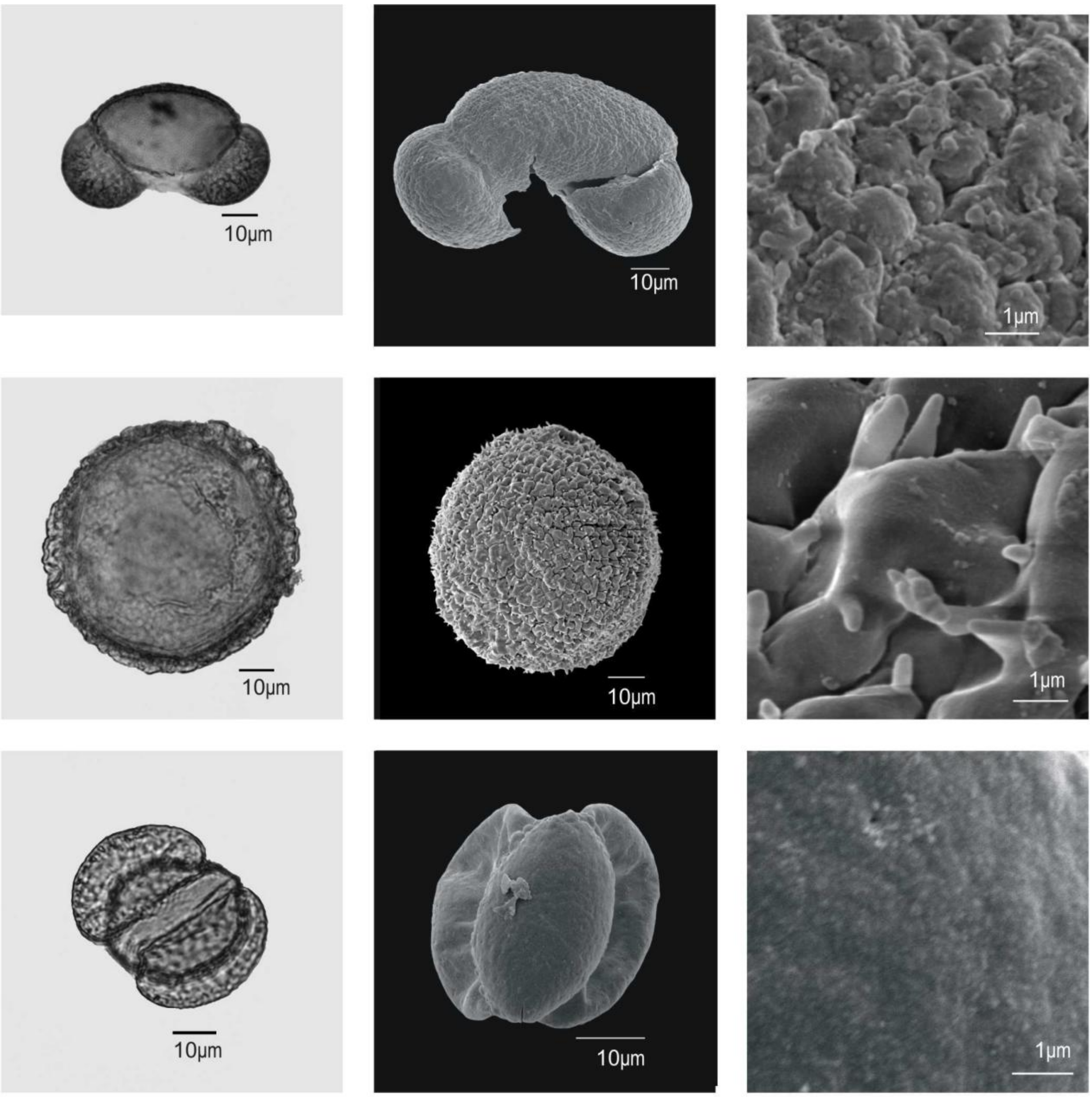
10µm
10µm
1µm
10µm
10µm
1µm
10µm
10µm
1µm

**Plate 9:**

Fig.1: ***Acer* sp.** LM; equatorial view

Fig.2: ***Acer* sp.** SEM; equatorial view

Fig.3: ***Acer* sp.** SEM; detail picture of the surface

Fig.4: **Apiaceae gen. indet.** LM; equatorial view

Fig.5: **Apiaceae gen. indet.** SEM; equatorial view

Fig.6: **Apiaceae gen. indet.** SEM; detail picture of the surface

Fig.7: ***Palmae* sp.1.** LM; polar view

Fig.8: ***Palmae* sp.1.** SEM; polar view

Fig.9: ***Palmae* sp.1.** SEM; detail picture of the surface

Fig.10: ***Palmae* sp.2.** LM;

Fig.11: ***Palmae* sp.2.** SEM;

Fig.12: ***Palmae* sp.2.** SEM; detail picture of the surface

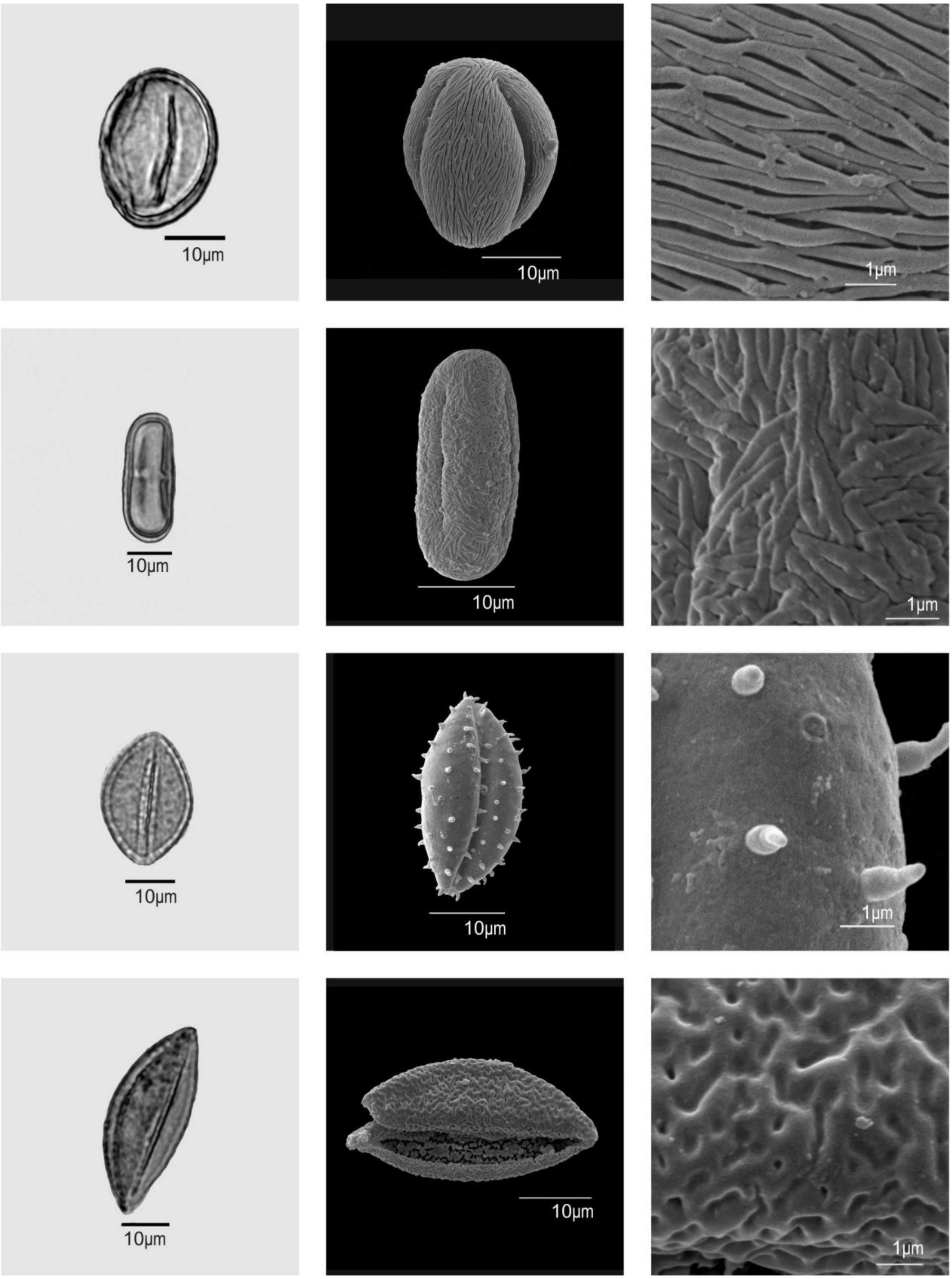
10µm
10µm
1µm
10µm
10µm
1µm
10µm
10µm
1µm
10µm
10µm
1µm

**Plate 10:**

Fig.1: ***Artemisia* sp.** LM; polar view

Fig.2: ***Artemisia* sp.** SEM; equatorial view

Fig.3: ***Artemisia* sp.** SEM; detail picture of the surface

Fig.4: **Liguliflorae Compositae gen. indet.** LM;

Fig.5: **Liguliflorae Compositae gen. indet.** SEM;

Fig.6: **Liguliflorae Compositae gen. indet.** SEM; detail picture of the surface

Fig.7: **Tubiflorae Compositae gen. indet.1.** LM; polar view

Fig.8: **Tubiflorae Compositae gen. indet.1.** SEM; polar view

Fig.9: **Tubiflorae Compositae gen. indet.1.** SEM; detail picture of the surface

Fig.10: **Tubiflorae Compositae gen.indet.2.** LM; polar view

Fig.11: **Tubiflorae Compositae gen.indet.2.** SEM; equatorial view

Fig.12: **Tubiflorae Compositae gen.indet.2.** SEM; detail picture of the surface

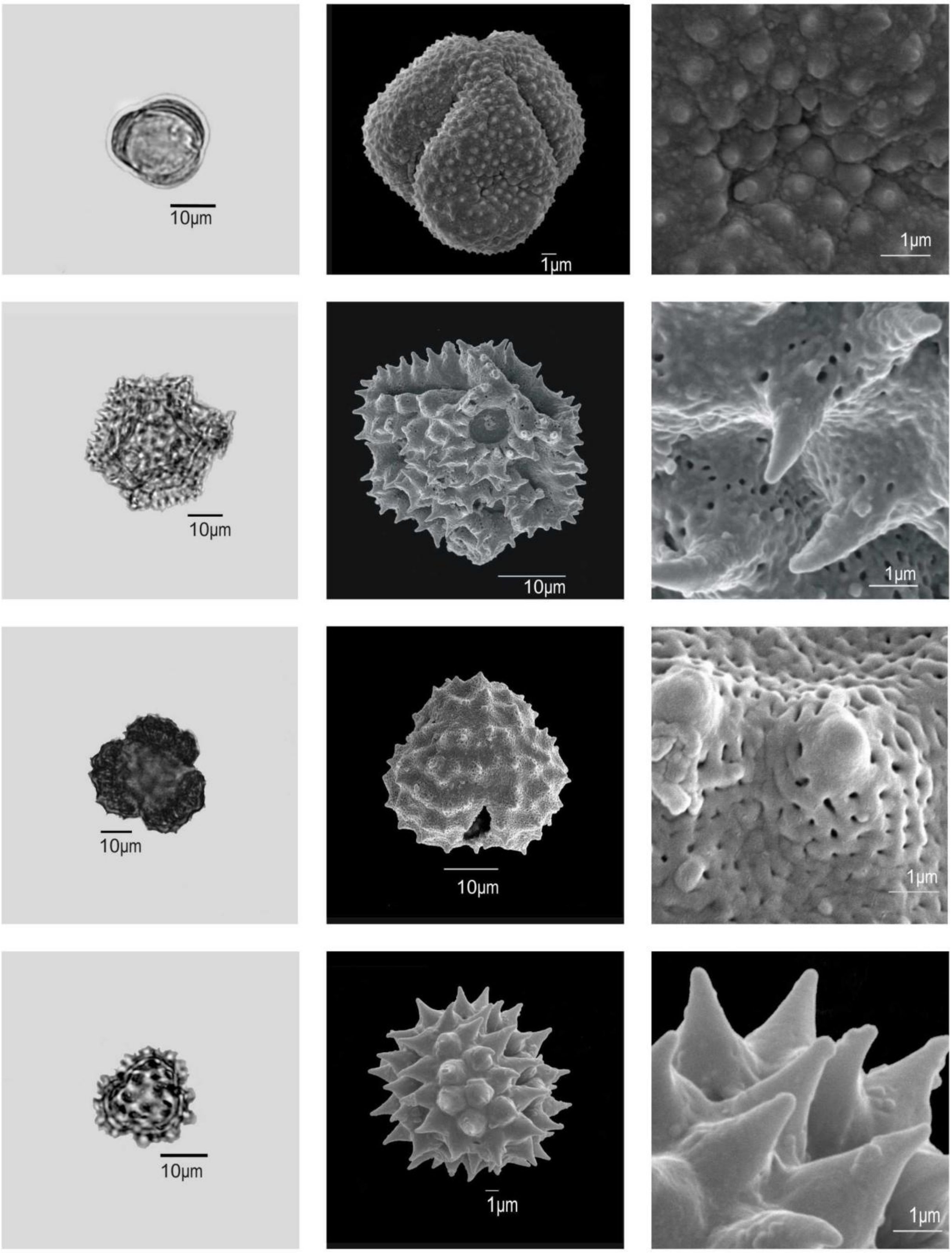
10µm
1µm
1µm
10µm
10µm
1µm
10µm
10µm
1µm
10µm
1µm
1µm

**Plate 11:**

Fig.1: **Tubiflorae Compositae gen. indet.3.** LM; equatorial view

Fig.2: **Tubiflorae Compositae gen. indet.3.** SEM; equatorial view

Fig.3: **Tubiflorae Compositae gen. indet.3.** SEM; detail picture of the surface

Fig.4: **Tubiflorae Compositae gen. indet.4.** LM; equatorial view

Fig.5: **Tubiflorae Compositae gen. indet.4.** SEM; equatorial view

Fig.6: **Tubiflorae Compositae gen. indet.4.** SEM; detail picture of the surface

Fig.7: ***Alnus* sp.** LM; polar view

Fig.8: ***Alnus* sp.** SEM; polar view

Fig.9: ***Alnus* sp.** SEM; detail picture of the surface

Fig.10: ***Betula* sp.** LM; polar view

Fig.11: ***Betula* sp.** SEM; polar view

Fig.12: ***Betula* sp.** SEM; detail picture of the surface

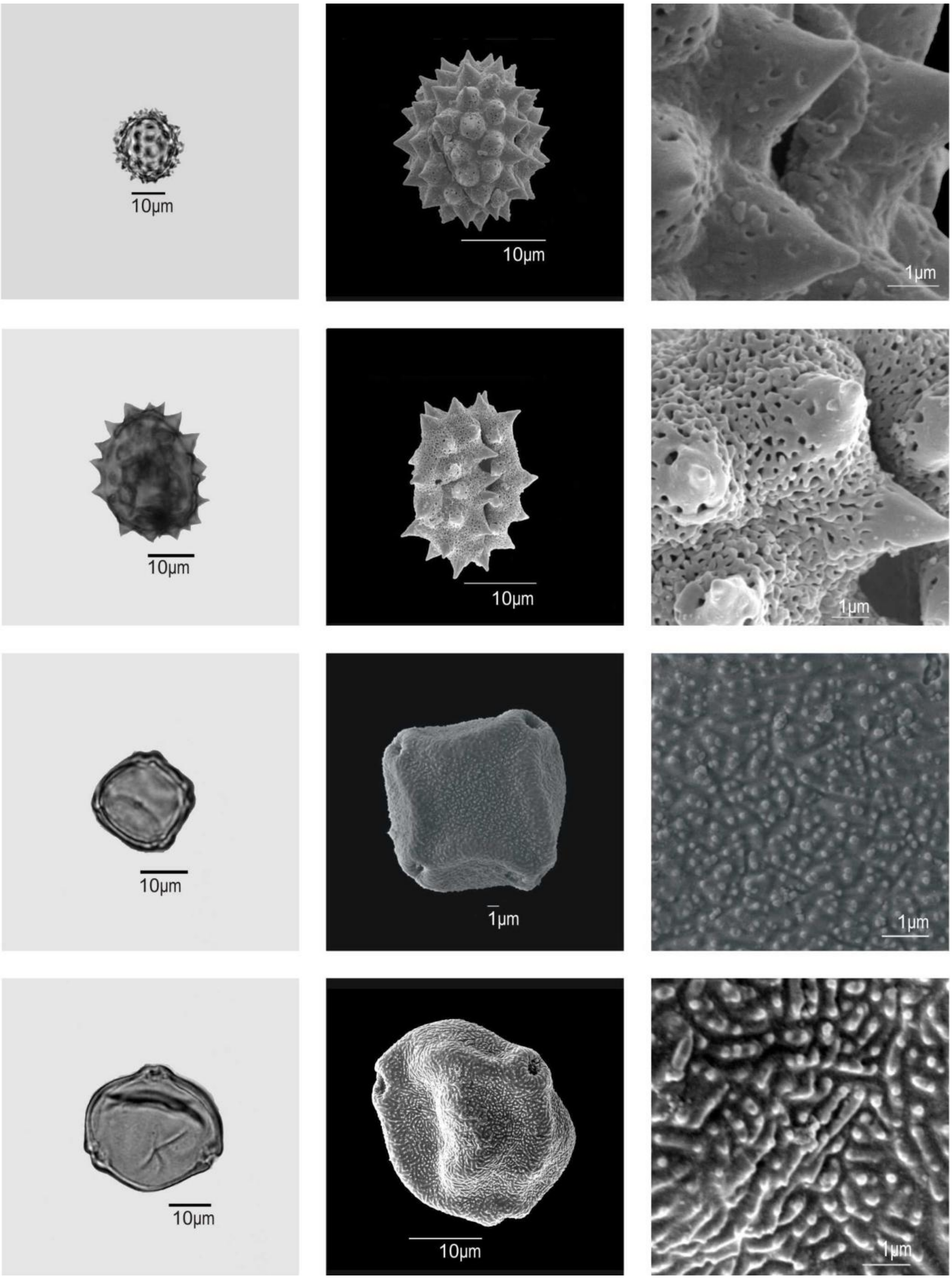
10µm
10µm
1µm
10µm
10µm
1µm
10µm
1µm
1µm
10µm
10µm
1µm

**Plate 12:**

Fig.1: ***Carpinus* sp.** LM; polar view

Fig.2: ***Carpinus* sp.** SEM; polar view

Fig.3: ***Carpinus* sp.** SEM; detail picture of the surface

Fig.4: **Caryophyllaceae gen. indet.** LM;

Fig.5: **Caryophyllaceae gen. indet.** SEM;

Fig.6: **Caryophyllaceae gen. indet.** SEM; detail picture of the surface and porus

Fig.7: **Chenopodiaceae gen. indet.1.** LM;

Fig.8: **Chenopodiaceae gen. indet.1.** SEM;

Fig.9: **Chenopodiaceae gen. indet.1.** SEM; detail picture of the surface and porus

Fig.10: **Chenopodiaceae gen. indet.2.** LM;

Fig.11: **Chenopodiaceae gen. indet.2.** SEM;

Fig.12: **Chenopodiaceae gen. indet.2.** SEM; detail picture of the surface and porus

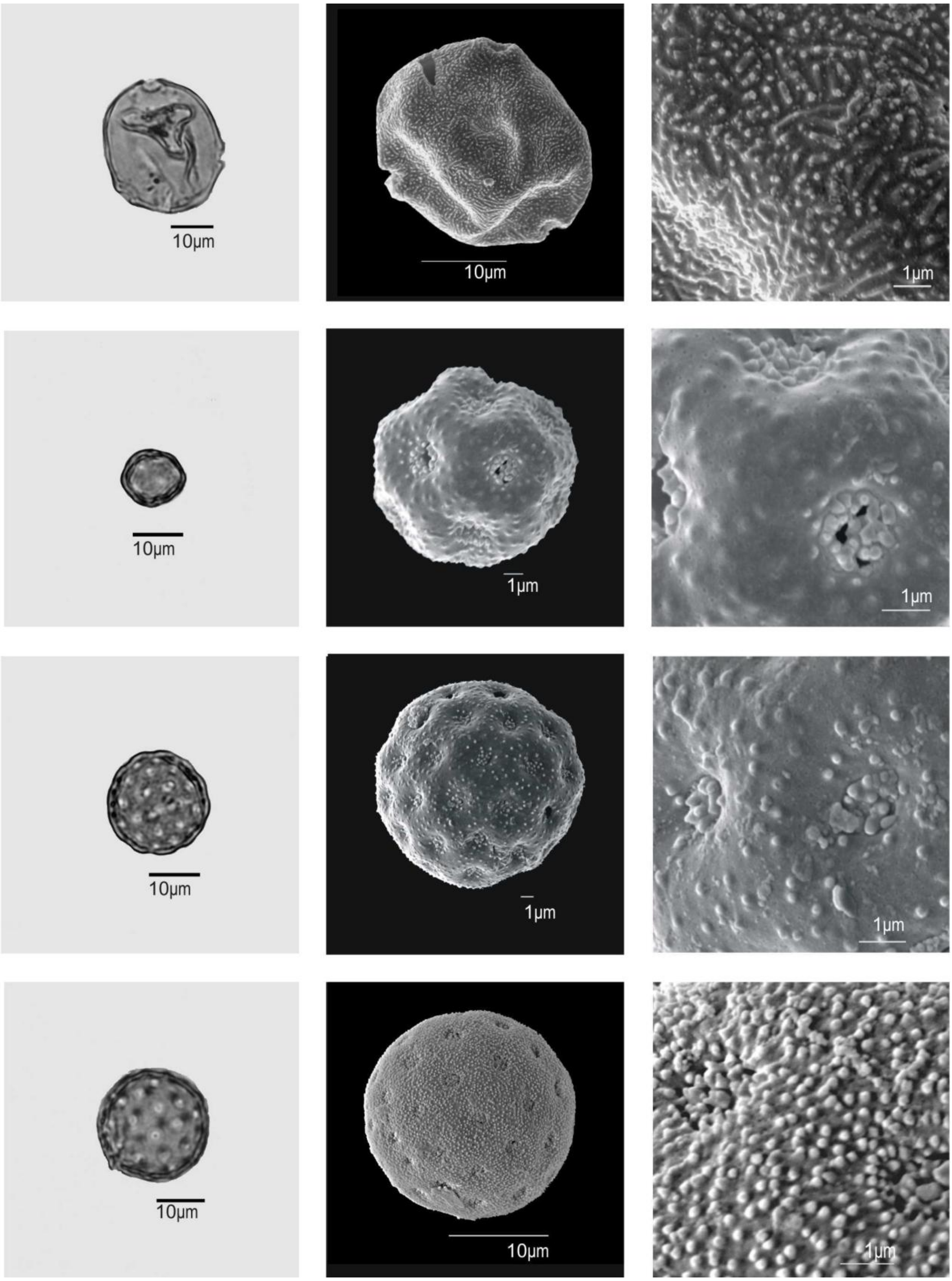
10μm
10μm
1μm
10μm
1μm
1μm
10μm
1μm
1μm
10μm
10μm
1μm

**Plate 13:**

Fig.1: **Chenopodiaceae gen. indet.3.** LM;

Fig.2: **Chenopodiaceae gen. indet.3.** SEM;

Fig.3: **Chenopodiaceae gen. indet.3.** SEM; detail picture of the surface and porus

Fig.4: ***Eleagnus* sp.** LM; polar view

Fig.5: ***Eleagnus* sp.** SEM; polar view

Fig.6: ***Eleagnus* sp.** SEM; detail picture of the surface

Fig.7: ***Phyllanthus* sp.1.** LM; equatorial view

Fig.8: ***Phyllanthus* sp.1.** SEM; equatorial view

Fig.9: ***Phyllanthus* sp.1.** SEM; detail picture of the surface at the pole

Fig.10: ***Phyllanthus* sp.2.** LM; equatorial view

Fig.11: ***Phyllanthus* sp.2.** SEM; equatorial view

Fig.12: ***Phyllanthus* sp.2.** SEM; detail picture of the surface around the colpus

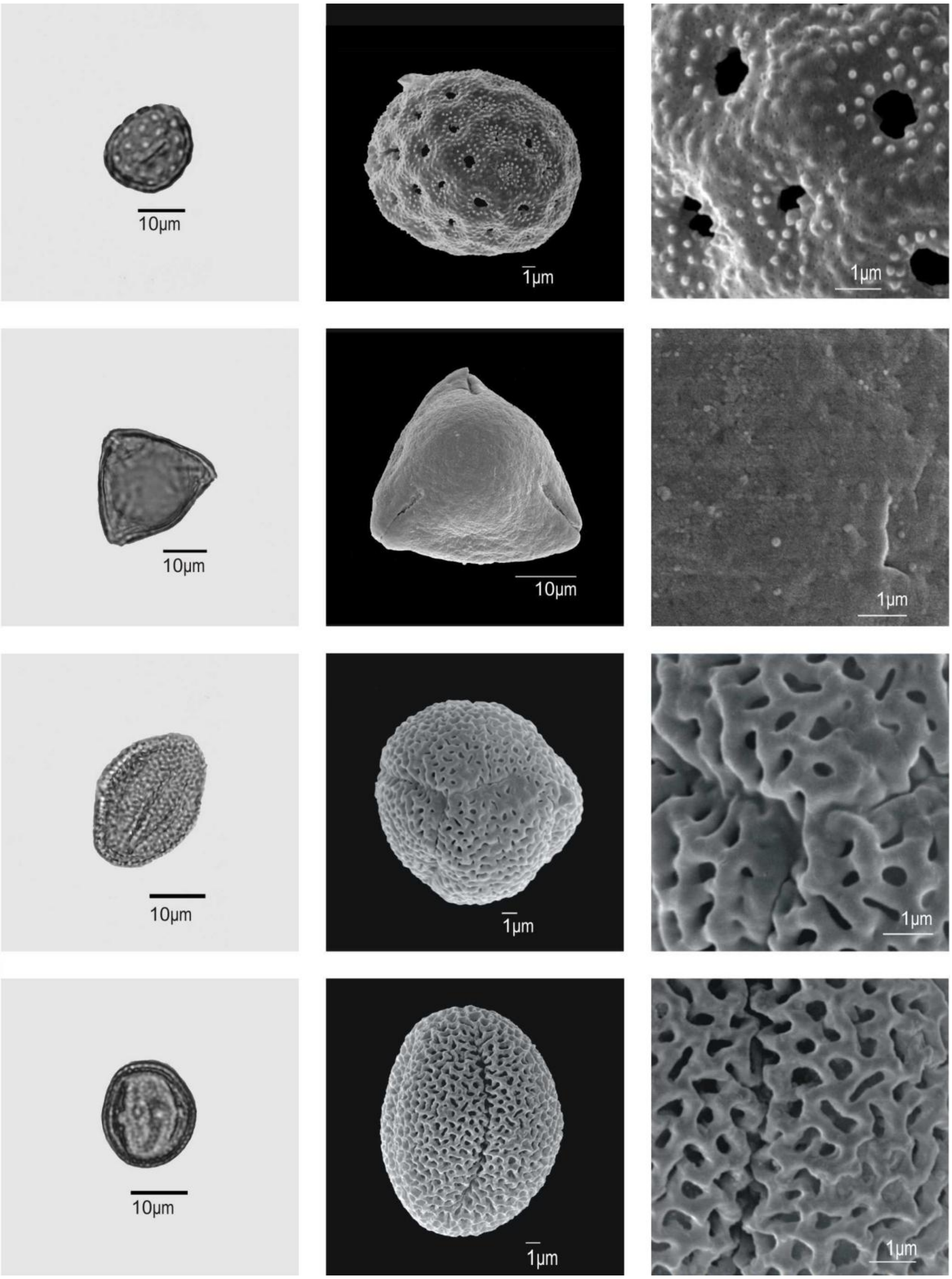
10µm
1µm
1µm
10µm
10µm
1µm
10µm
1µm
1µm
10µm
1µm
1µm

**Plate 14:**

Fig.1: ***Sapium* sp.** LM; equatorial view

Fig.2: ***Sapium* sp.** SEM; equatorial view

Fig.3: ***Sapium* sp.** SEM; detail picture of the surface around the colpus

Fig.4: ***Quercus* sp.1.** LM; equatorial view

Fig.5: ***Quercus* sp.1.** SEM; equatorial view

Fig.6: ***Quercus* sp.1.** SEM; detail picture of the surface

Fig.7: ***Quercus* sp.2.** LM; equatorial view

Fig.8: ***Quercus* sp.2.** SEM; equatorial view

Fig.9: ***Quercus* sp.2.** SEM; detail picture of the surface

Fig.10: ***Quercus* sp.3.** LM; equatorial view

Fig.11: ***Quercus* sp.3.** SEM; equatorial view

Fig.12: ***Quercus* sp.3.** SEM; detail picture of the surface

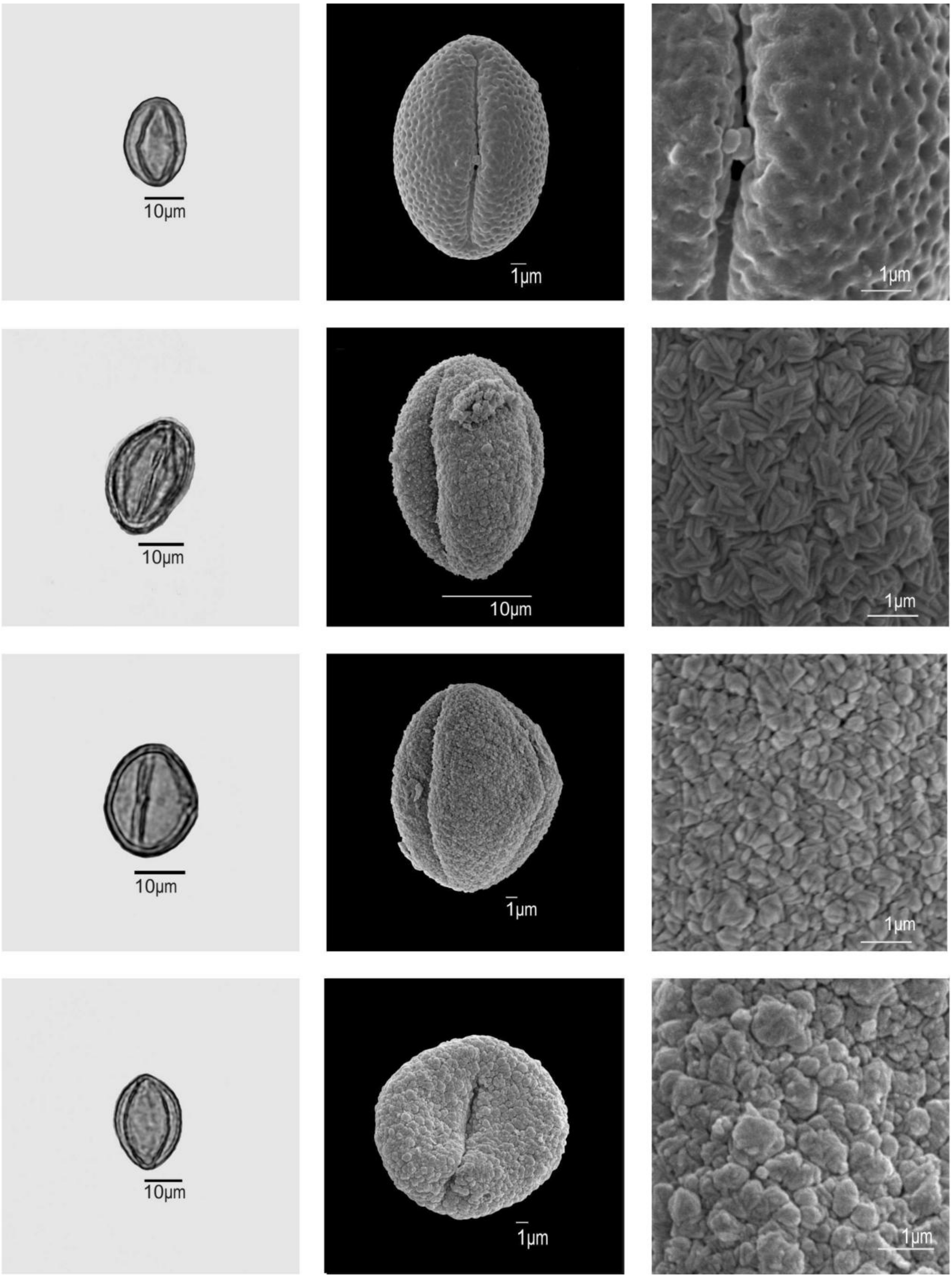
10μm
1μm
1μm
10μm
10μm
1μm
10μm
1μm
1μm
10μm
1μm
1μm

**Plate 15:**

Fig.1: ***Quercus* sp.4.** LM; equatorial view

Fig.2: ***Quercus* sp.4.** SEM; equatorial view

Fig.3: ***Quercus* sp.4.** SEM; detail picture of the surface

Fig.4: ***Quercus* sp.5.** LM; equatorial view

Fig.5: ***Quercus* sp.5.** SEM; equatorial view

Fig.6: ***Quercus* sp.5.** SEM; detail picture of the surface

Fig.7: ***Engelhardia* sp.** LM; polar view

Fig.8: ***Engelhardia* sp.** SEM; polar view

Fig.9: ***Engelhardia* sp.** SEM; detail picture of the surface

Fig.10: ***Juglans* sp.** LM;

Fig.11: ***Juglans* sp.** SEM;

Fig.12: ***Juglans* sp.** SEM; detail picture of the surface around a porus

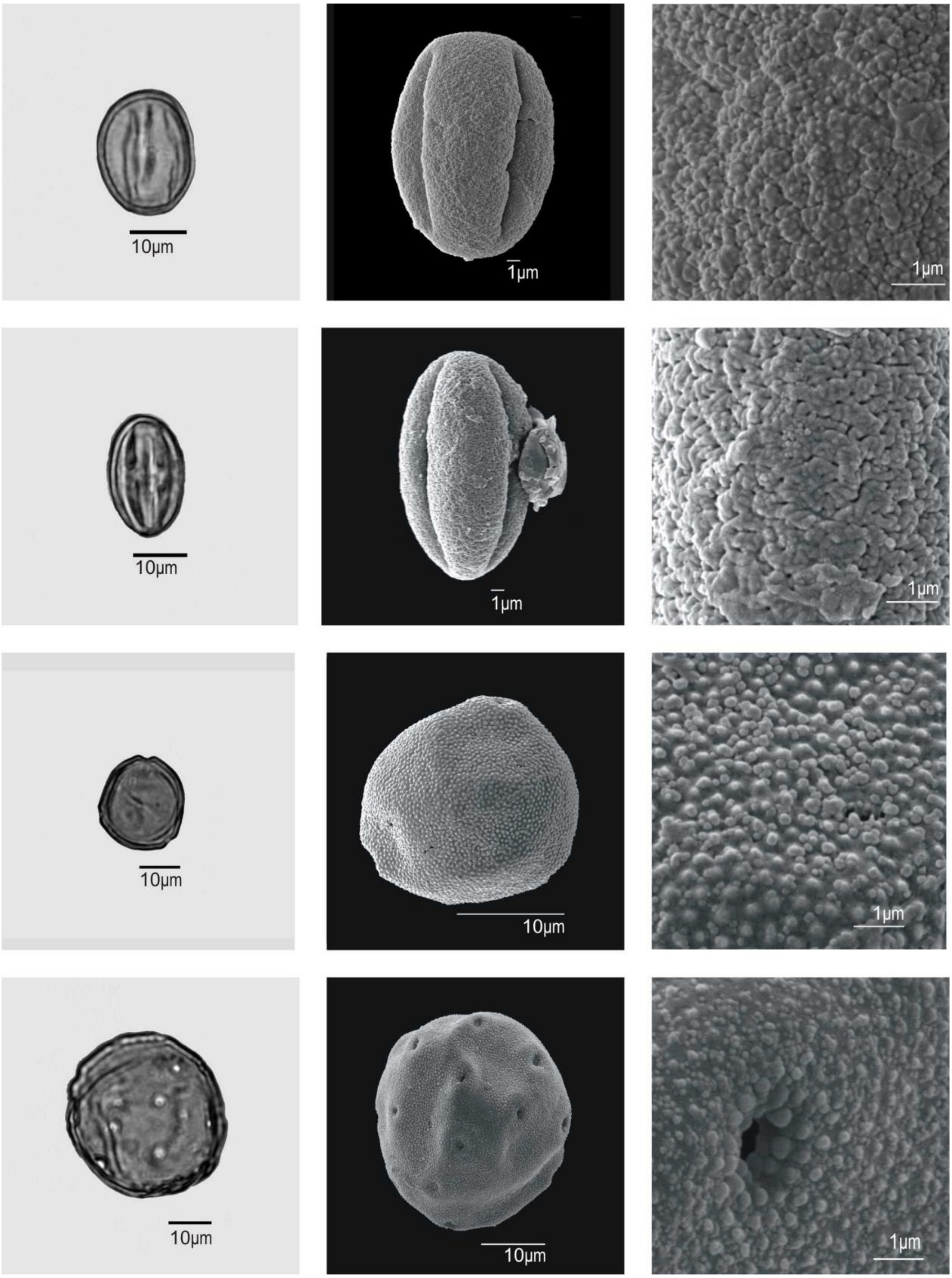
10µm
1µm
1µm
10µm
1µm
1µm
10µm
10µm
1µm
10µm
10µm
1µm

**Plate 16:**

Fig.1: **Mimosaceae gen. indet.** LM;

Fig.2: **Mimosaceae gen. indet.** SEM;

Fig.3: **Mimosaceae gen. indet.** SEM; detail picture of the surface between single pollen grains

Fig.4: ***Fraxinus* sp.** LM; equatorial view

Fig.5: ***Fraxinus* sp.** SEM; equatorial view

Fig.6: ***Fraxinus* sp.** SEM; detail picture of the surface

Fig.7: ***Ligustrum* sp.** LM; equatorial view

Fig.8: ***Ligustrum* sp.** SEM; polar view

Fig.9: ***Ligustrum* sp.** SEM; detail picture of the surface

Fig.10: **Poaceae gen. indet.1.** LM; polar view

Fig.11: **Poaceae gen. indet.1.** SEM; equatorial view

Fig.12: **Poaceae gen. indet.1.** SEM; detail picture of the surface

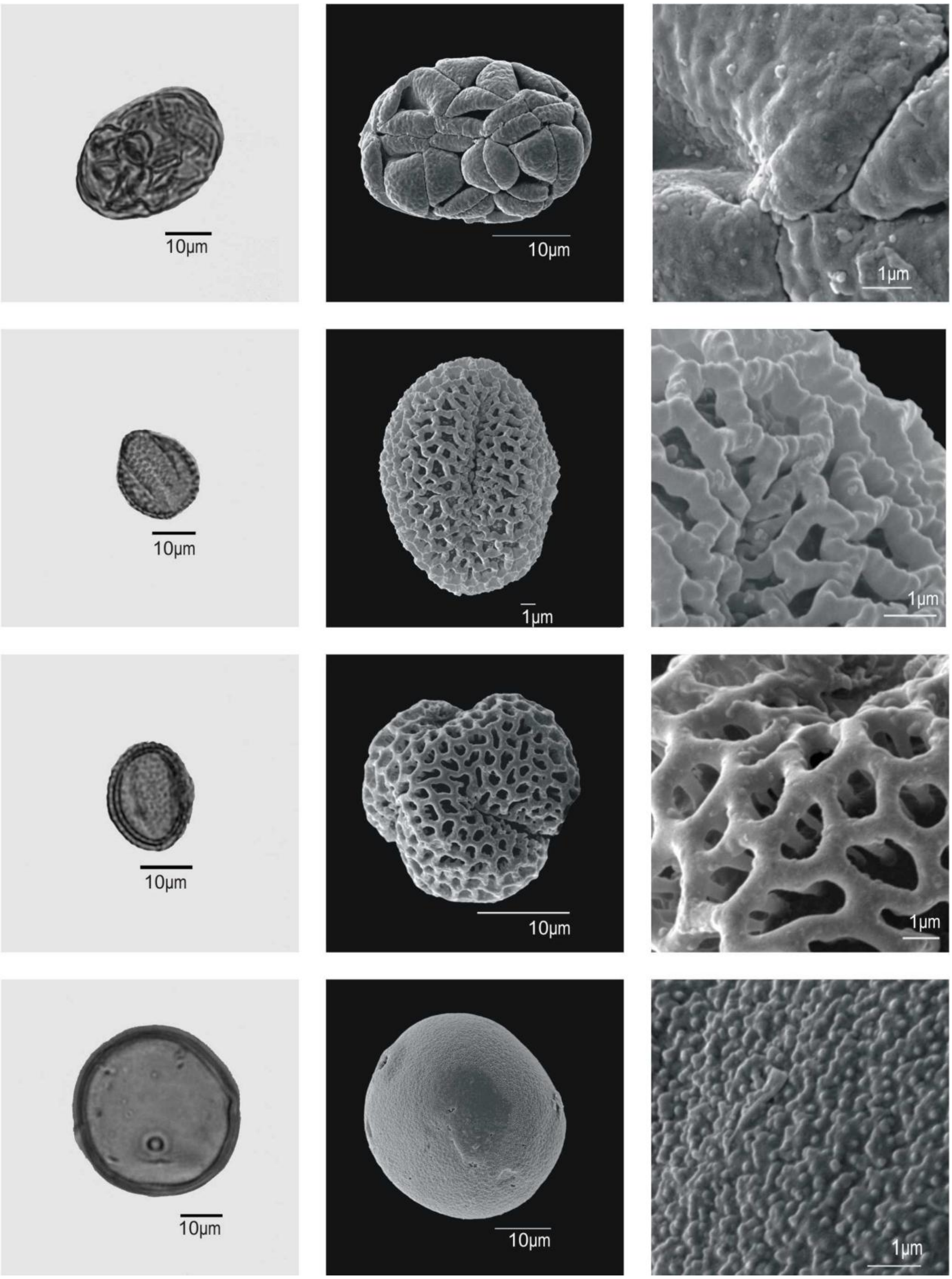
10µm
10µm
1µm
10µm
1µm
1µm
10µm
10µm
1µm
10µm
10µm
1µm

**Plate 17:**

Fig.1: **Poaceae gen. indet.2.** LM; equatorial view

Fig.2: **Poaceae gen. indet.2.** SEM; equatorial view

Fig.3: **Poaceae gen. indet.2.** SEM; detail picture of the surface

Fig.4: **Poaceae gen. indet.3.** LM; equatorial view

Fig.5: **Poaceae gen. indet.3.** SEM; equatorial view

Fig.6: **Poaceae gen. indet.3.** SEM; detail picture of the surface

Fig.7: ***Zanthoxylum* sp.** LM; equatorial view

Fig.8: ***Zanthoxylum* sp.** SEM; equatorial view

Fig.9: ***Zanthoxylum* sp.** SEM; detail picture of the surface

Fig.10: **Solanaceae gen. indet.** LM; polar view

Fig.11: **Solanaceae gen. indet.** SEM; polar view

Fig.12: **Solanaceae gen. indet.** SEM; detail picture of the surface

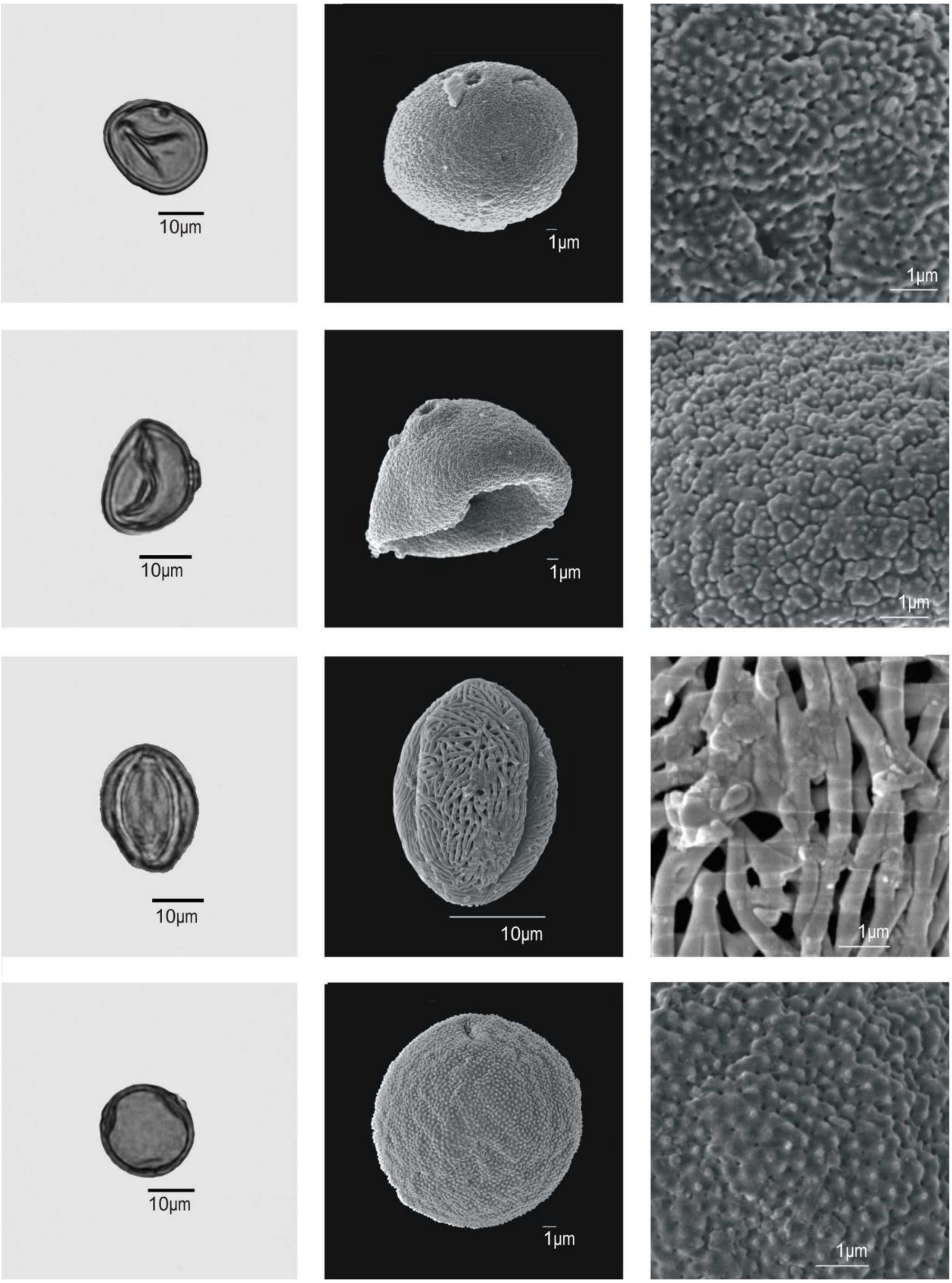
10µm
1µm
1µm
10µm
1µm
1µm
10µm
10µm
1µm
10µm
1µm
1µm

**Plate 18:**

Fig.1: ***Symplocos* sp.1** LM; polar view

Fig.2: ***Symplocos* sp.1** SEM; polar view

Fig.3: ***Symplocos* sp.1** SEM; detail picture of the surface

Fig.4: ***Symplocos* sp.2** LM; polar view

Fig.5: ***Symplocos* sp.2** SEM; polar view

Fig.6: ***Symplocos* sp.2** SEM; detail picture of the surface

Fig.7: ***Typha* sp.** LM; polar view

Fig.8: ***Typha* sp.** SEM; polar view

Fig.9: ***Typha* sp.** SEM; detail picture of the surface

Fig.10: ***Ulmus* sp.** LM; polar view

Fig.11: ***Ulmus* sp.** SEM; polar view

Fig.12: ***Ulmus* sp.** SEM; detail picture of the surface

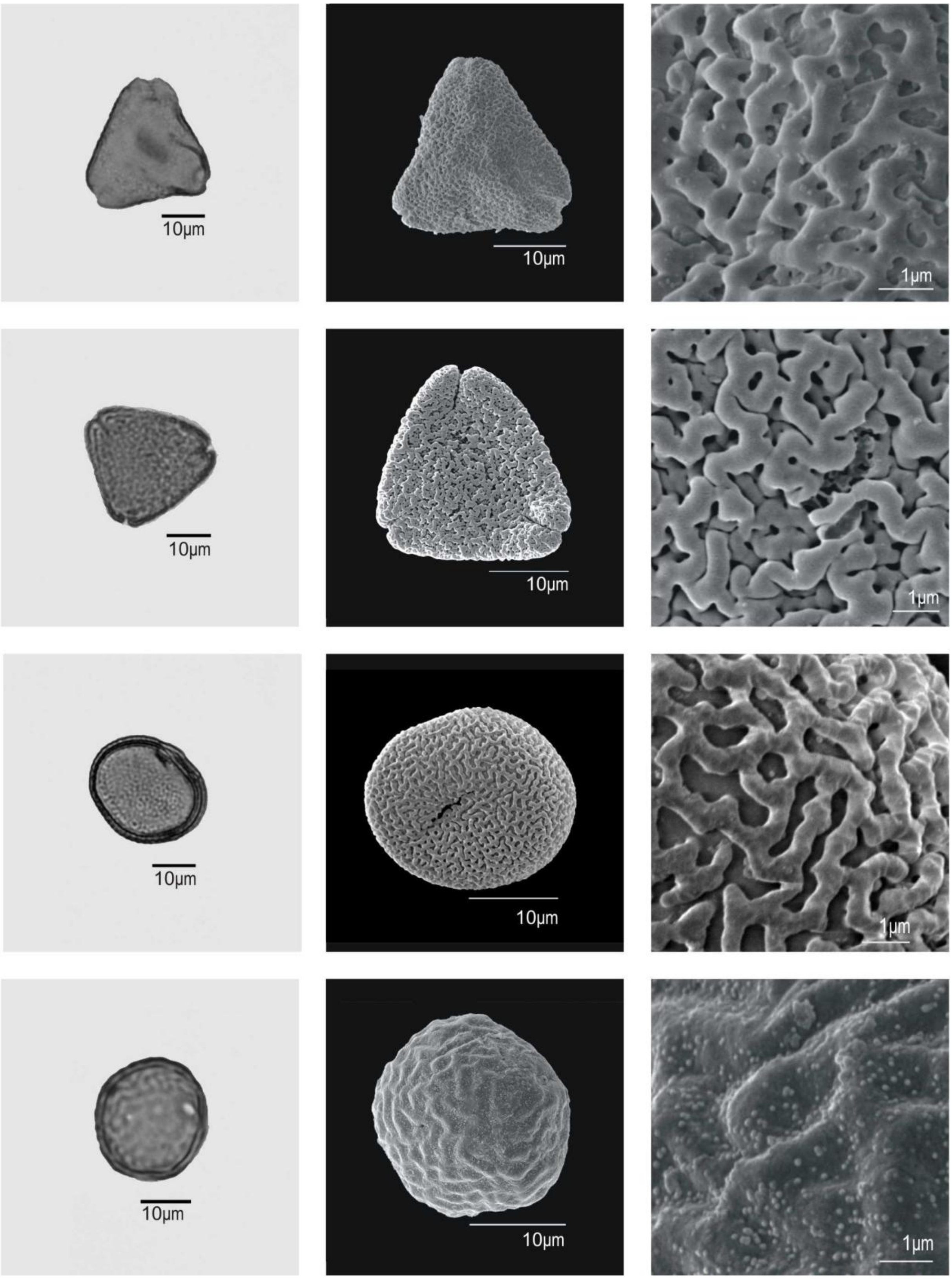
10µm
10µm
1µm
10µm
10µm
1µm
10µm
10µm
1µm
10µm
10µm
1µm

**Plate 19:**

Fig.1: ***Zelkova* sp.** LM; polar view

Fig.2: ***Zelkova* sp.** SEM; polar view

Fig.3: ***Zelkova* sp.** SEM; detail picture of the surface

Fig.4: **Fam. indet.1.** LM; equatorial view

Fig.5: **Fam. indet.1.** SEM; equatorial view

Fig.6: **Fam. indet.1.** SEM; detail picture of the surface around a colpus

Fig.7: **Fam. indet.2.** LM; equatorial view

Fig.8: **Fam. indet.2.** SEM; equatorial view

Fig.9: **Fam. indet.2.** SEM; detail picture of the surface

Fig.10: **Fam. indet.3.** LM; equatorial view

Fig.11: **Fam. indet.3.** SEM; equatorial view

Fig.12: **Fam. indet.3.** SEM; detail picture of the surface

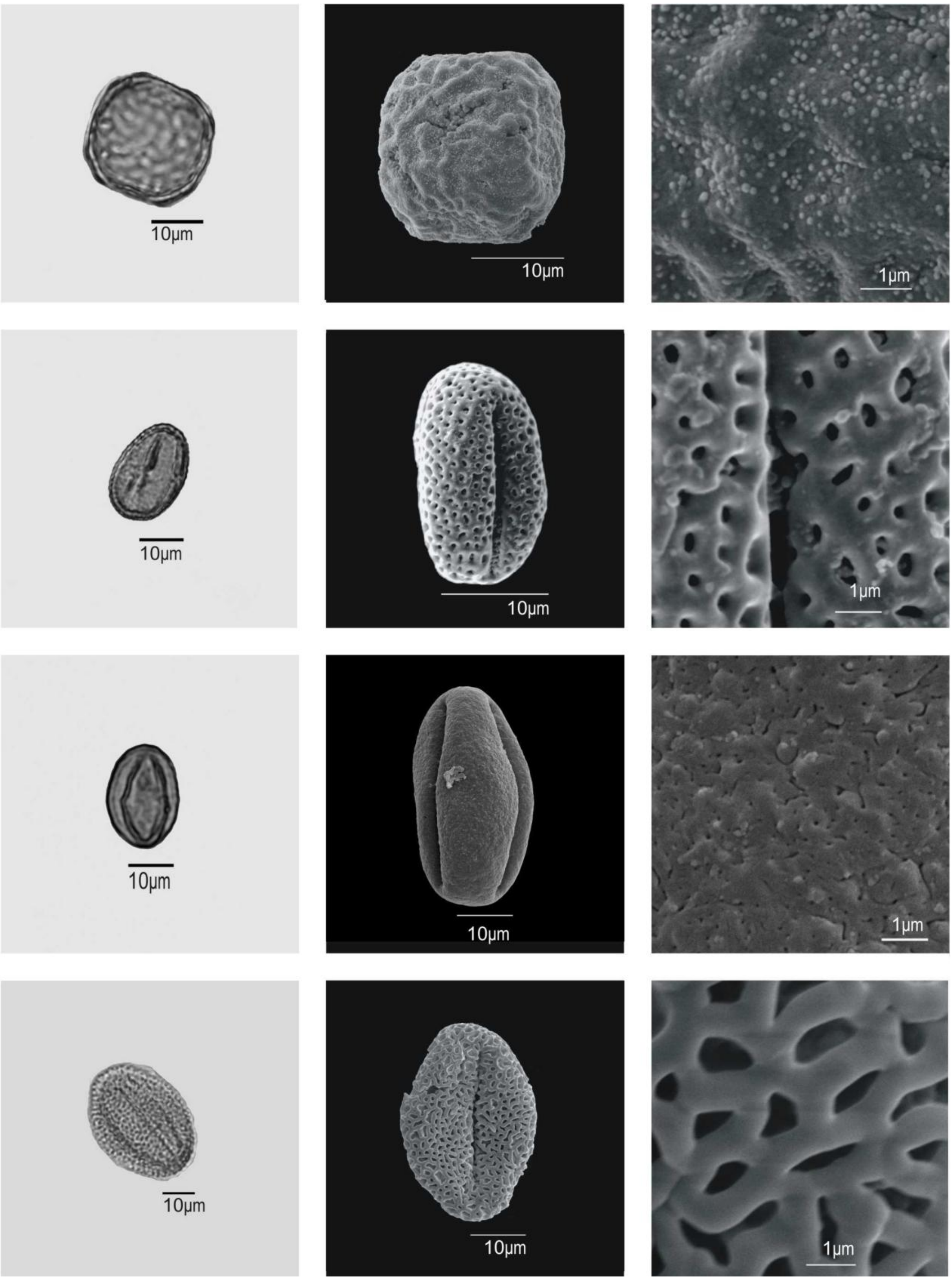
10μm
10μm
1μm
10μm
10μm
1μm
10μm
10μm
1μm
10μm
10μm
1μm

**Plate 20:**

Fig.1: **Fam. indet.4.** LM; polar view

Fig.2: **Fam. indet.4.** SEM; equatorial view

Fig.3: **Fam. indet.4.** SEM; detail picture of the surface

Fig.4: **Cyst indet.** LM;

Fig.5: **Cyst indet.** SEM;

Fig.6: **Cyst indet.** SEM; detail picture of the surface

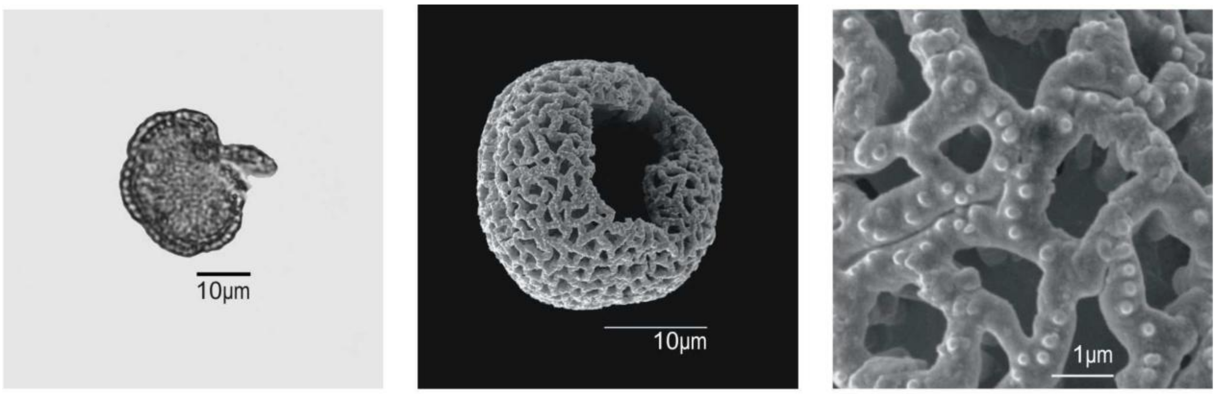
10µm
10µm
1µm

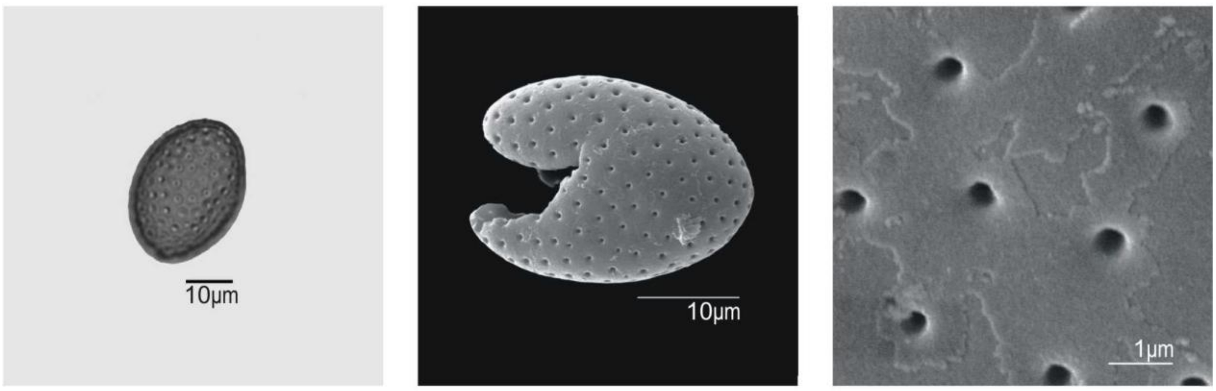
10µm
10µm
1µm

# References


Amana, K., Taira, A., 1992. Two-phase uplift of Higher Himalaya since 17 Ma. Geology 20, 391-394.

Banerji, M.L., 1963. Outline of Nepal phytogeography. Vegetatio 11, 288-296.

Booffield, M.E., 1993. Miocene to Holocene uplift and sedimentation in the northwestern Himalaya and adjacent areas. In: Schröder, J.F. (Ed.), Himalaya to the Sea: Geology, Geomorphology and the Quaternary, 43-71. Routledge, London.

Bordet, P., 1961. In: Recherches géologiques dans l'Himalaya du Népal, région du Makalu. Paris Editions du Centre National de la Recherche Scientifique, Paris 275 pp.

Bordet, P., Colchen, M., Le Fort, P., 1972. Some features oft the geology of the Annapurna range Nepal Himalaya. Himalayan Geology 2, 537-563.

Bossat, P., Ottinger, R., 1989. Rocks of the Murree Formation of northern Pakistan: indicators of a descending foreland basin of late Paleocene to middle Eocene age. Eclagae Geol. Helv. 82, 133-165.

Burback, D.W., Derry, L.A., France-Lanord, Ch., 1993. Reduction Himalayan sediment production 8 Myr ago despite an intensified monsoon. Nature 364, 48-50.

Cochran, J.R., 1990. Himalayan uplift, sea level and the record of Bengal fan sedimentation at the ODP led 116 sites, Cochran, J.R., Stow, D.A.V. (Eds.), Proc. Ocean Drilling Prog. Sci. Results 116, 397-413.

Cerling, T.E., Harris, J.M., MacFadden, B.J., Leakey, M.G., Quade, J., Eisenmann, V., Ehrlinger, J.R., 1997. Global vegetation change through the Miocene/Pliocene boundary. Nature, 389, 153-158.

Cole, D.R., Monger, H.C., 1994. Influence of atmospheric CO2 on the decline of C4 plants during the last deglaciation. Nature, 368, 533-536.

Corvinus, G., 1988. The mio-plio-pleistocene Litho- and Biostratigraphy of the Surai Khola Siwaliks in West Nepal: first results. Comptes Rendus de l'Académie des Science (Series II) 306 (20), 1471–1477.

Derry, L.A., France-Lanord, C., 1996. Neogene Himalayan weathering history and river $^{87}Sr/^{86}Sr$ impact in the marine Sr record. Earth Planet. Sci. Lett. 142, 59-74.

Dobremez, J.-F., 1972. Mise au point d'un methode cartographique d'etude des montagnes tropicals, le Nepal, ecologie et phytogeographic. Thése. University Scient16:46 17/05/2005 ifique et Medicale de Grenoble; France.

Dobremez, J.-F. 1972. Les grandes divisions phytogéographiques du Népal et de l'Himalaya. Bull. Soc. Bot. France 119, 111-120.

Dobremez, J.-F., Vigny, F. & Williams, L.H.J., 1972. Bibliographie du Népal III. 2, Botanique. Centre National de la Recherche Scientifique; Paris.

Erdtman, G., 1954. An introduction to pollen analysis. Chronica Botanica Company, Waltham, Mass., USA, 239 pp.

Faegeri, K., Iversen, J., 1989. Textbook of pollen analysis, John Wiley Sons, 328 pp.

Fort, M., Gupta, V.J., 1981. Plio-Pleistocene Midland Himalayan basins of Kathmandu, Pokhara and Kashmir. Neogene/Quaternary Boundary Field Conference, India, 1979, Proceedings, Geological Survey of India, pp. 37-43.

Fujii, R., Sakai, H., 2001. Paleoclimatic changes during the last 2.5 m.y. recorded in the Kathmandu Basin, central Nepal Himalayas. Journal of Earth Science, 20, 255-266.

Fujii R., Kuwahara Y. and Saki H.,2001. Mineral composition changes recorded in the sediments from a 248-m-long drill-well in central part of the Kathmandu Basin, Nepal. Journal of Nepal Geological Society, Vol. 25, pp 63-69.

France-Lanord, C., Derry, L.A., 1994. $\delta^{13}C$ of organic carbon in the Bengal fan: source evolution and transport of C3 and C4 plant carbon to marine sediments. Geochim. Cosmochim. Acta 58, 4809-4814.

Goddu, S.R., 2004. A study of Pleistocene lacustrine sediments at the southern front of the Tibetan Plateau: Dating and paleoclimate record. Dissertation at the Eberhard-Karls-Universität Tübingen.

Frank, W., Fuchs, G., 1970. Geological investigations in western Nepal and their significance for the geology of the Himalayas. Geologische Rundschau 59, 552-580.

Franz, H., Kral, F., 1975. Pollenanalyse und Radiocarbondatierung einiger Proben aus dem Kathmandubecken und aus dem Raum Jumla in Westnepal. Sitz. Ber. Öst. Akad. Wiss., math. Nat. Kl. Abt. I, Bd. 184, 1-5, 9-17.

Gansser, A., 1964. Geology of the Himalayas. Interscience, London, p.289.

Gupta, V., 1975. On the stratigraphic position of the Kathmandu Valley sediments, Nepal. Geographica Helvetica, 30, 27-28.

Hagen, T., 1968. Report on the geological survey of Nepal. 1, Denschar. Schweiz. Nat. Gesell. 86 Hf1, 185 pp.

Hagen, T., 1969. Report on the geological survey of Nepal Preliminary reconnaissance. Zürich Mémoires de la Societe Helvétique des Sciences Naturelles LXXXVI/1, 185.

Hagen, T., 1986. Nepal. Oxford and IBH Publishing, New Delhi, 264 pp.

Hashimoto, S., Ohta, Y., Akiba, C., 1973. Geology of the Nepal Himalayas. Saikon, Tokyo 286 pp.

Heim, A., Gansser, A., 1939. Central Himalaya: Geological observations of the Swiss expedition 1936. Mem. Soc. Helv. Sci. Nat 73 (1), 1-245.

Katel, T.P., Upreti, B.N., Pokharel, G.S., 1996. Engineering properties of fine grained soils of Kathmandu Valley, Nepal. Journal of Nepal Geological Society 13, 121-138.

Kral, F., Havinga, A., 1979. Pollenanalyse und Radiocarbondatierung an Proben der oberen Teile der Sedimentserie des Kathmandu-Sees und ihre vegetationsgeschichtliche Interpretation. Sitz Ber. Öst. Akad. Wiss., math. Nat. Kl. Abt. I, 188 (1-10), 45-61.

Le Fort, P., 1975a. Himalaya : the collided range: Present knowledge of the continental arc. American Journal of Science 275A, 1-44.

Liu, G., Einsele, G., 1994. Sedimentary history of the Tethyan basin in the Tibetan Himalaya. Geologische Rundschau 83, 32-61.

Natori, H., Takizawa, F., Motojima, K., Nagata, S., 19890. Natural gas in the Kathmandu Valley. Chishitsu News (Geology News from Geological Survey of Japan) 3312, 24-35.

Paudayal, K.N., Ferguson, D.K., 2004. Pleistocene palynology of Nepal. Quaternary International 117, 69-79.

Pècher, A., 1975. The Main Central Thrust of the Nepal Himalaya and the related metamorphism in the Modi-Khola cross section (Annapurna Range). Himalaya Geology 5, 115-132.

Pècher, A., 1977. Geology of the Nepal Himalaya: deformation and petrography in the Main Central Thrust zone, Vol. 268. Ecologie et géologie de l'Himalaya C.N.R.S. Paris coll.int., Paris Sciences de la Terra Ed. Cent. Natl. Rech. Sci. Paris, pp. 301-318.

Sah, R.B., 1992. A Survey of Vertebrate Palaeontological Records of Nepal Himalaya. J. Nat. His. Mus. Vol. 13, No. (1-4), 29-40.

Saijo, K., Kimura, K., 2007. Expansion of an ancient lake in the Kathmandu basin of Nepal during the Lake Pleistocene evidenced by lacustrine sediment underlying piedmont slope. Himalayan Journal of Sciences, Vol. 4, Issue 6, 41-48.

Sakai, H., Takigami, Y., Nakamuta, Y., Nomura, H., 1999. Inverted metamorphism in the Pre-Siwalik foreland basin sediments beneath the crystalline nappe, western Himalaya. Journal of Asian Sciences 17 (5-6), 725-737.

Sakai, H., Fujii, R., Kuwahara, Y., 2002. Changes in the despositional system of the Paleo-Kathmandu Lake cause by uplift of the Nepal Lesser Himalayas. Journal of Asian Earth Sciences 20, 15th International Himalaya-Karakoram-Tibet Workshop, 267-276.

Schweinfurth, U., 1957. Die horizontale und vertikale Verbreitung der Vegetation im Himalaja. Bonner Geographische Abhandlung 20. Dummer Verlag, Bonn.

Sharma, C.K., 1973. Geology of Nepal, Mani Ram Sharma, Kathmandu. 189pp.

Stainton, J.D.A., 1972. Forests of Nepal. John Murray; London.

Stearn, W.T., 1960. *Allium* and *Milula* in the central and eastern Himalaya. Bulletin of the British Museum of Natural History, Botany, 2, 159-191.

Stöcklin, J., Bharrarai, K.D., 1981. Geological map of Kathmandu area and central Mahabharat Range (1:250000). Department of Mines and Geology, His Majesty's Government of Nepal.

Tabata, H., Tsuchya, K., Shimizu, Y., Fujita, N., Matsui, K., Koike, F., Yumoto, T., 1988. Vegetation and climatic changes in Nepal Himalayas. I. Vegetation and climate in Nepal Himalayas as the basis of paleoecological studies. Proc. Indian Natl. Acad., 54: 530-537.

Upreti, B.N., 1999. An Overview of the stratigraphy and tectonics of the Nepal Himalaya. Journal of Asian Earth Sciences 17, 577-606.

West, R.M., Munthe, J., 1981. Neogene vertebrate palaeontology and stratigraphy of Nepal. Jour. Nepal Geol. Soc., 1, 1-14.

West, R.M., Dongol, G.M.S., Munthe, J., Hutchinson, H. Gupta, V.J., 1988. Late Neogene and Quaternary geology, paleontology and paleoenvironment of the Kathmandu Valley, Central Nepal and the Churia Hills, Western Nepal. In: The Paleoenvironment of East Asia from the Mid-Tertiary. Centre of Asian Studies, University of Hong Kong, 916-936.

West, R.M., 1996. The Cenozoic of Nepal: mountain elevation and vertebrate evolution. Journal of Nepal Geological Society, Vol. 14, pp. 11-19.

Yoshida, M., Gautam, P., 1988. Magnetostratigraphy of Plio-Pleistocene lacustrine deposits in the Kathmandu Valley, central Nepal. Proceedings of Indian National Science Academy 54 (A3), 410-417.

Yoshida, M., Igarashi, Y., 1984. Neogene to quaternary lacustrine sediments in the Kathmandu Valley, Nepal. Journal of Nepal Geological Society, Vol. 4, Special Issue, 73-100.

Zetter, R., 1989. Methodik und Bedeutung einer routinemäßig kombinierten lichtmikroskopischen und rasterelektronenmikroskopischen Untersuchung fossiler Mikrofloren. Courier Forschungsinstitut Senkenberg 109, 41-50.

Zetter, R., Ferguson, D.K., 2001. Trapaceae pollen in the Cenozoic. Acta Paleobotanica 41 (2), 321-339.

# Lebenslauf

13.09.1984 geboren in Linz

1991 – 1995 Volksschule

1995 – 2003 Gymnasium in Linz

2003 Matura am Bundesrealsymnasium Ramsauerstraße

2003 Inskription an der Universität Wien „Diplomstudium Biologie (A 437)“

2006 Spezialisierung „ Diplomstudium Paläobiologie (Stzw. A 443)“

09.12.2007 Beginn mit der Diplomarbeit: Palynological Investigation on Plio/Pleistocene Sediments of the Lukundol Formation, Kathmandu Basin, Nepal

Betreuer der Diplomarbeit: Dr. Reinhard Zetter

**Arbeit**

2007 Werkvertrag: „Bohrkernanalyse Hennersdorf – graphische Darstellung der Verteilung der Palynomorphen“ am Naturhistorischen Museum Wien

2008 Werkvertrag: „Analyse der Palynomorphenvergesellschaftungen aus verschiedenen Aufschlüssen des Pannons des Wiener Beckens“ am Naturhistorischen Museum Wien

2008 Werkvertrag: „Bericht über palynologische Detailbearbeitung Autobahnspange Korneuburg im Bereich Profil S Teiritzberg“ an der Geologischen Bundesanstalt Wien

2008 Arbeit an der Universität Wien als Tutorin (Kurs: Paläontologische Laborübungen)

**Publikationen und Abstracts**

Kern, A., Harzhauser, M., 2008. Tracing the late Miocene climatic change – a palynomorph-based pilot-study in the Vienna Basin. Journal of Alpine Geology, Pangeo 2008, 49, p. 52.

Harzhauser, M., Kern, A., Soliman, A., Minati, K., Piller, W.E., Danielopol, D.L., Zuschin, M., 2008. Centennial- to decadal-scale environmental shifts in and around Lake Pannon related to a major Late Miocene lake-level rise. Palaeogeography, Palaeoclimatology, Palaeoecology 270, p. 102 – 115.

Kern, A., Harzhauser, M., Soliman, A., Minarti, K., Piller, W.E., Danielopol, D.L., Zuschin, M., 2008. Oscillation of the paleoenvironment around Lake Pannon revealed by ultra-high-resolution pollen sampling. IPC/IOPC Joint Conference, 30. August - 5. September 2008, Bonn, Abstract volume, p. 140.

Kern, A., Harzhauser, M., Soliman, A., Minarti, K., Piller, W.E., Danielopol, D.L., Zuschin, M., 2008. Ultrahochauflösende Analysen spätmiozäner Palynofloren deuten auf zyklische Änderungen der Vegetationszoen rund um den Pannonsee. Jahrestagung ÖPG Dornbirn. Berichte Geol. B-A.14.

Kern, A., Harzhauser, M., Piller, W.E., Soliman, A., Zetter, R., 2007. High-resolution palynology and sub-Milankovitch cycles in Lake Pannon - coupled or decoupled?. NECLIME 2007, Bratislava.